



**Fausto Daniel dos Santos Queda**

Licenciado em Bioquímica

**Studies towards modified chitooligosaccharides: a  
new approach to NAG-NAM moiety**

Dissertação para obtenção do Grau de Mestre em  
Bioorgânica

Orientador: Maria Manuel Marques, Investigadora  
Auxiliar, FCT-UNL

Júri:

Presidente: Prof. Doutora Jorge Parola  
Arguente(s): Doutor Sérgio Raposo Filipe  
Vogais: Doutora Maria Manuel Marques  
Doutor Sérgio Raposo Filipe



Fausto Daniel dos Santos Queda, Copyright

A Faculdade de Ciências e Tecnologia e a Universidade Nova de Lisboa têm o direito, perpétuo e sem limites geográficos, de arquivar e publicar esta dissertação através de exemplares impressos reproduzidos em papel ou de forma digital, ou por outro qualquer meio conhecido ou que venha a ser inventado e de divulgar através de repositórios científicos e de admitir a sua cópia e distribuição com objectivos educacionais ou de investigação, não comerciais, desde que seja dado crédito ao autor e editor.



## Agradecimentos

Resolvi escrever esta secção como forma de exprimir a minha gratidão para todos aqueles que me acompanharam e ajudaram durante esta etapa que culmina uma série de provas e desafios algo longo dos últimos anos.

Antes de mais gostaria de agradecer à minha orientadora Prof. Maria Manuel Marques por me ter orientado e por ter acreditado nas minhas capacidades para a realização deste trabalho que se revelou um desafio desde o início, sem a sua orientação seria impossível ultrapassar todos os contratemplos.

Gostaria de agradecer às pessoas que trabalharam comigo, nomeadamente ao pessoal do laboratório 202, FCT-UNL, Alexandra Loupas, Cátia Santos, Luísa Carvalho, Luísa Maria, Marina Pires, Tomé Silva e Vasco Bonifácio, laboratório Bacterial cell surfaces and parhogenesis, ITQB-UNL Gonçalo Covas e Filipa Vaz pelo apoio, pela paciência e pelas horas em convívio, sem esquecer a Cecília Bonifácio e a Ana Teresa que juntamente com a Rede Nacional de RMN foram importantes para a realização deste projecto, bem como o financiamento PTDC/SAU-IMU/111806/2009 e PTDC/QEQ-QOR/2132/2012

Gostaria agora de agradecer à minha namorada Nídia Almeida, pelo apoio nesta jornada, que foi e tem sido uma peça fundamental para que as coisas decorressem da forma mais harmoniosa possível.

Quero também deixar um especial obrigado ao André Dias, João Cascão e Tiago Costa, pelos jantares de orientação e pelos momentos de diversão. À Helena Coelho e Mariana Romão por todo o apoio antes e durante a escrita.

Aos meus amigos de longa data Cristina Montenegro, Filipe Sério, José Ribeiro Mariana Mesquita, Samuel Figueiredo, Rita Nóbrega, Rui Oliveira, que embora uns mais distantes do que outros também eles peças fundamentais durante esta jornada.

Não podia deixar de agradecer aos quatro amigos que compõem a banda da qual faço parte, *The Big Odds*, Bruno Salgado, Fernando Dias, Gustavo Marques e Pedro Fonseca, que se não fossem eles a tirar-me do trabalho em alguns momentos teria sido muito mais difícil.

Quero também agradecer à minha mãe Alexandrina Santos por todo o apoio e paciência ao longo destes anos nesta etapa que agora termina. Ao meu pai Fernando Queda, que infelizmente não conseguiu ver o terminar desta caminhada, tendo sido vencido nesta recta final, mas que de certo, estaria muito orgulhoso por me ver completar este ciclo.

O meu obrigado a todos os outros que não menciono mas que foram eles também importantes durante estes últimos anos.



## Resumo

O **peptidoglicano** (PGN) bacteriano tem sido associado a infecções bacterianas e à resistência antibióticos. Desta forma, este trabalho surge no enquadramento do problema com qual a comunidade científica se tem vindo a deparar aquando da obtenção de fragmentos de peptidoglicano puros e em quantidade que permita a realização de estudos biológicos. A síntese de fragmentos de PGN é complexa e envolve inúmeros passos de síntese e o seu isolamento e purificação de fontes naturais é difícil.

Este trabalho consistiu em investigar uma estratégia que permitisse transformar um produto considerando um desperdício da indústria alimentar, **quitosano**, num produto valioso, mureína, um polímero de unidades alternadas de **NAG-NAM** que se encontram interligadas por pontes peptídicas. Para isso explorou-se uma aproximação **quimioenzimática**. Numa primeira estratégia procedeu-se à protecção regioselectiva dos grupos hidroxilo da posição O-6 com dois grupos, TBDPS e TPS, com consequentemente introdução da unidade lactil na posição O-3, apenas contando com o impedimento estéreo que estes grupos proporcionavam à entrada do grupo lactil.

Numa segunda estratégia, foi utilizado uma pinça molecular, "**molecular clamp**", com vista a forçar uma entrada da unidade lactil de uma forma alternada, recorrendo a uma di-esterificação, usando um ácido di-carboxílico nas posições O-6 alternadas.

As amostras obtidas por estas duas vias foram submetidas a uma hidrólise enzimática. As enzimas utilizadas foram a **lisozima** e mutanolizina. As amostras digeridas foram ainda avaliadas em relação à afinidade para a enzima **mCherry-PGRP-SA**. **Os produtos obtidos foram** avaliados quanto à sua quantidade relativa de NAG e NAM, por uma cromatografia de troca iónica.

Os resultados obtidos demonstraram que a via "**molecular clamp**" é a estratégia mais promissora permitindo a conversão de quitosano em unidade de NAG-NAM (1:1,18) numa composição semelhante à do PGN natural extraído de *S. aureus*.

**Palavras-chave:** Peptidoglicano, quitosano, NAG-NAM, quimioenzimática, *molecular clamp*, lisozima, mCherry-PGRP-SA.



## Abstract

The bacterial **peptidoglycan** (PGN) has been directly associated with bacterial infections and antibiotic resistance. This work deals with the scientific community problem of obtaining peptidoglycan in a pure and reliable amounts for biological studies. The synthesis of PGN fragments. The synthesis of PGN fragments involves multi-step approaches and the isolation and purification from natural sources is usually difficult.

This work consisted on the investigation of a strategy that allows conversion of a food industry disposal, **chitosan**, in the valuable murein, a polymer of alternated **NAG-NAM** units that are cross-linked via short peptide bridges. Thus a **chemoenzymatic** approach was explored.

In a first strategy a regioselective O-6-hydroxyl group protection was performed using two different groups, TBDPS and TPS, with subsequent introduction of the lactyl moiety at O-3 position relying on the steric hindrance of the groups at O-6.

On a second approach, a **molecular clamp** strategy was applied to block the access to some of the O-3 positions in alternate units. This approach involved a di-esterification at the -O6 positions of two alternate units, using a di-carboxylic acid, resulting in an alternated lactyl insertion in the following step.

After the completion of the chemical modification of chitosan, the samples obtained were digested with two lytic enzymes, **Lysozyme** and Mutanolysin. The digested samples were evaluated against its binding to the enzyme **mCherry-PGRP-SA**. Moreover the content in NAG:NAM of the samples produced was quantified by ionic chromatography.

to the results obtained in this study revealed that the molecular clamp strategy is a promising route to convert chitosan into NAG-NAM oligosaccharides in a composition, NAG:NAM ratio (1:1.18) similar to the PGN isolated from *S. aureus*.

**Key words:** peptidoglycan, chitosan, NAG-NAM, chemoenzymatic, molecular clamp, lysozyme, mCherry-PGRP-SA



## Figure index

Figure	Page
Figure 1.1 <i>Drosophila melanogaster</i> model of Toll and Imd pathway activation, adapted from Lemaitre <i>et al</i> (5)	2
Figure 1.2: Representation of PGN; (a) Gram-positive; (b) Gram-negative; adapted from Royet <i>et al</i> (71 <sup>b</sup> )	3
Figure 1.3 Bacterial cell wall representation; (a) Gram-positive bacteria cell wall; (b) Gram-negative bacteria cell wall adapted from	4
Figure 1.5: Schematic representation of glycosylation reaction; (a) via NAG donor; (b) via <i>N</i> -disubstituted donors	5
Figure 1.4 Schematic NAG-NAM retro-synthesis approaches	6
Figure 1.6 Retrosynthetic view of a dimeric PGN	7
Figure 1.7 Schematic NAG-NAM coupling to the peptide D-Ala-L-Lys-D-Gln-L-Ala, then coupled with five glycines and finally cleavage of the resin	7
Figure 1.8: Synthesis of glucosamine Donor (A) and Acceptor (B)	8
Figure 1.9 Synthesis of disaccharide NAG-NAM	9
Figure 1.10 Molecular skeleton of chitin (R=acetyl) and chitosan (R=H>50%)	9
Figure 1.11- Antiparallel chain arrangement in $\alpha$ -chitin.(1); parallel arrangement in $\beta$ -chitin. adapted from Colocar <i>et al</i> reference 33 <sup>(e)</sup> (2) ou Colocar A e B	11
Figure 1.12 Scheme of amine moiety protection with phthalic anhydride	12
Figure 1.13 Schematic water-influence in the solvent composition on the chitosan and phthalic anhydride, reaction product	12
Figure 1.14 Synthesis of a regioselective amphiprotic chitosan; (a) <i>N</i> -phthaloylation; (b) position 6 bromination; (c) position 6 azidation; (d) Husigen cycloaddition; (e) phthaloyl group removal	13
Figure 1.15 Synthetic scheme of <i>N</i> -(4-carboxybutyryl) chitosan derivatives using different mol ratios of glutaric anhydride	14
Figure 1.16 Synthesis of <i>N,N,N</i> -trimethyl <i>O</i> -carboxymethyl chitosan	16
Figure 1.17 <i>O</i> -3 and <i>O</i> -6 <i>N</i> -acetyl/phthaloyl chitosan simultaneous protection; (a) Silylation; (b) Acetylation; (c) Tosylation	16
Figure 1.18 Selective <i>O</i> -6 Tosylation then FGI; (b) <i>O</i> -6-ethyl benzoate chitin; (c) 6-deoxy-diethyl malonate chitin; (d) 6-(deoxydiethyl) phosphite chitin	17
Figure 1.19 <i>O</i> -6- <i>N</i> -phthaloyl chitosan selective protection; (a) Trytilation; (b) Silylation (TBDMS); (c) Silylation (TBDPS)	18
Figure 1.20 Synthesis of a regioselective amphiprotic chitosan; (a) <i>N</i> -phthaloylation; (b) position 6 bromination; (c) position 6 azidation; (d) Husigen cycloaddition; (e) phthaloyl group removal	19
Figure 1.21 Selective protection/deprotection of chitosan; (a) <i>N</i> -phthaloylation; (b) <i>O</i> -6 tritylation; (c) <i>O</i> -3 benzoylation; (d) <i>O</i> -6 trityl group removal; (e) <i>N</i> -phthaloyl group removal; (f) <i>O</i> -3 benzyl group removal.	20
Figure 1.22 Conversion of the azide moiety into amine group	21
Figure 2.1 PGN's sugar backbone retrosynthetic plan	23
Figure 2.2 5 hours chemical chitosan hydrolysis	23
Figure 2.3 Mechanism of chitosan acid assisted hydrolysis	23
Figure 2.4 TLC of 5 hours dialysis. (G) – I.5; (I) - inside of dialysis membrane; (F) - outside of dialysis membrane. Eluent 70% H <sub>2</sub> O 20% isopropanol 10% aqueous ammonia, revealed with 10% sulphuric acid in ethanol	24
Figure 2.5 MALDI-TOF spectra from II.8	25
Figure 2.6 <i>N</i> -modification synthesis strategy	26
Figure 2.7 MALDI-TOF spectra from II.10	27
Figure 2.8 Synthesis plan of PGN sugar backbone or murein; (A) asymmetric protection route; (B) silylation route	28
Figure 2.9 Generic strategy to the silylation route	29
Figure 2.10 Silylation of <i>N</i> -phthaloyl chitosan	30
Figure 2.11 Polymeric chitosan amine moiety protection	30
Figure 2.12 Schematic representation of lactyl moiety insertion	31
Figure 2.13 Sequence of deprotection reactions and <i>N</i> -acetylation	32

Figure 2.14 IR spectra of polymeric chitosan modifications, black – (I.30); red – (I.32); dark green – (I.47); blue – (II.18); light green – (II.24)	33
Figure 2.15 NMR CP/MAS spectra green I.32; black I.47;	33
Figure 2.16 Linkage between two odd units	34
Figure 2.17 Dicarboxylic acids synthesized during this work	34
Figure 2.18 Example of a molecular clamp reaction scheme	34
Figure 2.19 NMR CP/MAS green I.32; black II.33	35
Error! Reference source not found.	35
Figure 2.21 Silylation of the remaining O6 free positions	36
Figure 2.22 Muramic acid moiety insertion of O6 molecular clamp and O6-TBDMS <i>N</i> -phthaloyl chitosan	37
Figure 2.23 Sequence of deprotection and <i>N</i> -acetylation reactions	37
Figure 2.24 IR spectra of polymeric chitosan modifications, black (I.32); red (II.34); green (II.42); light blue (II.44); blue (II.48)	38
Figure 2.25 Comparison of lysozyme hydrolysis profiles, 206 nm	40
Figure 2.26 Hydrolysis profile of II.48 treated with mutanolysin; (green); (black) negative control	41
Figure 2.27 HPLC-UV/MS chromatogram of sample II.48; (red) II.48 + mutanolysin; (green) negative control	42
Figure 2.28 II.48 ESI+ MS, (8.18 min)	42
Figure 2.29 8% SDS-PAGE gel electrophoresis of the mCherry-PGRP-SA pull-down assay in the presence of native PGN	43
Figure 2.30 mCherry-PRGP-SA percentage of binding of the different samples	44
Figure 2.32 8% SDS-PAGE gel electrophoresis of the mCherry-PGRP-SA pull-down assay without native PGN	45
Figure 2.31 mCherry-PGRP-SA intensity in the PGRP-SA pull-down assay without native PGN	45
Figure 4.1 Schematic representation of hydrolysis reactions	48
Figure 4.2 Schematic representation of <i>N</i> -protection reactions	50
Figure 4.3 Schematic representation of molecular clamp synthesis	51
Figure 4.4 Schematic representation of molecular clamp insertion	56
Figure 4.5 Schematic representation of the protection of the remaining O6 free positions	58
Figure 4.6 Schematic representation of muramic acid moiety insertion	59
Figure 4.7 Schematic representation of protecting group removal and <i>N</i> -acetylation reaction	60
Figure 4.8 Schematic representation of silylation of <i>N</i> -protected chitosan	62
Figure 4.9 Schematic representation of lactyl moiety insertion	63
Figure 4.10 Schematic representation of all deprotection reactions and <i>N</i> -acetylation	65
Figure 4.11 HPLC-UV eluent profile	67
Figure 4.12 Eluent profile for the anionic exchange chromatography	70



## Table index

<b>Table</b>	<b>Page</b>
Table 2-1 Summary of the hydrolysis' work	23
Table 2-2 Summary of first enzymatic, lysozyme, digestion	40
Table 2-3 Summary of the second enzymatic study (92 hours)	41
Table 4-1 Summary of the hydrolysis' work	52
Table 4-2 HPLC UV protocol eluent composition	67
Table 4-3 Concentration gradient used during the HPLC-UV program	67
Table 4-4 Concentration gradient used during the HPLC-MS program	68
Table 4-5 SDS gel composition	69
Table 4-6 Loading Buffer	69
Table 4-7 Electrophoresis Buffer	69
Table 4-8 Concentration gradient used during the anionic exchange chromatography program	70



## List of abbreviations

[M+]	Molecular Ion
<sup>13</sup> C NMR	Carbon Nuclear Magnetic Resonance
<sup>1</sup> H NMR	Proton Nuclear Magnetic Resonance
Ac	Acetyl
Ar	Aromatic
alloc	Allyloxycarbonyl
Bn	Benzyl
CDI	1,1'-Carbonyldiimidazole
CHPTMAC	3-Chloro-2-Hydroxy-Propyl Trimethyl Ammonium Chloride
d	Doublet
DA	Deacetylation Degree
DAP	Diaminopimelic
DCC	<i>N,N'</i> -Dicyclohexylcarbodiimide
DCM	Dichloromethane
DIC	Carbodiimide
DMF	Dimethylformamide
DMSO	Dimethylsulfoxide
DP	Polymerisation Degree
DS	Degree Of Substitution
EC	Effective Concentration
equiv.	Equivalent
Et	Ethyl
Fmoc	Fluorenylmethyloxycarbonyl
g	Gram
GNBP	Gram-Negative Binding Protein
GPC	Gel Permeation Chromatography
h	Hour
HPLC	High Performance Liquid Chromatography
Hz	Hertz
Im	Imidazole
IR	Infra-Red

J	Coupling Constant
m	Multiplet
MALDI	Matrix-Assisted Laser Desorption/Ionization
Me	Methyl
MHz	Megahertz
min	Minute
mL	Milliliter
mmol	Millimole
Mn	Number Average Molecular Weight
MS	Molecular Sieves
MS	Mass Spectroscopy
Mw	Weight Average Molecular Weight
MW	Molecular Weight
N.D.	Nothing Detected
NAG	<i>N</i> -Acetyl Glucosamine
NAM	<i>N</i> -Acetyl Muramic Acid
NMR	Nuclear Magnetic Resonance
PDI	Polydispersity Index
PGN	Peptidoglycan
PGRP	Peptidoglycan Recognition Protein
Ph	Phenyl
Phth	Phthaloyl
ppm	Parts Per Million
q	Quartet
rt	Room Temperature
s	Singlet
SN2	Substitution Nucleophilic Bi-Molecular
T	Temperature
t	Triplet
TA	Teichoic Acid
TBAF	Tetra- <i>N</i> -Butylammonium Fluoride
TBDMS	Tert-Butyldimethylsilyl

TBDPS	Tert-Butyldiphenylsilyl
TCA	Trichloroacetyl
TCP	Trichlorophthalimide
TEA	Triethylamine
TFA	Trifluoroacetic Acid
THF	Tetrahydrofuran
TLC	Thin Layer Chromatography
TMC	<i>N,N,N</i> -Trimethyl Chitosan
TMHTMAPC	<i>N,N,N</i> -Trimethyl <i>O</i> -(2-Hydroxy-3-Trimethylammonium Propyl)
TMS	Trimethylsilyl
TPS	Triphenylsilyl
Tr	Trityl
Troc	Trichloroethoxycarbonyl
Ts	Tosyl
UV	Ultraviolet
$\delta$	Chemical Shift

<b>1</b>	<b>INTRODUCTION</b>	<b>1</b>
<b>1.1</b>	<b>BACTERIAL INFECTIONS</b>	<b>1</b>
<b>1.2</b>	<b><i>DROSOPHILA MELANOGASTER</i> INNATE IMMUNE RESPONSE</b>	<b>1</b>
<b>1.3</b>	<b>BACTERIAL CELL-WALL</b>	<b>3</b>
1.3.1	SYNTHETIC APPROACHES TO PGN	5
<b>1.4</b>	<b>CHITIN AND CHITOSAN</b>	<b>9</b>
1.4.1	CHEMICAL MODIFICATION OF CHITIN AND CHITOSAN	10
1.4.1.1	N-modifications	11
1.4.1.2	O-modification	16
<b>2</b>	<b>RESULTS AND DISCUSSION</b>	<b>21</b>
<b>2.1</b>	<b>PRELIMINARY STUDIES</b>	<b>22</b>
2.1.1	CHITOSAN HYDROLYSIS	23
2.1.2	N-MODIFICATION OF THE OLIGOMERS PRODUCED	26
<b>2.2</b>	<b>POLYMERIC CHITOSAN CHEMICAL MODIFICATION</b>	<b>28</b>
2.2.1	O-6 SILYLATION ROUTE	29
2.2.2	MOLECULAR CLAMP ROUTE	34
<b>2.3</b>	<b>ENZYMATIC STUDIES OF THE FINAL PRODUCTS</b>	<b>39</b>
2.3.1	ENZYMATIC DIGESTION	39
2.3.2	MCHERRY-PGRP PULL-DOWN ASSAYS	43
2.3.3	MONOSACCHARIDE COMPOSITION ANALYSIS	46
<b>3</b>	<b>CONCLUSIONS AND FINAL REMARKS</b>	<b>49</b>
<b>4</b>	<b>EXPERIMENTAL PROCEDURE</b>	<b>51</b>
<b>4.1</b>	<b>GENERAL METHODS</b>	<b>51</b>
<b>4.2</b>	<b>GENERAL PROCEDURES FOR CHITOSAN MODIFICATION</b>	<b>52</b>
4.2.1	CHITOSAN HYDROLYSIS	52
4.2.1.1	General procedure for chemical hydrolysis	52
4.2.2	CHITOSAN N-PROTECTION	53
4.2.3	CHITOSAN O <sub>6</sub> -PROTECTION	54
4.2.3.1	Molecular Clamp route	54
4.2.3.2	Silylation route	62
4.2.4	MURAMIC ACID MOIETY INSERTION	66
4.2.5	N-ACETYLATION	66
<b>4.3</b>	<b>GENERAL PROCEDURES TO EVALUATE THE FINAL PRODUCT</b>	<b>66</b>
4.3.1	ENZYMATIC DIGESTION	66
4.3.1.1	HPLC-UV protocol	67
4.3.1.2	HPLC-MS protocol	67
4.3.2	MCHERRY-PGRP PULL-DOWN ASSAY	68
4.3.2.1	Electrophoresis	69
4.3.3	MONOSACCHARIDE COMPOSITION ANALYSIS	69
<b>5</b>	<b>BIBLIOGRAPHY</b>	<b>71</b>
<b>6</b>	<b>APPENDIX</b>	<b>79</b>



# 1 Introduction

## 1.1 Bacterial Infections

There is a huge biodiversity of bacteria, in fact bacteria are the most abundant of all organism with an approximate population of  $5 \times 10^{30}$  individuals. These bacteria have a large number of shapes and sizes and can be found everywhere even if in radioactive waste or at the Mariana Trench.<sup>1</sup>

Although the majority of bacteria are harmless, there are a few, called pathogenic bacteria that are responsible for the bacterial infections. In matter of fact the two most deadliest diseases caused by bacterial infections are tuberculosis, caused by the *Mycobacterium tuberculosis*, which kills almost two million people every year and pneumonia, caused by *Streptococcus pneumoniae*, Gram-positive, and *Pseudomonas aeruginosa*, Gram-negative bacteria, killing almost four million people every year.

The innate immune system is the first line of host defence against infection by pathogens. Infection by pathogenic microbes trigger several host-pathogen complex interactions that are mediated by pattern recognition receptors (PRR) that are highly conserved in evolution. Thus, during the early stages of infections, the innate immune responses play crucial roles in host defense and exert an intense influence on the resulting generation of adaptative immune responses. The understanding of the PRR that mediate the innate responses and their subsequent effect after receptor ligation will open room for the discovery and/or improvement of vaccines.<sup>2</sup>

In order to understand these immunologic responses, insects are the most usual model organism used in these investigations, since there are many mechanisms and pathways of their immune system that have been conserved during the species evolution. *Drosophila melanogaster*, or commonly fruit fly is one particular insect used in these kind of studies, since its genome was sequenced in the year of 2000, and *Drosophila melanogaster* has a high rate of reproduction, leading to the emergence of new generations in a short period of time.<sup>3</sup>

## 1.2 *Drosophila melanogaster* innate immune response

Although the *Drosophila melanogaster* genome sequence has been fully discovered its innate immune response to a bacterial infection is still under investigation..<sup>4</sup> Figure 1.1 shows the actually accepted model of innate immune response of *Drosophila melanogaster* the two pathways of innate immune response are highlighted, the Toll and Imd pathways, which are responsible for inducing an antimicrobial peptide production response.

*Drosophila* flies recognize the presence of peptidoglycan (PGN) with the help of specific PGN receptors: PGRPs (PGN recognition proteins). Depending on the composition of the injected PGN and the PGRP receptor involved, one of the two distinct signaling pathways is activated to produce antimicrobial peptides capable of killing the infected pathogen.

In *Drosophila*, the Toll pathway is required for resistance to Gram-positive bacteria, containing a lysine-type PGN, as well as fungi and yeast pathogens. The Toll receptor is activated when bacterial lysine-type PGN is recognized by PGRPs, specifically PGRP-SA and PGRP-SD, as well as Gram-negative binding proteins (GNBPs).<sup>5</sup> These proteolytic cascades,

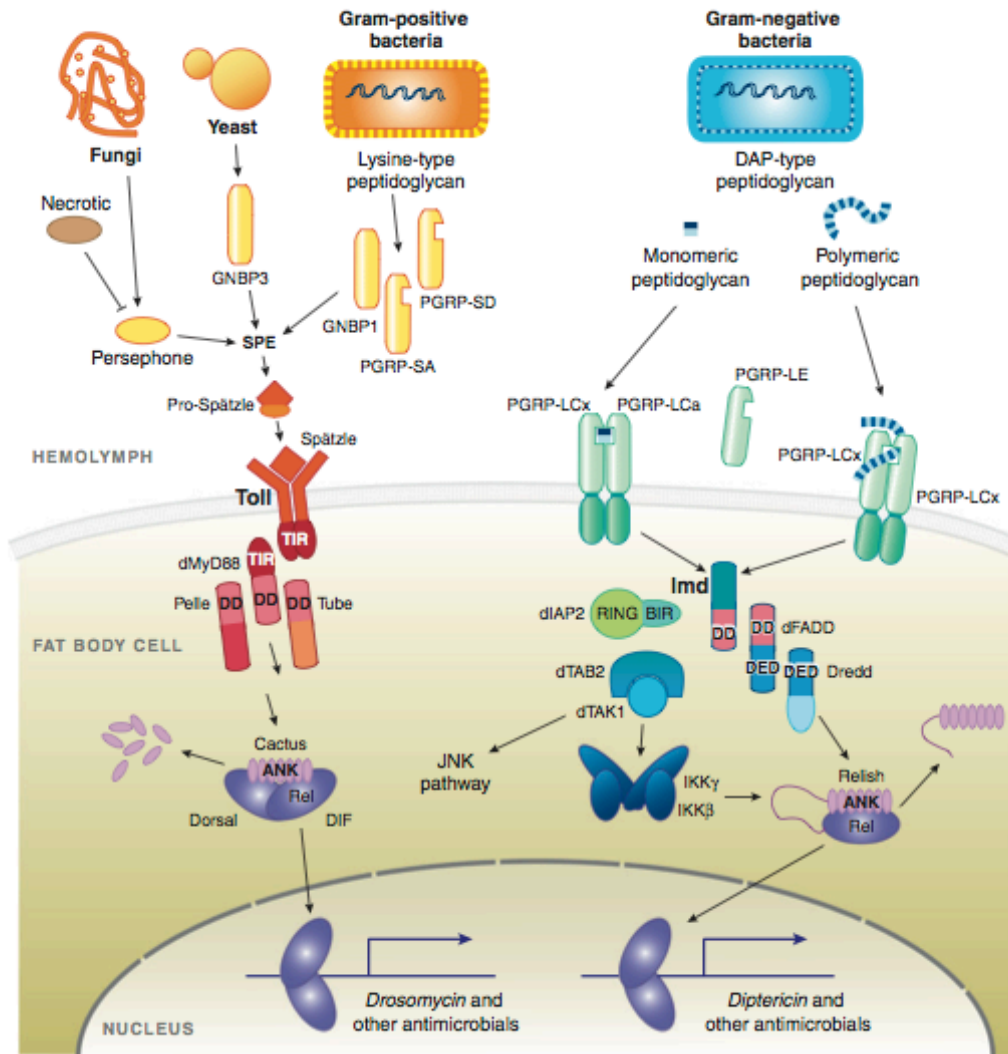


**Figure 1.1 *Drosophila melanogaster* model of Toll and Imd pathway activation, adapted from Lemaitre *et al* (5)**

which are not yet well characterized, lead to activation of Spätzle-processing enzyme (SPE) that leads to the Spätzle cleavage in the hemolymph. The processed Spätzle binds as a dimer to Toll leading to its dimerization in the plasma membrane leading to activation of three proteins MYD88, Tube and Pelle and recruiting to the Toll receptor in the cytoplasmic region. Subsequently, Cactus is phosphorylated and degraded by proteasome. Transcription factors Dif and Dorsal are released and moved through the nucleus and then activate the transcription genes that encode several antimicrobial peptides leading to the immune response.<sup>6</sup>

The Imd pathway is directly associated to activation by Gram-negative bacteria, possessing diaminopimelic acid-type PGN (DAP-PGN). The Imd pathway is activated by recognition of monomeric DAP-PGN by PGRP-LC/LE, then Imd interacts with dFADD which binds the apical caspase Dredd, enhancing the cell death activity and proteolytic processing the Dredd.<sup>7</sup> At the same time a cascade is activated leading to the phosphorylation of IKK signaling complex which also phosphorylate the Relish. This leads to its cleavage and the Rel domain translocate to the nucleus, where it activates the transcription genes that encode several antimicrobial peptides leading to the immune response.<sup>7-9</sup>

Despite all the studies developed to understand innate immune response and the recognition process between host and bacteria during bacterial infection, some questions remain unanswered. How host receptors can recognize high molecular weight fragments of PGN at the surface of bacteria remains unsolved. Until today it is not clear which are the structural requirements for PGN recognition by PGRPs.

### 1.3 Bacterial Cell-Wall

Bacteria can be divided in two major groups the Gram-positive, with lysine-type PGN, and the Gram-negative, possessing a DAP-PGN, as it is shown in Figure 1.2. Gram-

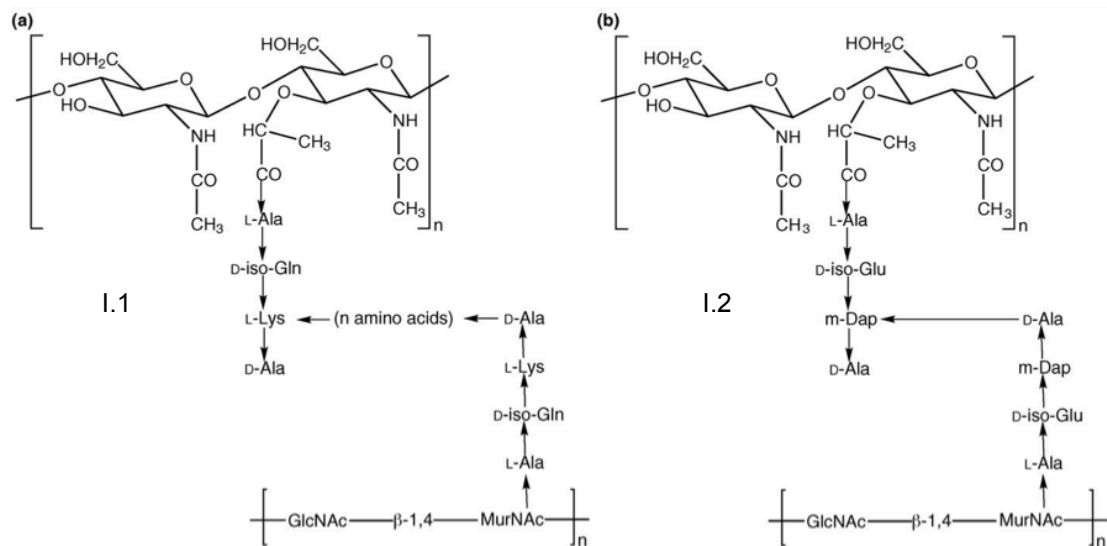


**Figure 1.2: Representation of PGN; (a) Gram-positive; (b) Gram-negative; adapted from Royet et al (71<sup>b</sup>)**

positive bacteria cell wall has in its composition, PGN also called murein, teichoic acids (TA) and a cytoplasmatic lipid membrane. Gram-negative bacteria cell wall has in its composition cytoplasmatic membrane, DAP-PGN, also an outer lipopolysaccharide membrane, porins and lipoproteins.

These different components in their cell wall provides different characteristics and properties to these two groups of bacteria, properties such as thickness and permeability of the cell-wall, leading to a higher permeability in the Gram-negative bacteria and higher thickness in the Gram-negative ones, Figure 1.3.

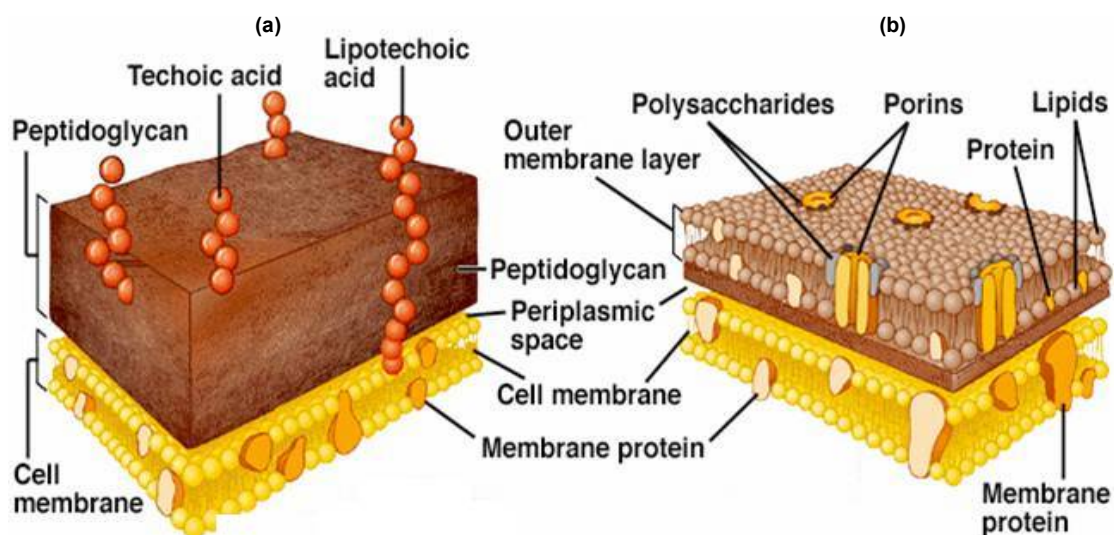


**Figure 1.3 Bacterial cell wall representation; (a) Gram-positive bacteria cell wall; (b) Gram-negative bacteria cell wall adapted from <http://medimoon.com/wp-content/uploads/2013/04/gramstructure.jpg>**

PGN is the major component of the bacteria cell wall, is normally composed by a disaccharide, monomer, of *N*-acetyl glucosamine (NAG) and *N*-acetyl muramic acid (NAM) and a tetra-peptide, L-Ala, D-iso-Gln, L-Lys, D-Ala, in the Gram-positive bacteria and L-Ala, D-iso-Glu, m-DAP, D-Ala, in the Gram-negative bacteria. However, several modifications in both the glycan structure, and the aminoacids in the cross-linking bridge and the peptide stem, have been reported leading to numerous new structures of PGN. These modifications can be as varied as a glycine in the first position, a *D*-iso-glutamate in the second position or a *D*-serine in the fifth position.<sup>10</sup> The most common modification of the glycan strands include *N*-deacetylation and *O*-acetylation at the NAM residue, these modification can occur with different ratios and degree of modification.<sup>11</sup>

It has been shown that PGRP-SA is capable of recognizing small PGN fragments, isolated and purified from the cell wall of two Gram-positive pathogens *Staphylococcus aureus* and *Streptococcus pneumoniae*.<sup>12</sup> The follow-up of this research line<sup>13</sup> has been hampered by limited availability of high-molecular weight PGN fragments in pure form from natural sources.

In order to overcome this limitation S. Filipe group has been creating and analyzing *S. aureus* and *S. pneumoniae* mutants that produce PGN with different levels of polymerization degree at their bacterial surface. The group has also been studying how these bacteria may hide PGN from external recognition.<sup>14</sup>

Thus, a critical limitation for further PGN investigation, is the limited availability of PGN in pure form from natural sources, and the need of ligand purification in reliable

amounts. Indeed, the extraction and purification process of PGN presents several difficulties, due to the presence of TA and proteins that can contaminate the PGN fragments.<sup>15 16, 17</sup>

### 1.3.1 Synthetic approaches to PGN

The vast majority of glycoconjugates possessing NAG residues are linked via a 1,2-*trans* linkage. Glycosylation of the 4-hydroxyl group of NAG derivatives is notoriously difficult, due to the well-known lack of reactivity of this hydroxyl group which is due to a combination of steric hindrance and to the involvement of the N-acetyl group in a hydrogen-bonded network.<sup>18</sup> The glycosylation of complex aglycones with glycosyl donors bearing a 2-

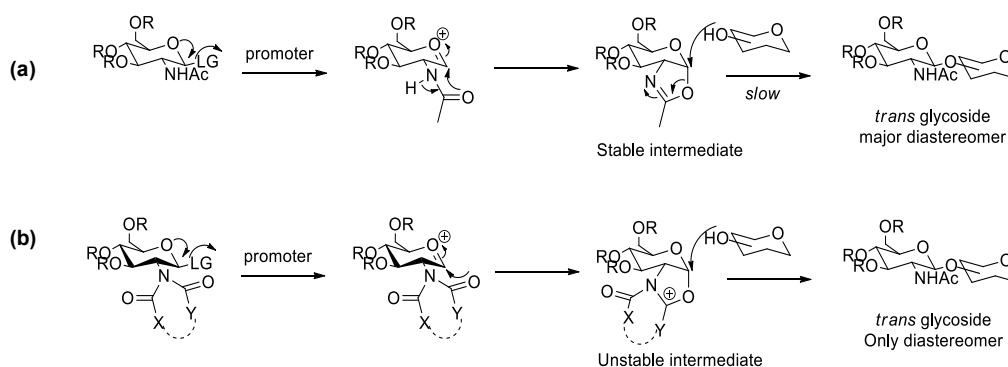


**Figure 1.5: Schematic representation of glycosylation reaction; (a) via NAG donor; (b) via N-disubstituted donors**

acetamido-2-deoxy functionality is usually unfeasible, due to the formation of a rather stable 1,2-*O,N*-oxazoline intermediate during glycosidation (Figure 1.5-A), which significantly decreases the rate of glycosylation and yields. One strategy to avoid the formation of this stable intermediate consists on the use of disubstituted donors (Figure 1.5-B), by blocking the amino group.

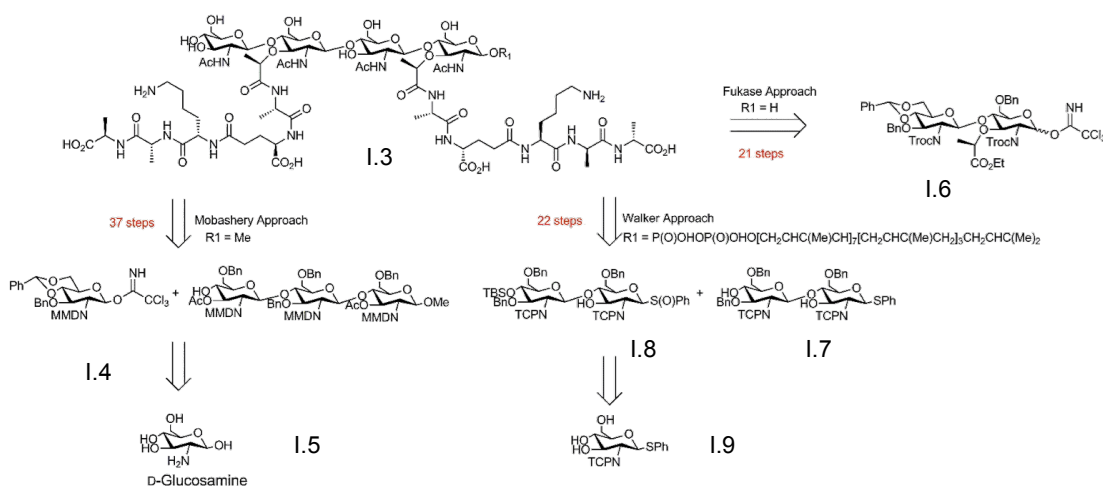


**Figure 1.4 Schematic NAG-NAM retro-synthesis approaches**

Due to the high biological significance of bacterial PGN, some ingenious synthetic approaches have been developed (Figure 1.4). Special efforts have been dedicated to efficient synthetic approaches of glucosamine oligosaccharides. Indeed excellent synthetic strategies for general PGN fragments have been reported.<sup>15-17</sup>

Due to the difficulty in using NAG units, mentioned above, and in order to control the regioselectivity and enantioselectivity of the glycosylation step, the majority of these synthetic sequences developed so far involve a huge number of steps, as in Mobasherv's approach, 37 steps, with many protection and deprotection steps.<sup>17</sup> Traditionally, as Fukase reported in the first synthesis of more than threesaccharide units, the amino group is protected with a temporarily protecting group (trichloroethoxycarbonyl – Troc, allyloxycarbonyl – alloc, trichloroacetyl – TCA and many others) which is replaced by acetyl group in a final stage of the synthesis, as it will be further explain.<sup>19</sup>

On the other hand, Walker approach, uses as amino protecting group, TCP – trichlorophthalimide, instead of Troc. These two strategies seemed similar, once it depends on a donor and acceptor synthesis and then combine those two units through a new glycosidic bond.

Moreover, despite the long multi-step sequences, these approaches involve many laborious work-ups/purifications/separations and costly reagents.

Preliminary results revealed that the PGN minimal structure required to activate the *Drosophila* Toll pathway is a dimeric mucopeptide, not yet synthesised, and that the free reducing end of the *N*-acetyl muramic acid residue is needed for activity.<sup>12</sup>

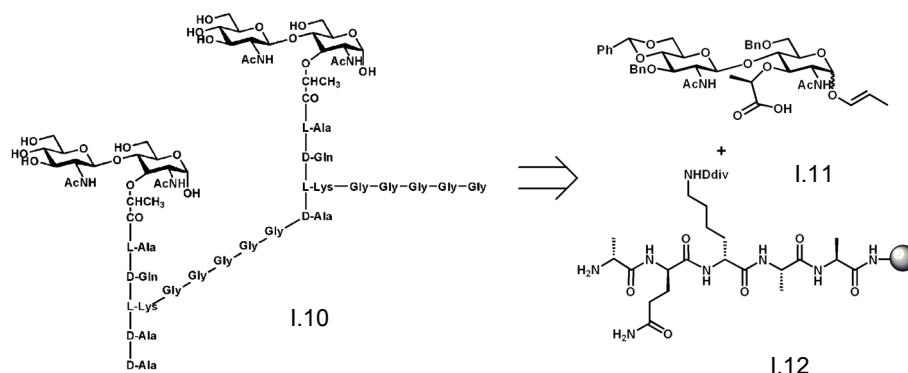


**Figure 1.6 Retrosynthetic view of a dimeric PGN**

Although some excellent strategies for general PGNs synthesis have been reported in the literature, one of the major difficulties associated with this particular PGN synthesis is the attachment of a disaccharide unit into a peptide chain linked to a solid support, and the cross-link peptide bridge assembly in such a macromolecule.

In a retrosynthetic overview, it can be divided in three fragments, a disaccharide NAG-NAM and two peptide chains, one that is directly bind to the NAM unit and the order that cross-link with other peptide chain as can be seen in Figure 1.6.

In our group, we have already synthesized a NAG-NAM disaccharide has already been synthesized with a pentapeptide attached D-Ala-L-Lys-D-Gln-L-Ala-L-Ala. The first

attempts were performed by preparing the NAG-NAM unit adapting the Fukase's approach where the key step consisted on a stereoselective  $\beta$ -(1,4) glycosylation. The peptide was synthesized through Fmoc SPS (solid phase synthesis) with a global yield of 70%.<sup>20</sup>

As we can see in Figure 1.7, we used a 3:1 ratio (disaccharide:peptide) were used in the first step with a common coupling protocol, then the Div group of lysine was removed

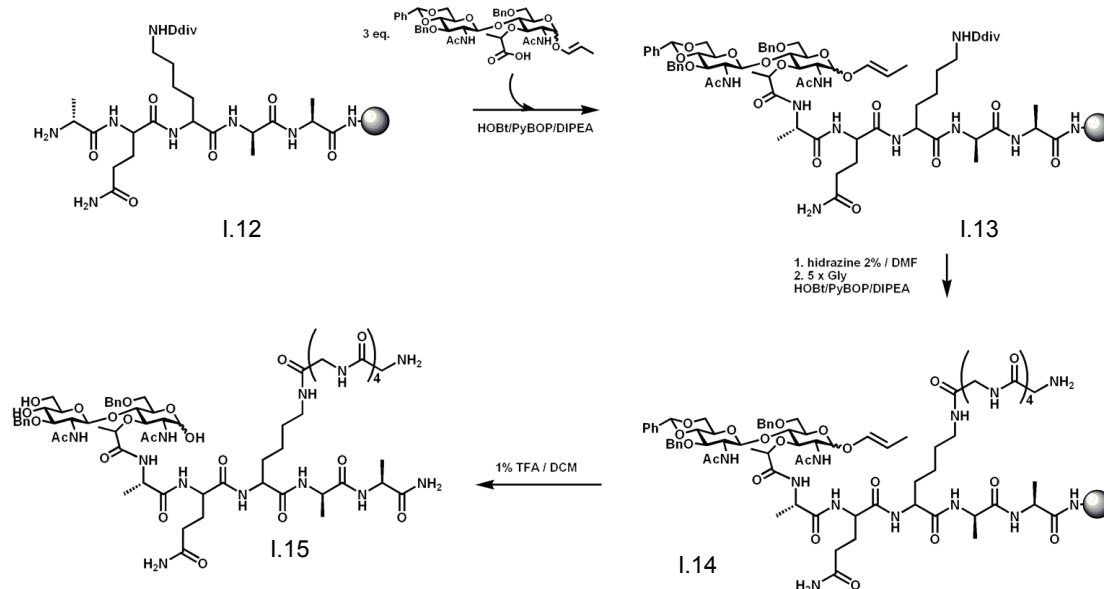
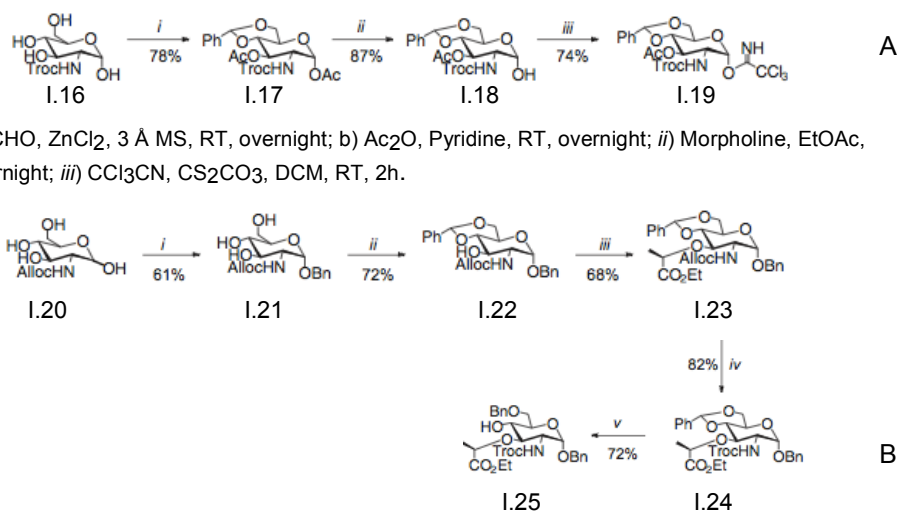


**Figure 1.7 Schematic NAG-NAM coupling to the peptide D-Ala-L-Lys-D-Gln-L-Ala, then coupled with five glycines and finally cleavage of the resin**

and then coupled with a five glycines group, with the same coupling protocol. The final step was the cleavage of the resin with 1% TFA/DCM, giving the glycopeptide with a yield of 3%. Additionally we have developed the solid-phase synthesis of a glycopeptide, and monitoring by high resolution magic angle spinning NMR.<sup>21</sup>

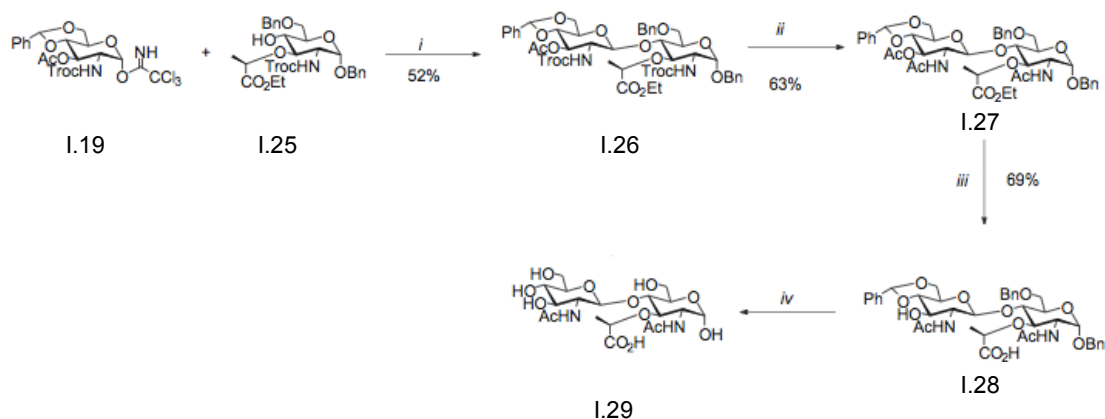
Recently the group have developed an efficient regioselective one-pot synthesis of



i) BnOH, AcCl, 80°C, 3h; ii) PhCHO, ZnCl<sub>2</sub>, overnight; iii) Ethyl L-(S)-2-trifluoromethanesulfonyloxypropionate, NaH, DCM, RT, 3h; iv) Pd(PPh<sub>3</sub>)<sub>4</sub>, AcOH, TrocCl, RT; v) BH<sub>3</sub>Me<sub>2</sub>N, BF<sub>3</sub>OEt<sub>2</sub>, RT, 3h.

**Figure 1.8: Synthesis of glucosamine Donor (A) and Acceptor (B)**

glucosamine building blocks<sup>22</sup> (Figure 1.8 and Figure 1.9). A properly *N*-protected glucosamine fully silylated at *O*-3, *O*-4 and *O*-6, was the key intermediate to achieve glucosamine building blocks, with a different substitution pattern, *via* a one-pot sequential procedure.



*i*) TMSOTf, DCM, 3A MS, -15 °C; *ii*) Zn-Cu, THF: AcOH: Ac<sub>2</sub>O (1:1:1), then Ac<sub>2</sub>O/pyridine; *iii*) LiOH, THF:1,4-dioxane:H<sub>2</sub>O; *iv*) Pd(OH)<sub>2</sub>, H<sub>2</sub>, AcOH, RT.

**Figure 1.9 Synthesis of disaccharide NAG-NAM**

A one-pot strategy seems to be the most attractive way to achieve NAG-NAM disaccharides in opposition to the several synthetic strategies developed for the synthesis of carbohydrates and especially for the construction of complex oligosaccharides,<sup>23</sup> Figure 1.9.

Such an approach allows the protection of the hydroxyl groups with suitable groups while avoiding multi-step sequences, difficult and challenging purification methods and it provides control for a regioselective glycosylation.<sup>19, 20, 22</sup>

Recently, the group has also reported the synthesis of a versatile intermediate towards NAM-NAG disaccharide, using a strategy that involves a multi-step approach with many purification steps.<sup>24</sup> Despite the novelty of the approach and the key intermediate formed, the overall yield of the NAM-NAG moiety was only 2% in 11 steps. Due to the lack of resources, lack of pure and homogenous PGN, and an extremely hard-core synthesis providing PGN fragments with extremely low yields, our goal consists on finding the right strategy towards PGN synthesis. The use of a renewable starting material, such as a natural polymer would open a completely new and sustainable route to achieve PGN fragments of controlled degree of polymerization and high purity.

Chitin is a polymer that shares the same basic carbohydrate backbone as that of PGN. The advantage of the abundance and structure of chitin, a biopolymer having immense potential for chemical modification and for structural possibilities.

## 1.4 Chitin and Chitosan

Chitin is the second most abundant polysaccharide after cellulose, can be obtained by extraction from crustaceans shells and can also be found in the cell wall of some fungi and algae. Chitin is constituted by  $\beta$ -1-4-*N*-acetylglucosamine (GlcNAc) and *D*-glucosamine (GlcN) units, Figure 1.10.<sup>24-26</sup> Chitosan is the copolymer, linear heteropolysaccharide, product of chitin's deacetylation reaction<sup>27</sup>, with a DA (degree of acetylation) <50%, while chitin has DA=100%. Being a natural biopolymer, chitin has properties as non-toxic, biocompatible,

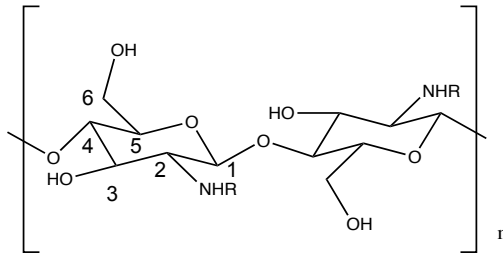


**Figure 1.10** Molecular skeleton of chitin (R=acetyl) and chitosan (R=H>50%)

biodegradable and has been explored in many distinct areas such, anti-bacterial agent<sup>28</sup>, fat-binding agent<sup>29</sup>, cell protection from carcinogenesis<sup>30</sup>, hypocholesterolemic agent<sup>31</sup>, antioxidant<sup>32</sup>, matrix for drug release<sup>33</sup> artificial skin<sup>34</sup> and wound dressing material<sup>35</sup>. Chitin has three different conformations  $\alpha$ -,  $\beta$ - and  $\gamma$ -chitin that depend on the animal source.<sup>36</sup>

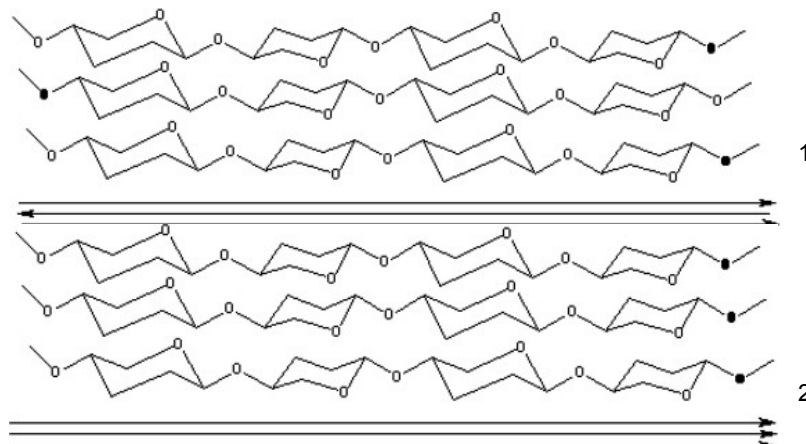


**Figure 1.11-** Antiparallel chain arrangement in  $\alpha$ -chitin.(1); parallel arrangement in  $\beta$ -chitin. adapted from Colocar aqui autores reference 33<sup>(e)</sup> (2) ou Colocar A e B

Due to its poor solubility many strategies have been developed in order to obtain derivatives by chemical modification, with the objective of maximize their properties in the application field but this problem still the major setback in the use of chitin and chitosan.<sup>37, 38</sup> Depending on the source and consequently the conformation of the chitin, different solubilities are associated.  $\alpha$ -Chitin has more intramolecular forces, hydrogen-bonds associated, than  $\beta$ -chitin that is more used due to this fact.<sup>38</sup> Chitin showed to be soluble in water but its DA must be in a range between 45-55%.<sup>39</sup> Several solvents have proved to dissolve chitin and chitosan, depending on its natural source has a different solubility, as shown in table 1.<sup>40</sup>

**Tabela 1-1: List of solvents and ionic liquids used to dissolve chitin and chitosan**

Chitin	Chitosan
<i>N,N</i> -dimethylacetamide, 5-10%(wt) LiCl,	Diluted acids (phosphoric, sulfuric, citric, sebacic, acetic)
<i>N,N</i> -dimethylacetamide, <i>N</i> -methyl-2-pyrrolidone, 5-8%(wt) LiCl	Dimethylsulfoxide
Methanol saturated with calcium chloride dihydrate	<i>p</i> -Toluene sulfonic acid
1-allyl-3-methylimidazolium bromide	10-Camphrosulfonic acid
1-butyl-3-methylimidazolium acetate	1-butyl-3-methylimidazolium chloride
1-butyl-3-methylimidazolium chloride	1-butyl-3-methylimidazolium acetate
hexafluoroacetone or hexofluoro-2-propanol	1-allyl-3-methylimidazolium acetate

In order to follow the degree of deacetylation or the depolymerization progress, and accomplish the characterization of the chitoligomers many technics have been used to provide this information, such as MALDI-TOF, <sup>1</sup>H-NMR and chromatographic techniques as GPC.<sup>41-43</sup> The degree of deacetylation can be calculated directly from the observation of the peak's intensity on the <sup>1</sup>H-NMR spectra as shown in equation 1.

$$D_{deac} (\%) = \left[ 1 - \left( \frac{\frac{1}{3}I_{CH_3}}{\frac{1}{6}I_{(H2-H6)}} \right) \right] \times 100 \quad (1)$$

While the applications of chitin and chitosan in a wide range of areas, have been reviewed by several authors, the regioselective and chemoselective modification of these polymers has been scarcely reported.<sup>26, 44</sup>

The low molecular weight chitosan has greater potential for application in many different areas, due to the higher solubility. In order to obtain low molecular weight chitosan, many strategies of hydrolysis have been explored. This depolymerization reaction can occur by chemical hydrolysis, by the use of a strong protic acid such as nitric acid<sup>45</sup>, diluted sulfuric acid<sup>46</sup> and hydrochloric acid<sup>43, 47, 48</sup>, which is the most common way of hydrolysis of chitosan, or via enzymatic hydrolysis.<sup>49</sup> Additionally the physical mechanism of depolymerization via the ultrasonic depolymerization<sup>42, 50</sup>, which is directly affected by the geometry of the glass-wear used, has also been reported<sup>42</sup>. Apart from that there are also alternative methods, such as  $\gamma$ -irradiation depolymerization<sup>29</sup> and depolymerization assisted by microwave<sup>51</sup>.

#### 1.4.1 Chemical modification of chitin and chitosan

Chitosan and chitin have distinct functional groups with different reactivities: O-6 - a primary hydroxyl group; O-3 - a secondary hydroxyl group; and the amine group (figure 1.6).

During the last few years, some developments on the chemoselective and regioselective modification of chitosan have been reported.

#### 1.4.1.1 N-modifications

The protection of the amine group in chitosan is fundamental in order to achieve different physical properties with consequently easier handling and to achieve different applications. Thus several methods were developed, such the phthaloylation, acylation or carboxyacylation and quaternization. These methods and the chemical methodology used will be discussed in the following sections.

##### 1.4.1.1.1 N-Phthaloylation

One method to prepare the *N*-phthaloyl chitosan consists on using aqueous acetic acid reaction media. Changes in the concentrations of aqueous AcOH to 10.0% maximum did not affect the regularity of the products, Figure 1.12. It should be emphasized that the irregular structure of the chitosan intermediate and acidic conditions caused by partial hydrolysis of phthalic anhydride allowed a homogeneous reaction in pure water. Since the *N*-

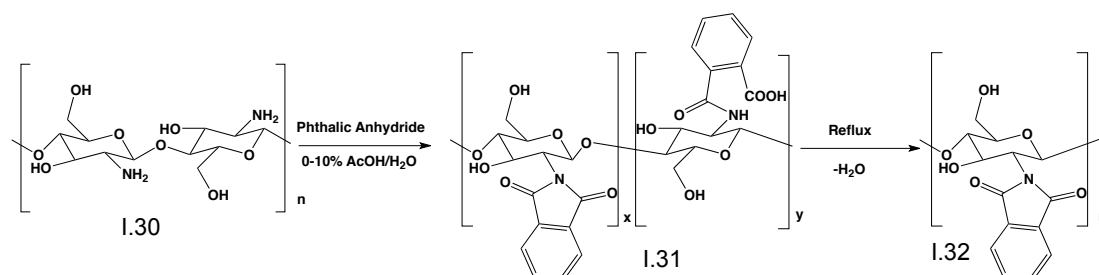
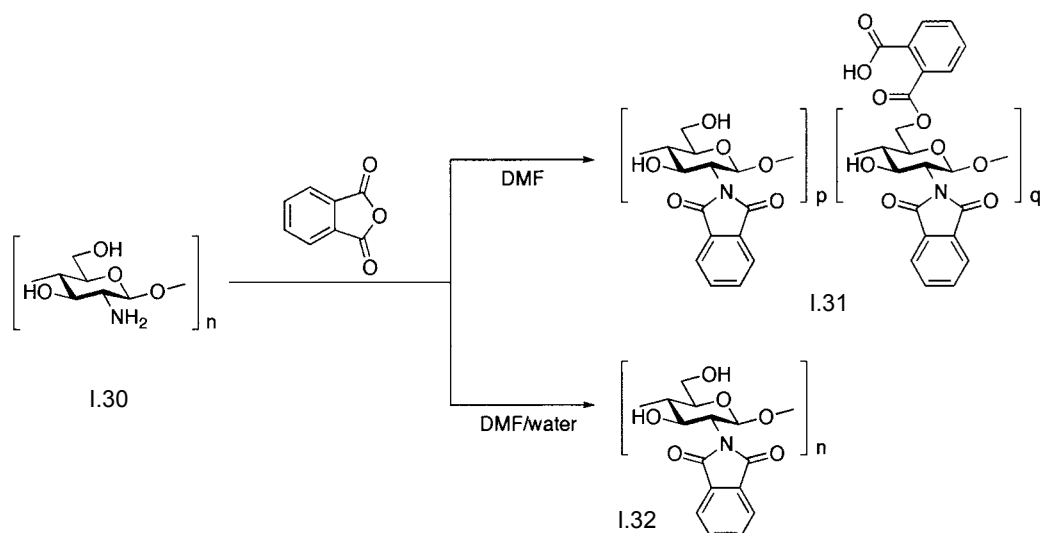


Figure 1.12 Scheme of amine moiety protection with phthalic anhydride

phthaloylation of chitosan is one of the most important reactions for the design of advanced materials, a reaction that requires no organic solvents will great contribute to the advancement of green chemistry.<sup>52</sup>



**Figure 1.13 Schematic water-influence in the solvent composition on the chitosan and phthalic anhydride, reaction product**

Other method consists on reacting fully deacetylated chitosan with phthalic anhydride in DMF with 5% of a co-solvent, such as ethanol, water, ethylene glycol and methyl cellosolve. Treatment of chitosan with phthalic anhydride, generally results in partial *O*-phthaloylation in addition to the *N*-phthaloylation. However in the present of 5% water, as co-solvent the partial *O*-6 phthaloylation are removed by hydrolysis, resulting in a 1.0 degree of *N*-substitution in chitosan, Figure 1.13.<sup>53</sup>

#### 1.4.1.1.2 *N*-carboxylacylation

*N*-carboxymethylchitosan is the most typical amphiprotic chitosan with amine and carboxylic acid groups in the molecule. It is a unique macromolecular structure that provides

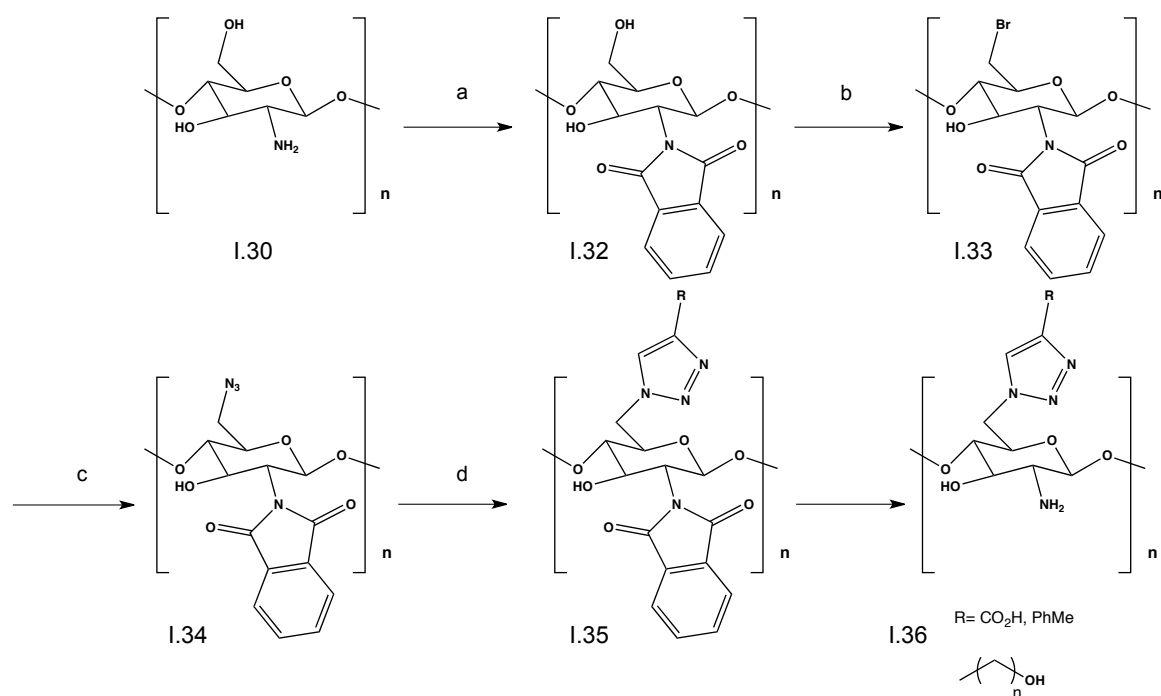


**Figure 1.14 Synthesis of a regioselective amphiprotic chitosan; (a)*N*-phthaloylation; (b) position 6 bromination; (c) position 6 azidation; (d) Husigen cycloaddition; (e) phtaloyl group removal**

specific properties and applications. However, preparing regioselective amphiprotic chitosan can be difficult by *N*- and *O*-carboxymethyl esterification using monochloroacetic acid. This derivative can be prepared *via* copper-catalyzed Huisgen cycloaddition, as it is shown further on Figure 1.14.<sup>54</sup>

*N*-carboxymethyl chitosan is obtained by using glyoxylic acid: the product is a glucan carrying pendant glycine groups. The solubility of chitosan in aqueous solutions of lithium and magnesium halides varies in the following order: LiCl < LiBr < LiI; MgCl<sub>2</sub> < MgBr<sub>2</sub> < MgI<sub>2</sub>. A method for selective production of mono-*N*-(2-carboxyethyl)chitosan (NCE-chitosan) was developed *via* synthesis in gel (concentration of chitosan 4–20%) of the magnesium halides solution (1.1–3.5 M) using acrylic acid. The use of MgI<sub>2</sub> or MgBr<sub>2</sub> in the reaction, provides relative greater amount of the monosubstituted amino groups (73–87%) in comparison with their absence. It is known that the bioactivity of carboxymethyl chitosan vary according to the ratio mono:-disubstitution- of the amino groups.<sup>55</sup>

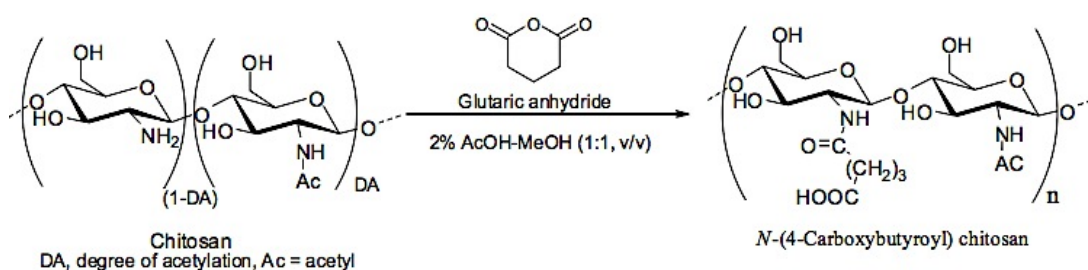


**Figure 1.15 Synthetic scheme of *N*-(4-carboxybutyryl) chitosan derivatives using different mol ratios of glutaric anhydride**

Water-soluble *N*-(4-carboxybutyryl), **Figure 1.15**, chitosan derivatives with different degrees of substitution (DS) were synthesized to study the antimicrobial activity of chitosan. Chitosan in a solution of 2% aqueous acetic acid–methanol was reacted with different amounts of glutaric anhydride to give *N*-(4-carboxybutyryl) chitosans at different DS. The chemical structures and DS were characterized NMR spectroscopy, which showed that acylation took place at the amine group. This synthesis gives a new chitosan derivative, soluble in water-, diluted acid or diluted base. The antimicrobial activity was investigated against the most economic plant pathogenic bacteria of *Agrobacterium tumefaciens* and *Erwinia carotovora* and fungi of *Botrytis cinerea*, *Pythium debaryanum* and *Rhizoctonia solani*. The antimicrobial activity of *N*-(4-carboxybutyryl) chitosans revealed to be more efficient than the native chitosan with the increase of the DS. A compound of DS 0.53 was the most active one with minimum inhibitory concentration (MIC) of 725 and 800 mg/L against *E. carotovora* and *A. tumefaciens*, respectively and also in mycelial growth inhibition against *B. cinerea* (EC<sub>50</sub> = 899 mg/L), *P. debaryanum* (EC<sub>50</sub> = 467 mg/L) and *R. solani* (EC<sub>50</sub> = 1413 mg/L).<sup>56</sup>

A different approach to carboxyalkylation of chitosan consist on gel state approach by using aza-Michael addition and substitution reactions. Various reagents were applied including acrylic and crotonic acids, and halocarboxylic acids. The reaction of chitosan with

halocarboxylic acids showed no target product formation, either in solution or in the gel state. In the case of acrylic, crotonic, halocarboxylic acids, the reaction performed in the gel state (concentration of chitosan 20–40%) showed higher degree of substitution at lower reaction time and temperature than in diluted solutions (concentration of chitosan 0.5–2%). This method provided higher yield of the product per reaction volume, lower reaction time and temperature, lower consumption of solvents and reagents, and no need for stirring of the reaction mixture. All of these factors make the gel technique advantageous for large-scale production and turn the synthesis of these compounds more environmental friendly.<sup>57</sup>

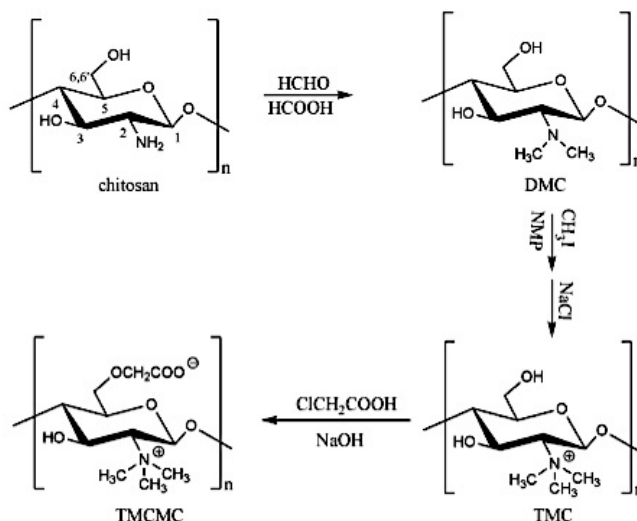


**Figure 1.16 Synthesis of *N,N,N*-trimethyl *O*-carboxymethyl chitosan**

*O*-Methyl free *N,N,N*-trimethyl chitosan (TMC) can be synthesized by treating chitosan with formic acid and formaldehyde, followed by methylation with  $\text{CH}_3\text{I}$ . Then TMC is carboxymethylated by monochloroacetic acid to obtain *N,N,N*-trimethyl-*O*-carboxymethyl chitosan (TMCMC), Figure 1.16. Their antibacterial activity was investigated against *Staphylococcus aureus* and *Escherichia coli*. It seems to be a decreasing of the antibacterial activity of TMC as the degree of substitution increased at pH 5.5, however the structure activity relationship was the opposite at pH 7.2. TMCMC seems to have less activity than TMC, and also its activity decreased as the degree of carboxymethylation increased. The experimental results showed that the antibacterial activity of *N,N,N*-trimethyl amino group was lower than other non-quaternized amino groups, and carboxymethylation did not enhance the antibacterial activity directly.<sup>58</sup>

#### 1.4.1.1.3 Quaternization

*N,N,N*-Trimethyl *O*-(2-hydroxy-3-trimethylammonium propyl) chitosans (TMHTMAPC) with different degrees of *O*-substitution can be prepared by reacting *O*-methyl-free *N,N,N*-trimethyl chitosan (TMC) with 3-chloro-2-hydroxy-propyl trimethyl ammonium chloride (CHPTMAC). The products were investigated for antibacterial activity against *Staphylococcus aureus* and *Escherichia coli* at pH 5.5 and pH 7.2 conditions. TMHTMAPC exhibited enhanced antibacterial activity compared with TMC, and the activity of TMHTMAPC

increased as well as the DS increased. The use of divalent cations showed to be related to the lost of antibacterial activity of *O*-carboxymethyl chitosan and *N,N,N*-trimethyl-*O*-carboxymethyl chitosan. However it did not occur with such intensity in the repression on the antibacterial activity of TMC and TMHTMAPC. This indicated that the free amino group on chitosan backbone is the main functional group interacting with divalent cations.<sup>59</sup>

The antioxidant properties of quaternized chitosan conjugated with gallic acid or caffeic acid were tested against hydroxyl-radical, superoxide-radical and DPPH-radical were evaluated *in vitro*, respectively. The scavenging activities of the obtained gallic acid-quaternized chitosan and caffeic acid-quaternized chitosan seemed to be a remarkable improvement over those of either chitosan or quaternized chitosan. Moreover, the scavenging effect indices of the products were all higher than 90% at a concentration of 1 mg/mL. Since gallic acid-quaternized chitosan and caffeic acid-quaternized chitosan are easily prepared and possess improved potential activities, these materials may represent an attractive new platform for another utilization of chitosan.<sup>60</sup>

### 1.4.1.2 O-modification

Various protecting groups have been used for the protection of chitin's and chitosan's hydroxyl groups, in an attempt to modify chitosan derivatives properties, such as solubility, and to enable N-selective modifications. The most commonly used hydroxyl protecting groups are: acetyl, tosyl, trityl and silyl groups, such as trimethylsilyl (TMS) or *tert*-butyldimethylsilyl (TBDMS), Figure 1.17.<sup>61, 62</sup>

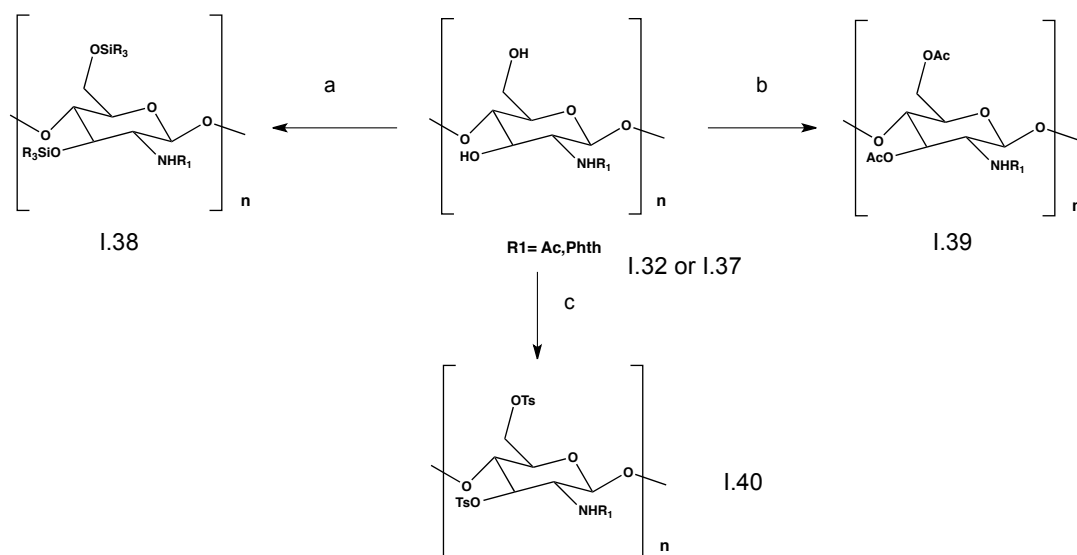


**Figure 1.17 O-3 and O-6 N-acetyl/phthaloyl chitosan simultaneous protection; (a) Silylation; (b) Acetylation; (c) Tosylation**

Usually O-modification at the O-6 position is commonly performed by the regioselective protection of the amine group with phthaloyl group.

The primary hydroxyl group in position 6 is very versatile, since is more reactive than the secondary hydroxyl in the position 3, enabling a wide variety of transformations. It can be regioselectively protected or transformed into different functionalities, such as a halide, an

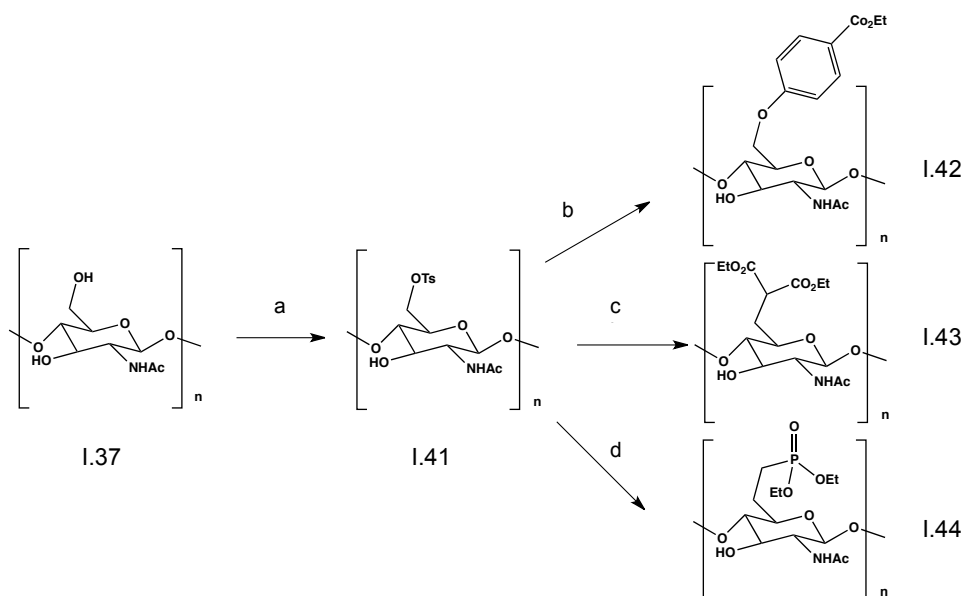


**Figure 1.18 Selective O-6 Tosylation then FGI; (b) O-6-ethyl benzoate chitin; (c) 6-deoxy-diethyl malonate chitin; (d) 6-(deoxydiethyl) phosphitechitin**

azide or an amine group.

Usually the O-6 position is selectively protected with bulky groups such as the triphenylmethyl group or the silyl groups, leaving the position O-3 capable of future modification. In these procedures the *N*-phthaloyl protected derivative is frequently used, increasing the solubility in organic solvents and thereby enabling the introduction of the proper group at the primary alcohol. At the end, the phthaloyl group can be easily cleaved by treatment with hydrazine.

The advantage of O-6-protected polymers, is the protection of the more reactive, primary hydroxyl, group leads to an increase of polymer solubility in organic solvents.

Trityl group is also placed in the polymer to increase the solubility in organic solvents. It is usually introduced reacting the *N*-protected chitin or chitosan with trityl chloride in pyridine.

Tosyl group is also very used as protecting group of O-6 position, since it has a good leaving character making tosylated polymer a very useful intermediate for further reactions at position O-6. Several nucleophiles such as sodium iodide, sodium borohydride, and potassium thioacetate<sup>63</sup> were used to substitute the tosyl group to yield iodo-, deoxy-, and acetylthio- chitin derivatives, respectively, Figure 1.18.

The preparation of tosylated derivative could be achieved by reaction of chitin with

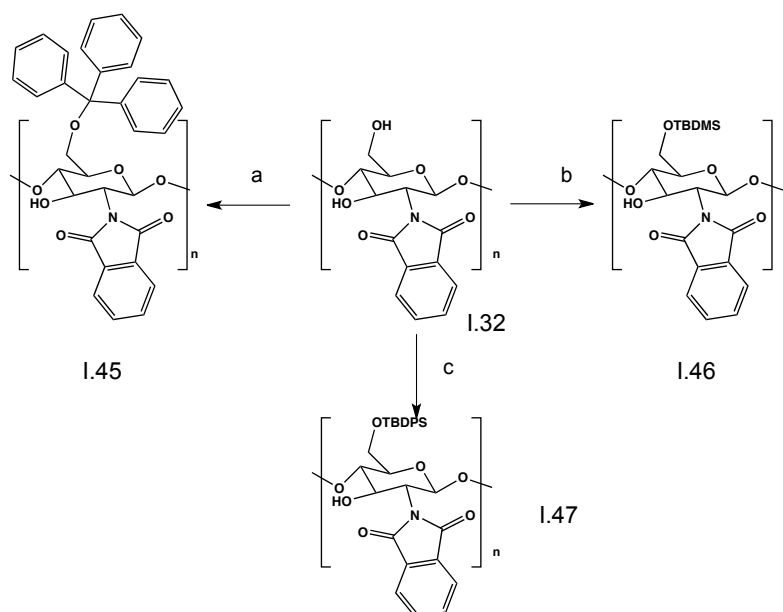


**Figure 1.19 O-6-*N*-phthaloyl chitosan selective protection; (a) Trytilation; (b) Silylation (TBDMS); (c) Silylation (TBDPS)** tosyl chloride (*p*-toluenesulfonyl chloride) in a DMAc/LiCl solvent system.<sup>63-65</sup>

Once functionalized, the resultant tosylated and fully *N*-acetylated chitin can react with the sodium salts of ethyl *p*-hydroxybenzoate, diethyl malonate, and diethyl phosphite, in DMAc, to afford the corresponding chitin derivatives of O-6-ethyl benzoate-chitin, 6-deoxy-diethyl malonate-chitin, and 6-(deoxydiethyl) phosphitechitin, respectively, Figure 1.19.<sup>64, 66</sup>

O-6 modification of N-protected chitosan is a strategy commonly employed to modify

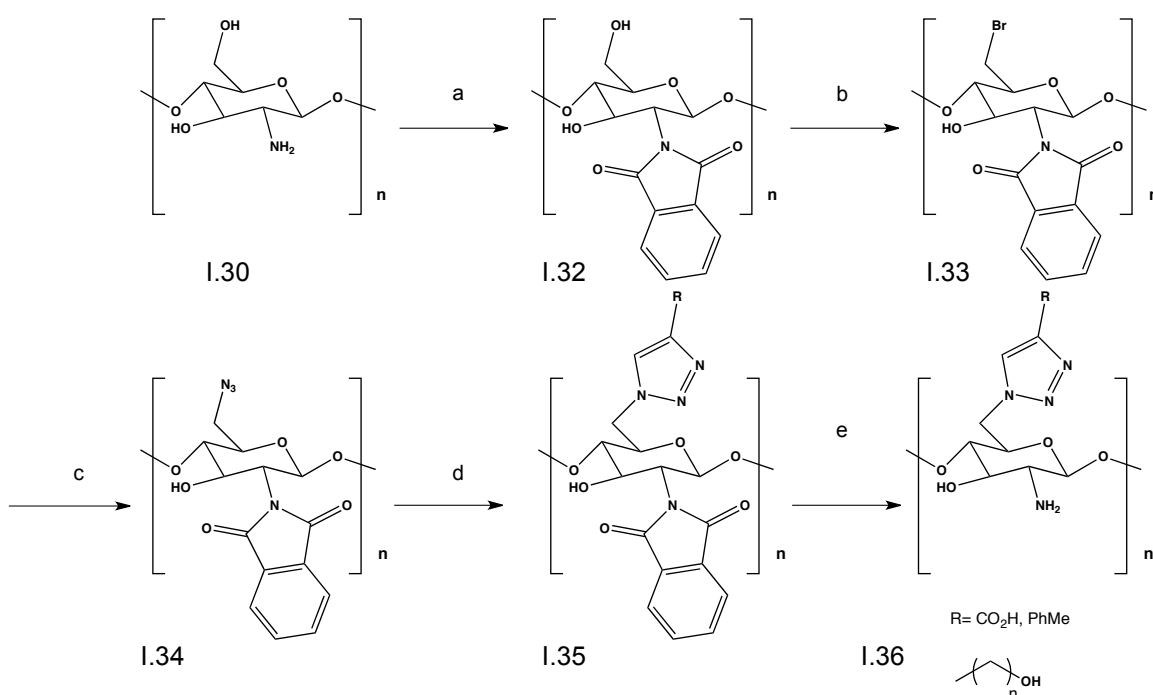


**Figure 1.20 Synthesis of a regioselective amphiprotic chitosan; (a) N-phthaloylation; (b) position 6 bromination; (c) position 6 azidation; (d) Huisgen cycloaddition; (e) phthaloyl group removal**

chitosan and create an amphiprotic polymer. These modifications offer several advantages, since the resulting polymer possesses tunable solubility and a nanosized structure which enable several applications such as drug delivery systems. Usually, this amphiprotic character can be achieved by placing a suitable group in position O-6 such as a carboxylic acid, which can make the polymer soluble under basic or acidic conditions. In neutral aqueous solution, a click chemistry approach has been developed, producing polymer nanoparticles, leading to the synthesis of a regioselective amphiprotic chitosan derivative.

The hydroxyl group can be converted to the brominated derivative that in turn is transformed in the azide derivative. The azide moiety at the C-6 position is then successfully converted to a 1,4-triazole linker with an appropriate R group, by a Huisgen cycloaddition between 6-azido-6-deoxy-N-phthaloyl-chitosan and an adequate propiolate in the presence of Cu(I) catalyst.<sup>54, 67</sup>

The same group also verified that the chitin type ( $\alpha$  or  $\beta$ ) has a high influence on some chemical modifications. After an exhaustive study of reaction conditions, the authors verified that functionalization of hydroxyl groups of squid  $\beta$ -chitin with trityl or benzyl groups

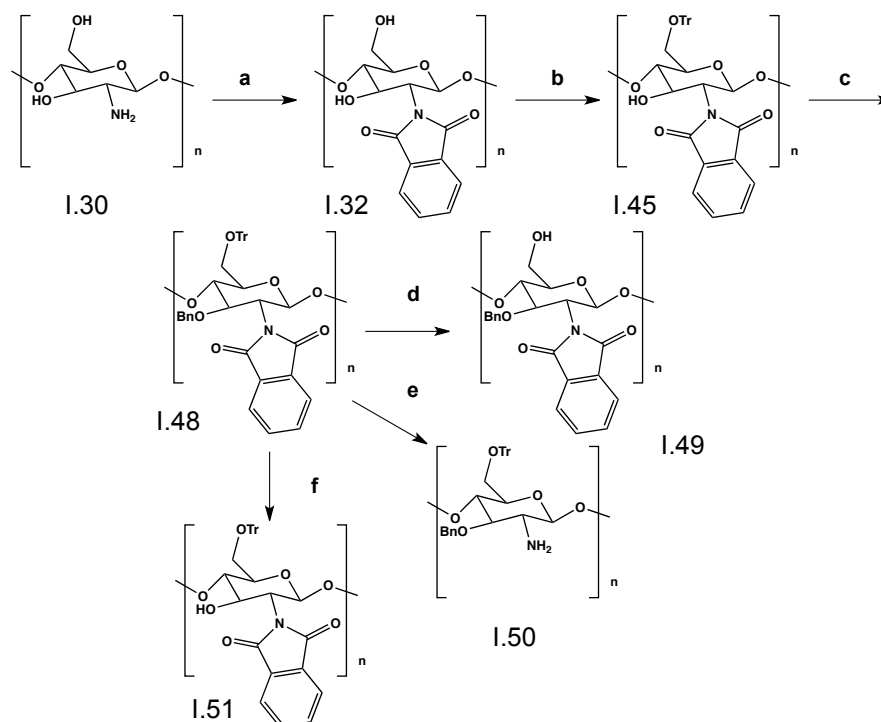


**Figure 1.21** Selective protection/deprotection of chitosan; (a) *N*-phthaloylation; (b) *O*-6 tritylation; (c) *O*-3 benzylation; (d) *O*-6 trityl group removal; (e) *N*-phthaloyl group removal; (f) *O*-3 benzyl group removal.

proceeded much more easily than those of shrimp  $\alpha$ -chitin. While in  $\alpha$ -chitin, the *O*-6-trityl derivative is prepared by reaction of trimethylsilylated chitin, the  $\beta$ -chitin was found to exhibit higher reactivity and direct tritylation of  $\beta$ -chitin was achieved in a quantitative way, Figure 1.21.

3,6-*O*-Dibenylation of  $\beta$ -chitin was also accomplished in simple one-step reaction, to afford the corresponding protected derivatives that exhibited good affinity for organic solvents.<sup>68</sup>

For the regioselective protection of chitin, Figure 1.21, the benzyl group was also explored as an efficient protecting group for *O*-3 position, in combination with other protective groups including triphenylmethyl (trityl) for *O*-6 and acetyl or phthaloyl for *N*-2. Chitin was first silylated to form 3,6-*O*-trimethylsilyl derivative that was further reacted with trityl chloride to afford 6-*O*-trityl-chitin. This derivative was benzylation to give 3-*O*-benzyl-6-*O*-trityl-chitin, in which the trityl, benzyl, and acetyl groups could be selectively removed to afford three different derivatives with a free reactive hydroxyl of amine group at *O*-6, *O*-3, or *N*-2, respectively.<sup>60</sup>

Azide moiety in position 6 can also be transformed in an amine group via formation of a triphenylphosphinimine intermediate that is hydrolyzed using aqueous hydrazine, which also led to the removal of the *N*-phthaloyl group. This sequence gave 6-amino-6-deoxy-chitosan, which, unlike chitosan, is soluble in water at neutral pH, Figure 1.22.<sup>69</sup>

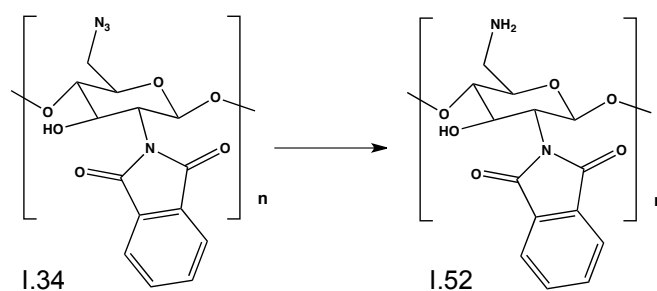


**Figure 1.22 Conversion of the azide moiety into amine group**

Conversion of the O-6 primary hydroxyls to carboxylate groups could be achieved using TEMPO/NaBr/NaClO oxidation systems making the water-insoluble  $\alpha$ -chitin become water-soluble.<sup>70</sup>

Chitosan is highly versatile biopolymer and can be easily converted in a wide range of functional groups, due to the possibility of chemoselective modification of its functional groups. Biological studies with PGN are limited by the difficulty in obtaining the pure, homogeneous and high molecular weight fragments of PGN. Adding these two facts we thought “*Is it possible to we convert chitosan into PGN’s sugar backbone?*” and it is in this context that the present work was developed. We aimed to contribute to a sustainable and efficient route that enables the conversion of available chitin/chitosan into valuable PGN fragments.

## 2 Results and Discussion

Since biological studies to investigate how the host receptors can recognize high molecular weight fragments of PGN at the surface of bacteria are limited by the amount and purity of natural PGN, we embraced the challenge of preparing pure and homogenous PGN fragments in order to overcome the major setback in this research field.

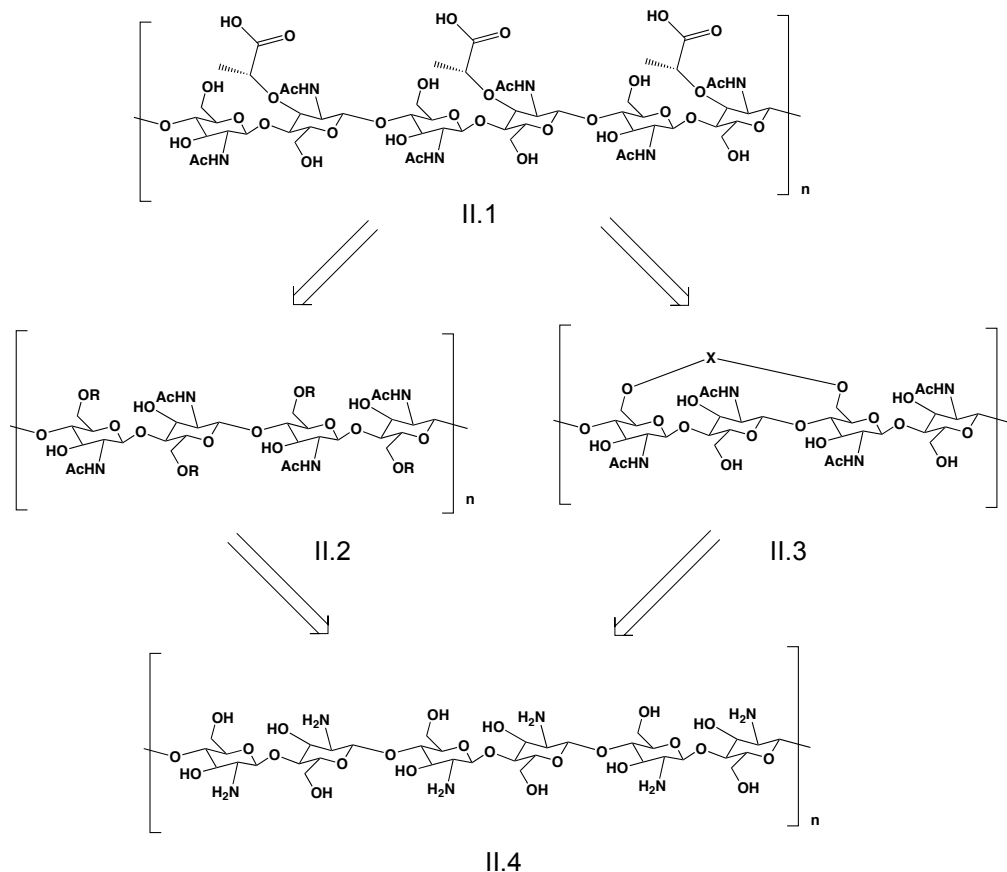


**Figure 2.1 PGN's sugar backbone retrosynthetic plan**

To achieve this goal, we envisaged that a biopolymer, that shares the same basic carbohydrate skeleton as PGN, could be used as starting material towards PGN. The aim consisted on combining chemical and enzymatic methods to modify the polymer in order to convert it into NAG-NAM units.

Chitin is a  $\beta$ -1,4-linked NAG biopolymer thus, to convert chitin into PGN, a lactyl unit must be introduced in alternating NAG units to which peptides may be connected. The main advantage of this proposal is the fact that chitin/chitosan already have the challenging  $\beta$ -1,4 glycosidic bond installed between NAG/glucosamine units and many orthogonal protection/deprotection strategies to achieve enantioselective glycosylation as well as the preparation of donors and acceptors will be avoided.

Chitin is very abundant in the biomass of shellfish discarded every year, is commercially available with different degrees of polymerization. However chitin's low solubility represents a limitation to the required chemical modification. On the other hand chitosan, the

alkaline derivative of chitin, has a better solubility profile and is amenable to chemical modifications.

In an initial stage of the project we aimed at preparing small chitooligomers and perform its structural elucidation. The idea was to establish a methodology for obtaining chitooligomers of controlled molecular weight for further chemical modification towards PGN.

In a second stage of the project the main aims were:

- To perform chitin/chitosan regioselective chemical modification;
- To establish a methodology to introduce the lactyl unit into alternating units of NAG in the modified chitin/chitosan;
- To digest NAM-NAG polymers by lysozyme-like enzymes to release homogenous NAM-NAG polymers;
- To characterize the fragments obtained using different spectroscopic and chromatographic techniques;

According to the retrosynthetic analysis depicted in figure XX, two different strategies were explored to introduce the lactyl moiety in alternating protected glucosamine units. After removal of the protecting groups, the NAG-NAM content was evaluated by using enzymatic assays through muramidases and lysozyme digestion. The amount of NAG-NAM units present in the final polymers, and thus the success of the approaches, was analyzed by HPLC-UV and HPLC-MS analyzes. Additionally PGRP affinity to the prepared samples was also evaluated by pull-down assays and by SDS-PAGE electrophoresis.

This work and the results obtained will be presented and discussed in the present chapter that is organized as follows:

- Preliminary studies;
- Polymeric chitosan chemical modification;
- Enzymatic studies of the final products

## **2.1 Preliminary studies**

To date, X-ray crystallography of PGRPs has been performed with a NAM unit attached to a penta or a tripeptide stem, performed to achieve the structure of human PGRPs.<sup>71</sup> Thus interaction studies of PGRPs with higher molecular fragments involving both NAM and NAG units have not been reported so far.

In this context, the first approach to produce NAM-NAG polymers from chitosan consisted on the preparation of small chitooligomers of controllable DP that could be isolated, characterized for further functionalization. The main idea was to develop a protocol in order to obtain oligomers of small molecular weight that could be further transformed with a control over the polymer size.

### 2.1.1 Chitosan hydrolysis

Several authors have already performed Chitosan hydrolysis, as mentioned in Section 1.4. Most of the reported procedures covering chemical and physical hydrolysis, have

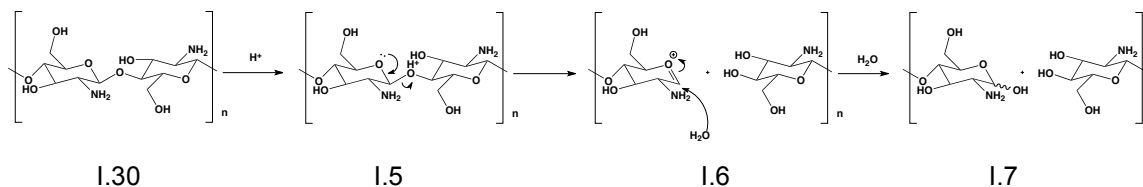


Figure 2.3 Mechanism of chitosan acid assisted hydrolysis

limited control over the DP of the fragments, involve harsh conditions, and/or are difficult to reproduce. For the current project a reproducible procedure with control over the DP would be desirable. Hence first experiments were carried aiming at exploring novel hydrolysis conditions as well as developing a protocol that allows control of the DP (solvent, reaction time, temperature, concentration) in order to obtain fragment of low molecular weight. Acidic medium was chosen for the hydrolysis experiments, and the mechanism of acid assisted

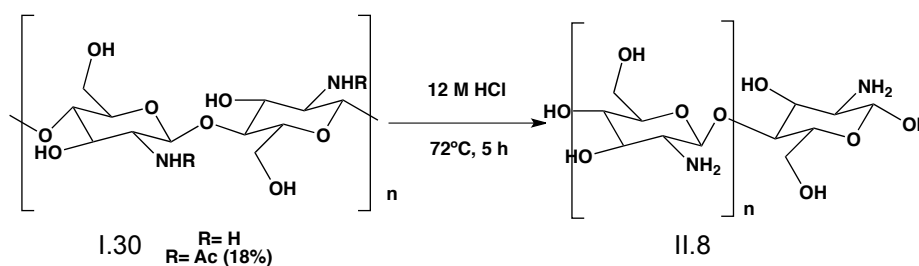


Figure 2.2 5 hours chemical chitosan hydrolysis

hydrolysis of chitosan is depicted in Figure 2.3. An investigation of several hydrolysis methods and conditions was performed, as summarized in Table 2-1.

Table 2-1 Summary of the hydrolysis' work

Concentração de quitosano	Tempo (h)	Condições	Isolamento	Resultados				
				DA (%)	DP	Mn (Da)	Mw (Da)	PDI
10 mg/mL (5% ácido acético)	6	Banho de ultrassons	Centrifugação a 5000 rpm e liofilização	Nada aconteceu				
	4	Sonda de ultrassons						
	6	Sonda de ultrassons						
40 mg/mL (HCl 1M)	6	Banho de ultrassons	Neutralização e evaporação do solvente	N. D.				
20 mg/mL (HCl 12M)	0.5 - 1	72°C						
20 mg/mL (HCl 12 M)	3							

20 mg/mL (HCl 12 M)	4	Evaporação do solvente e precipitação com acetona	2-16			
	5	Evaporação do solvente e diálise	11	2-15	674	860

<sup>a</sup> The acetylation degree was calculated based on equation 1; <sup>b</sup> the n, Mn, Mw and DPI (Mw/Mn) were calculated through MALDI-TOF analysis

First methods explored consisted on the use of a physical, ultrasonic assisted hydrolysis using an ultrasound bath over 6 hours, 10 mg/mL of chitosan in diluted acetic acid (5%) (table 2.1, entry 1). This method would represent a milder approach compared to the harsh conditions reported using concentrated solutions of HCl.<sup>43, 47, 48</sup> The results obtained demonstrated that this is not a good approach since the chitosan did not dissolve in the reaction media and little depolymerization was observed (table 2.1, entry 4). A literature procedure was then adopted,<sup>42</sup> in which an ultrasound probe was used, under the same previous conditions [10 mg/mL of chitosan in acetic acid (5%)]. Different reaction times were tested and after 4 hours, no depolymerization was observed. When the reaction time was extended to 6 hours, also no results were obtained (table 2.1, entry 2-3). Due to probe limitations, it was not possible to increase the acid concentration. Thus other conditions were next tested, using the ultrasound bath, and treating chitosan with a solution of 1 M HCl, 40 mg/mL of chitosan. The reactions were monitored by TLC and when HCl was used hydrolysis fragments were observed on the TLC plate corresponding to different chitooligomers obtained

(Figure 2.4).

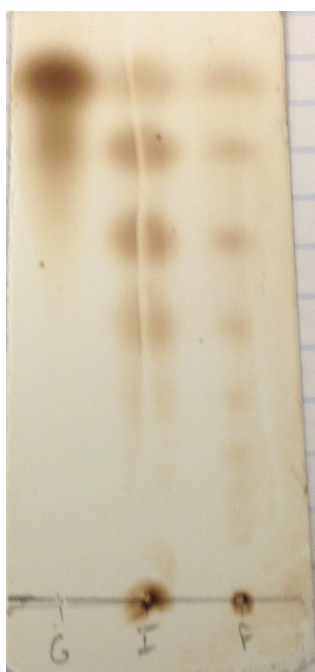


**Figure 2.4** TLC of 5 hours dialysis. (G) – I.5; (I) - inside of dialysis membrane; (F) - outside of dialysis membrane. Eluent 70% H<sub>2</sub>O 20% isopropanol 10% aqueous ammonia, revealed with 10% sulphuric acid in ethanol

Concerning the work-up/quench of the reaction, in the first experiments to the mixture was centrifuged and then the supernatant was lyophilized. It was expected that the soluble fractions of the oligomers would contain the oligomers of lower DP. However this was not observed at the TLC glimpse of hydrolysis. Next a new work-up procedure was employed.

Furthermore a new reaction condition was tested (Table 2.1, entry 8), consisting on the treatment of chitosan in a 2 % (w/v) concentration in HCl 12 M. The use of a strong acid would promote a more efficient hydrolysis improving the amount of chitooligomers produced. Once again the problem of work-up remained, and in order to avoid HCl evaporation, the acid was first neutralized with a solution of 10 M NaOH, which generated a huge amount of NaCl. This procedure hindered any sort of characterization. Next it was decided to proceed with the HCl evaporation as much as possible on a rotary evaporator, and use as less NaOH as possible to bring the pH value to 3. Next step consisted on the separation of the oligomers by dialysis. The pH value (3) was the minimum pH advisable to use with the dialysis

membranes. The dialysis process was performed to separate the hydrolysis product in two

fractions: outside the dialysis membrane oligomers with a maximum weight of 1500 Da; and inside the membrane oligomers  $\geq 1500$  Da.

The fractions obtained (outside and inside of the dialysis membrane), were then analyzed by MALDI-TOF (Figure 2.5), TLC (Figure 2.4) and GPC. It was concluded that the oligomers isolated from the reaction performed with 5 hours hydrolysis, II.8, as shown in 1, Figure 2.4 and Figure 2.5, a distribution of chitooligomers with a  $M_n=674$  and  $M_w=860$  which led us to conclude that these conditions were ideal to obtain small DP chitooligomers. By direct analysis of Figure 2.5, one can observe: consecutive  $m/z=161$  Da gaps that represent the glucosamine unit;  $m/z=524$  Da represent a  $DP_3+Na^+$  which was the ionization ion used in this experiment. In this acquisition window it is possible to identify chitooligomers from  $DP_3$  to  $DP_{12}$ . However in the data sheet of the entire MALDI-TOF experiment it is possible to identify chitooligomers from  $DP_2$  to  $DP_{15}$ .

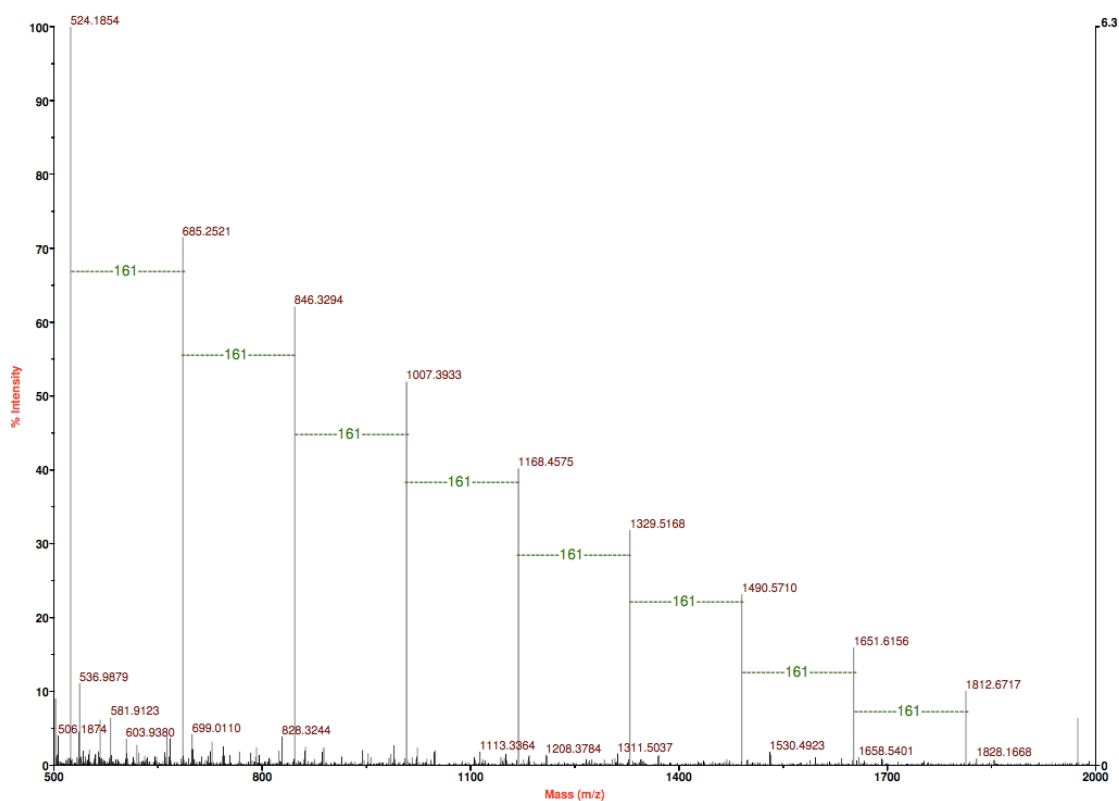


Figure 2.5 MALDI-TOF spectra from II.8

The GPC analysis was compromised by the lack of control samples to validate the results. The control samples consist of samples of small oligomers that are expensive but are currently being prepared in our lab. These controls will allow to perform the GPC analysis and establish the molecular weight of the oligomers prepared and validate the MALDI-TOF experiments carried. Nevertheless, for some samples analyzed the GPC analysis is in accordance with the mass spectrometry data.

Concerning the hydrolysis yield, for the reaction carried with 5 hours, a two-time dialysis was performed (table 2.1, entry 8) and 1.85 g of oligomers were obtained outside of the dialysis membrane, leading to a yield of 92.5 %. As a preliminary result but we expected

to obtain a fraction of oligomers lightly higher on Mn and Mw, and also narrow the DP if possible.

The reaction was further tested with 3 and 4 hours of hydrolysis (table 2.1, entry 6, 7). The results obtained demonstrated a change in Mn and Mw as shown in table 2.1. The results obtained suggested that the DP range was not only dependent on the reaction time. It could be obtained by dialysis but it seems impossible.

### 2.1.2 N-modification of the oligomers produced

In order to separate the obtained mixture of oligomers of different DP into fractions of the same molecular weight, and further convert them in the sugar backbone of PGN, the next step consisted on the regioselective protection.

Several amine-protecting groups were then considered. The aim was to protect the amine with a group that not only protects the amine from reaction in an advanced stage of the synthesis but also prevents H bond donor activity of the amine moiety, increasing the solubility in organic solvents. Two protecting groups were chosen, phthalic anhydride and 1,2-di-phenyl maleic anhydride, in order to evaluate the influence of the steric hindrance of a N-

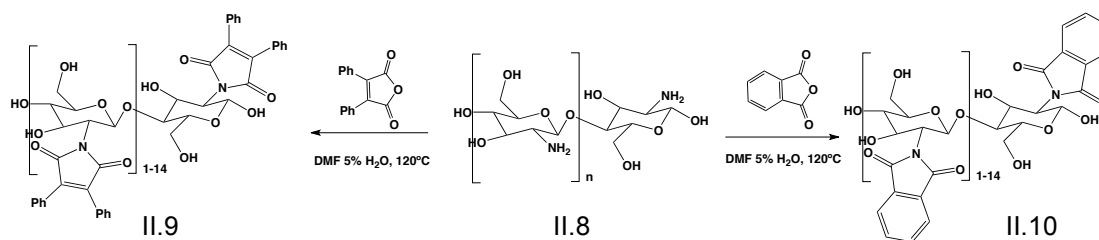
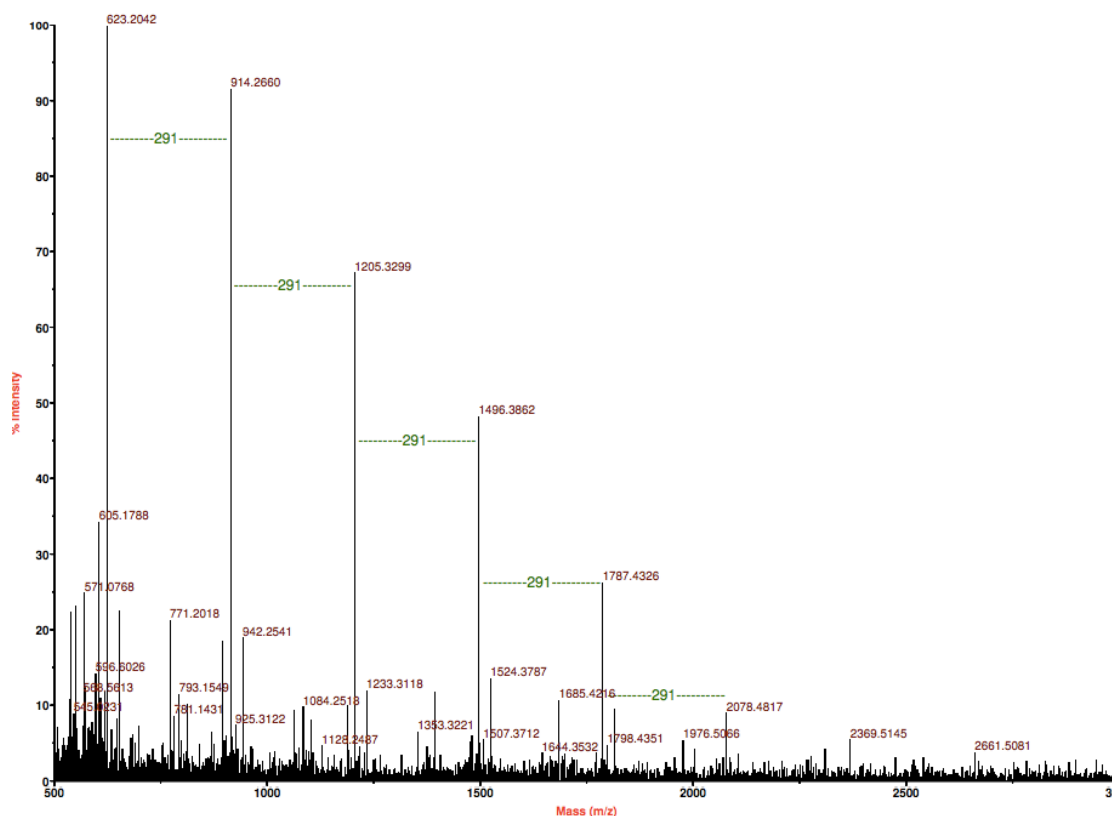


Figure 2.6 N-modification synthesis strategy

protecting group in the lactyl insertion in a later stage.

Most reported procedures for chitosan N-phthaloylation<sup>62</sup> are carried in DMF. Due to the problems of product isolation in DMF, dioxane and THF were considered as alternative solvents. However, this reaction requires high temperature and thus the solvent boiling point is crucial. Reactions were then carried with DMF containing 5% of water to prevent the O-6 protection.<sup>53</sup>

After isolation, precipitation with a mixture of ice water and methanol 1:1, the products were characterized by MALDI-TOF and NMR. The MALDI-TOF analysis, Figure 2.7,



**Figure 2.7 MALDI-TOF spectra from II.10**

confirmed the presence of oligomers with a DP5, however as the starting material had DP15 and during the work-up process no loss of higher molecular weight *N*-phthaloyl chitosan occurred. It could indicate that the MALDI-TOF protocol used for sample preparation was not the most appropriated to analyze this sample. Since MALDI-TOF analysis requires a volatile solvent to apply the sample onto the matrix, automatically excluding DMF, the sample was dissolved in water. As the oligomers of small DP ones were the most soluble in water, the higher DP oligomers might have been excluded from the analysis and that would justify the observed obtained chromatogram.

To proceed with the use of these oligomers, a proper characterization is required, as well as pure samples of small oligomers to be used as control in GPC analysis. These facts led us to focus on the modification of polymeric chitosan, using the know-how of working with oligomers as preliminary studies to the chemical modification of polymeric chitosan. Thus to proceed with the established aims of preparing NAG-NAM polymers, the next step consisted in the use of the commercial chitosan directly in the chemical modification.

The oligomers produced herein are currently being separated to obtain oligomers of defined DP.

## 2.2 Polymeric chitosan chemical modification

In our demand to convert chitosan into the PGN's sugar backbone, two distinct strategies were designed to block alternated O-3 position: an approach in which all the O-6 position are equally protected with the same group (the influence of the group steric hindrance was evaluated); and an approach in which a molecular clamp is used to create different accessibilities to O-3 (Figure 2.8). As the chitosan has the same basic scaffold as murein the challenge consisted on finding the right strategy to achieve discrimination between alternate O-3 positions to insert the lactyl group and achieve the muramic acid moiety. Acetylation of the amine moiety was performed in a later stage to recreate the NAG-NAM sequences.

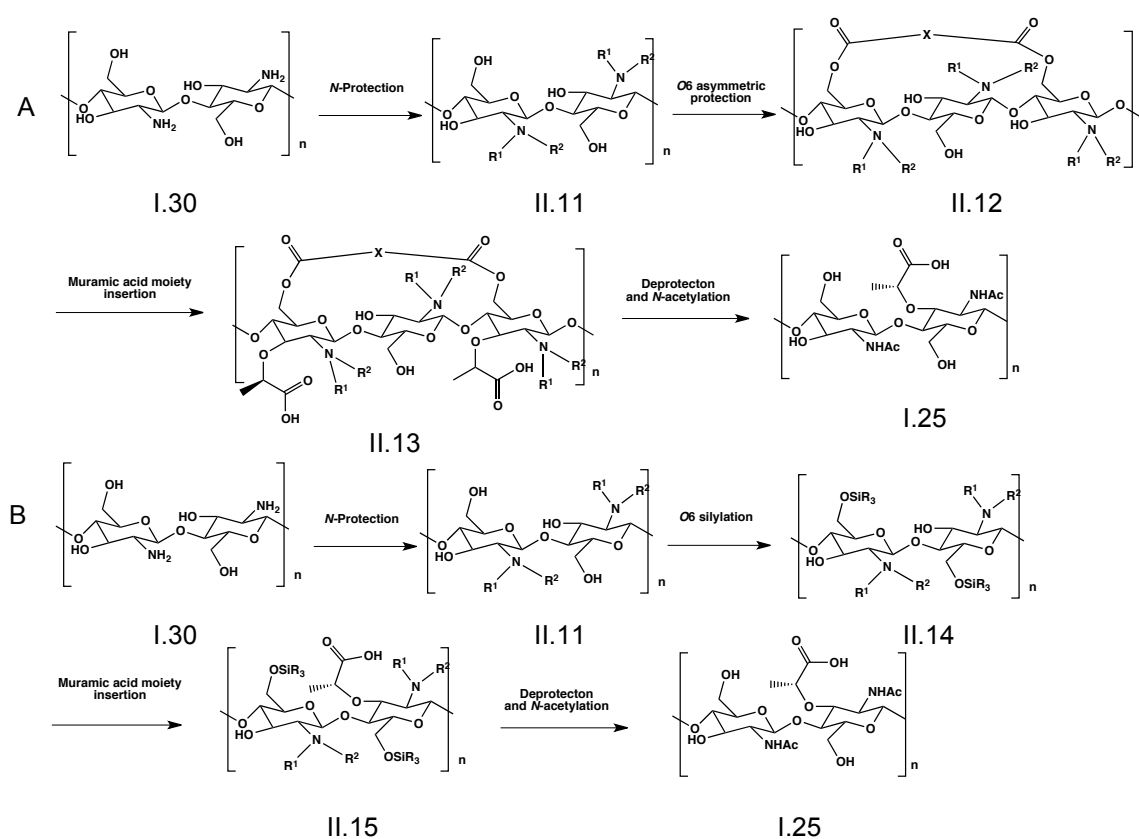
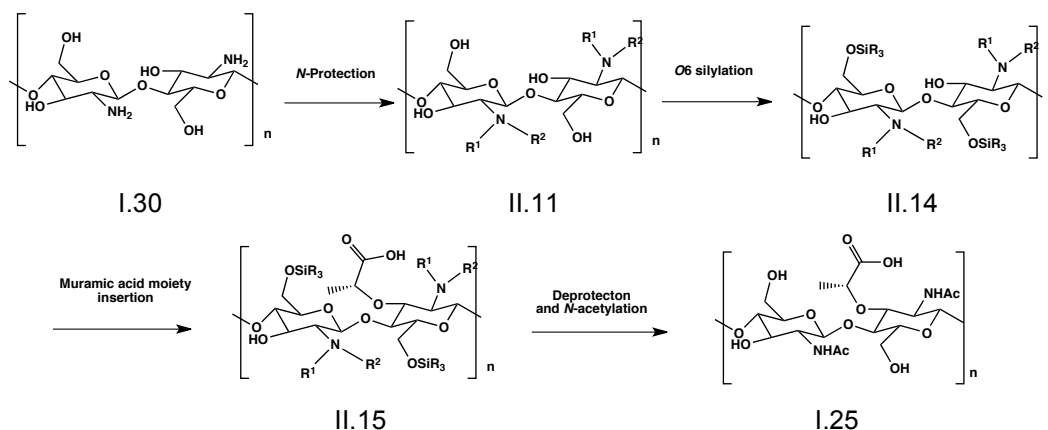


Figure 2.8 Synthesis plan of PGN sugar backbone or murein; (A) asymmetric protection route; (B) silylation route

### 2.2.1 O-6 Silylation route

To establish the best route for chitosan modification towards the murein main scaffold, the first and most direct route consisted on the exploration of a purely statistical insertion of lactyl moiety. With this tough in mind a silylation route was first considered, which basically consisted on the silylation of all the O-6 positions, after an amine moiety protection with a proper group, as shown in section 2.1.2.



**Figure 2.9 Generic strategy to the silylation route**

As Figure 2.9 shows the strategy relied on amine moiety protection, (two different groups were considered), followed by regioselective O-6 silylation, with distinct groups varying on their bulkiness. After O-6 protection the insertion of the lactyl moiety at O-3 position, was performed varying the equivalents of the corresponding reagent to evaluate the statistical distribution of that insertion, and finally a sequence of deprotection steps, starting with N-deprotection followed by N-acetylation and the O-6 silyl group removal.

Since the polymeric chitosan was used as starting material, the terminal O-4 hydroxyl group was despised, as well as the reducing end, once the polymeric chitosan has a DP about 1800. This commercial chitosan was ready available and was amenable to manipulate. However the characterization of the products obtained revealed even more difficult than the previous oligosaccharides obtained from the hydrolysis (preliminary results). So the samples obtained in this route were characterized based on IR and NMR CP/MAS. The first protection steps have already been reported in the literature for similar structures, so these procedures were adopted for the N-protection and O-6-silylation.<sup>62</sup>

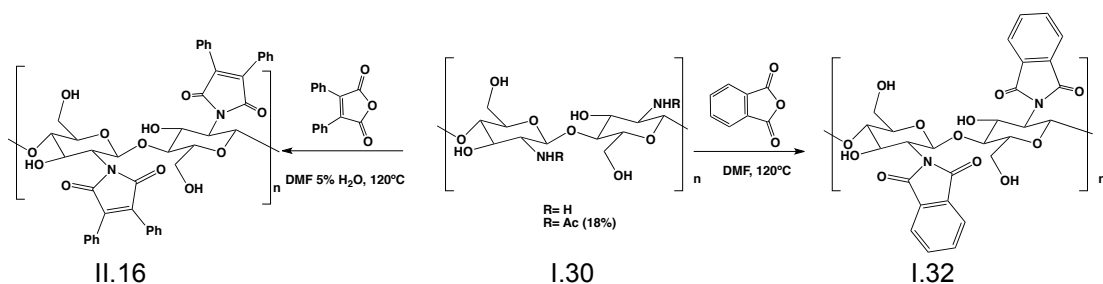


**Figure 2.11 Polymeric chitosan amine moiety protection**

As in the previous preparation of chitooligosaccharides, the first step of the strategy was the *N*-protection with phthalic anhydride and 1,2-di-phenyl maleic anhydride (Figure 2.11). The product isolation seems to be easier than the oligomers isolation, as expected, though a simple quench with ice water, generated a precipitate in a 72% and 80% yield, in the phthalic anhydride and 1,2-di-phenyl maleic anhydride respectively. Despite the high yields obtained, the protection with DPM anhydride, of II.16, decreased the solubility of the protected chitosan derivative in every solvent, even DMF or DMSO. Thus it was decided to continue the synthesis plan with I.32. In fact we planned to use II.16 in a later stage of the work, but due to time constrictions it was not possible to complete the plan with this substrate

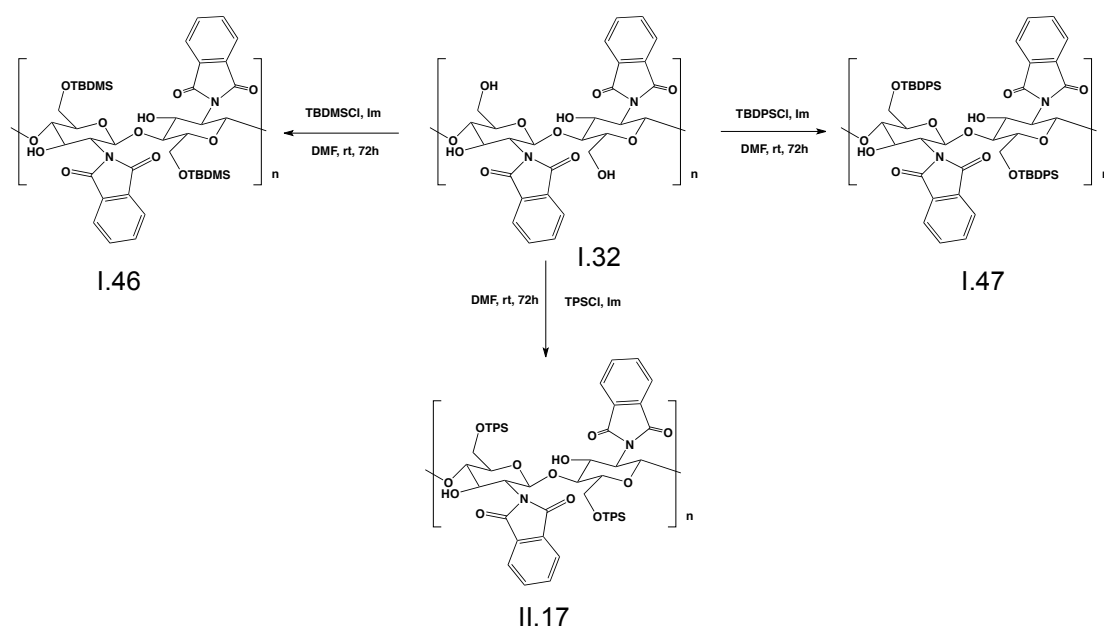


**Figure 2.10 Silylation of *N*-phthaloyl chitosan**

and understand the role of *N*-protecting group in the lactyl moiety insertion.

The second step of the synthesis consisted on the silylation of *O*-6 positions of the *N*-Phth derivative, and several silyl groups were tested, as shown in Figure 2.10. The aim was to understand if the bulkiness of the *O*-6 protecting group influences the lactyl moiety insertion and if it is possible to block some *O*-3 positions. In the literature it has been demonstrated that only the chitosan protection with TDBMSCl – was complete, DS = 1.0. Reported procedures for the chitosan protection with TBDPSCI mention DS of 0.82 but there

is no data for the protection with TPSCI. However, all 3 silyl groups were explored.<sup>62</sup> At this point the data indicated that the chitosan derivate obtained possessed the O-3 position free, and was ready for the lactyl moiety insertion. Until this point the products isolated were characterized mainly with IR spectroscopy and compared with the literature results<sup>62</sup> concluding that this synthesis was effective until this point. Then we proceeded to the next synthetic step, lactyl moiety insertion, as will be further discussed. For the lactyl moiety

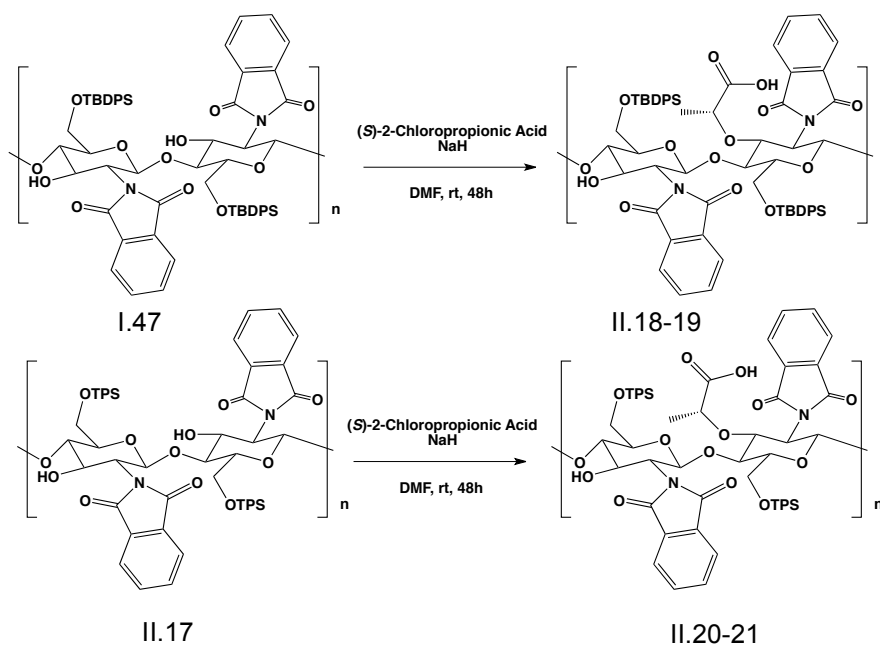


**Figure 2.12 Schematic representation of lactyl moiety insertion**

insertion the first attempt was performed with 0.5 equiv. of (*S*)-2-chloropropionic acid. This procedure has already been used in our group to introduce a lactyl moiety in glucosamine.<sup>20</sup> This first trial confirmed that with this strategy the lactyl moiety could be successfully introduced at the modified chitosan, which was confirmed by IR spectra analysis by the appearance of the carboxylic acid bands.

(*S*)-2-chloropropionic acid was used in 2 and 4 equiv. for each O-3 position in alternate units, which effectively represents 1 and 2 equiv. of all O-3 positions, but for further reference we will designate as 2 and 4 equiv. of (*S*)-2-chloropropionic acid.

The O-6-TBDMS derivative was in fact prepared, however in a preliminary stage it was decided to use groups with higher volume in order to prevent the lactyl moiety to be introduced in adjacent glucosamine units. So at this stage we focused only on the bulky protecting groups.

In this procedure, Figure 2.12, NaH was used to form the sodium salt of the starting material making it soluble in DMF and also making it more nucleophilic. Since we had no way of quantify how many O-3 positions react it was not possible, at this stage, to determine the DS and also if the insertion was alternated or not.

Due to the fact that the O-silylation reaction was not complete, according to literature,  $DS < 1.0$ , it suggested that some of the O-6 positions, which were not protected, could also react with (S)-2-chloropropionic acid. However, at this stage, there was no way of confirming alternate introduction of the lactyl moiety, which was evaluated later enzymatic studies.

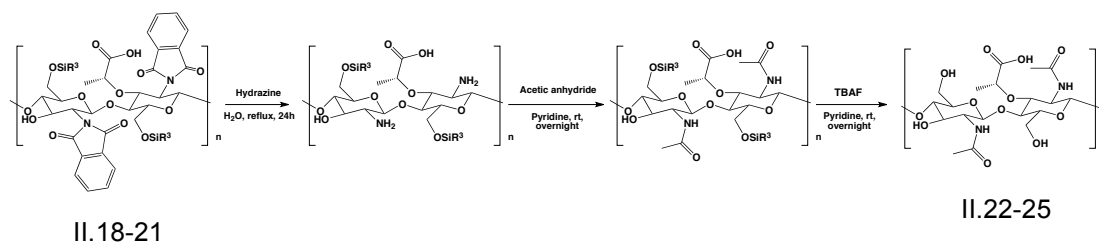


**Figure 2.13 Sequence of deprotection reactions and N-acetylation**

In the final stage of the silyl route to PGN's sugar backbone, a set of reactions were executed, Figure 2.13, starting by the phthaloyl group removal, leaving the amine group free to be selectively acetylated. Subsequently, silyl group removal was performed, by using TBAF in pyridine. Due to the little amount of product obtained, to the product was directly used in the enzymatic studies.

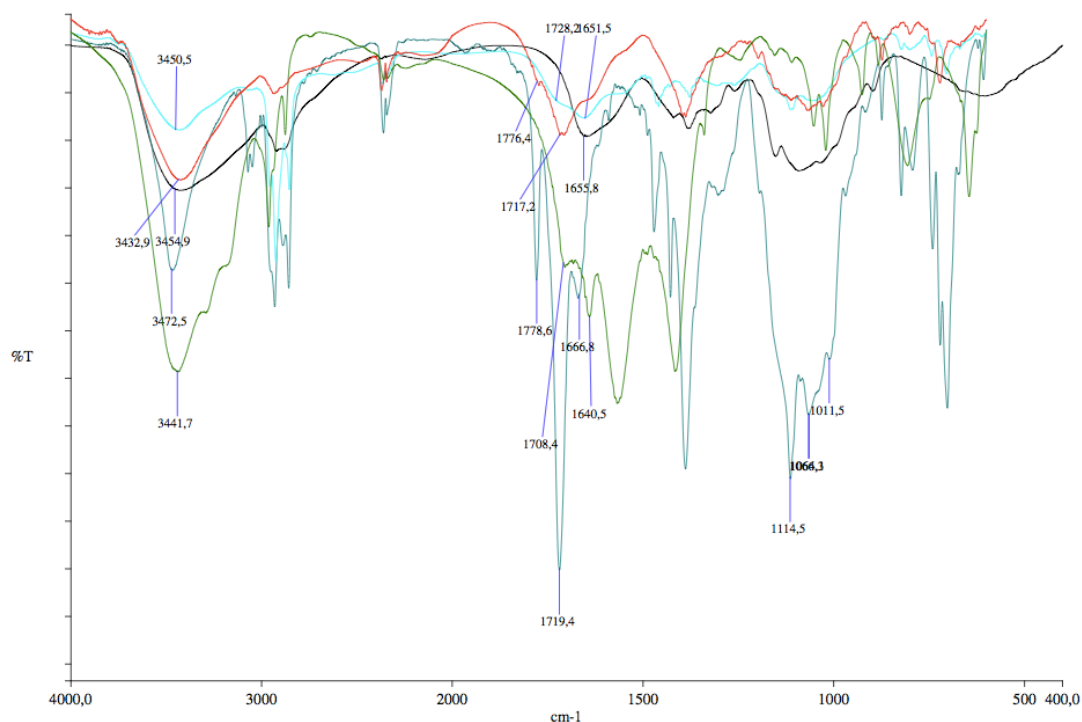


**Figure 2.14 IR spectra of polymeric chitosan modifications, black – (I.30); red – (I.32); dark green – (I.47); blue – (II.18); light green – (II.24)**

The IR showed to be a useful technique to analyze the silylated derivatives and monitor the reaction, once it was observed the decrease and shrinkage of the O-H band,  $3400\text{--}3450\text{ cm}^{-1}$ , and also the appearance of the O-Si band. Some bands overlap in the region of the pyranose band at  $1100\text{--}1000\text{ cm}^{-1}$ , Figure 2.14. In the final step we make sure that the lactyl moiety was successfully insert by the  $1668\text{ cm}^{-1}$  band, carboxylic acid band. Also in NMR CP/MAS spectra, Figure 2.15, it is noticed the change after O6-TBDPS

protection, once the aromatic region, 134 – 122 ppm, changes by the appearance of a signal at 127.9 ppm relative to the two phenyl groups of TBDPS, also at the aliphatic region 40 – 20 ppm, there is notice the appearance of a signal, 26,5 ppm relative to the terc-butyl group. After the lactyl moiety insertion step and the final steps of deprotection and acetylation, the final products were characterized by IR, unfortunately we still waiting for the NMR CP/MAS results.

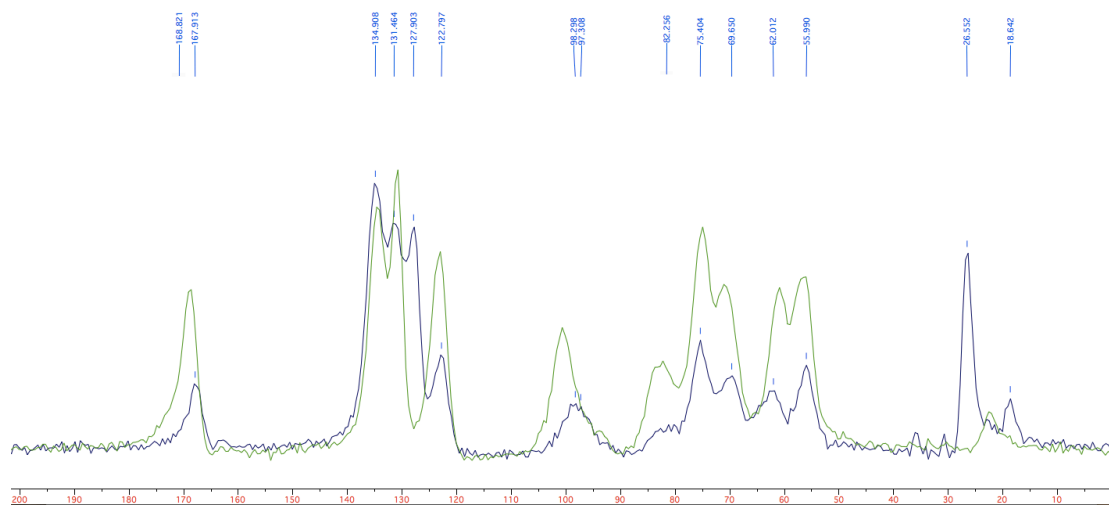
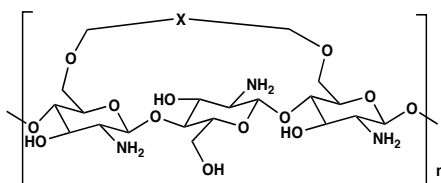


**Figure 2.15 NMR CP/MAS spectra green I.32; black I.47;**

### 2.2.2 Molecular clamp route

Since the objective was to obtain alternate NAG-NAM sequences, without depending as much as we can of statistical insertion of the muramic acid moiety, the structure of the



II.29

Figure 2.16 Linkage between two odd units

starting material was analysed - chitosan, to understand how could this problem could be overcome. Once the chitosan has a  $\beta$ -1,4 linkage, it means that every functional group position in the pyranose ring of an unit is the in the opposite position of the next unit, so in every odd unit the position of all functional groups are the same. With this idea we realized that if a linkage, such as a molecular clamp between two consecutive odd sugar units would create a blockage in the even unit placed between this two odd units, as shown in Figure 2.16. In this case an esterification between two O6 positions was considered. However the chain length needed to link those positions was still to be determined.

This strategy began with the design of a proper scaffold for the molecular clamp. A dicarboxylic acid was considered, in which the two O-6 positions could be linked. Suresh and

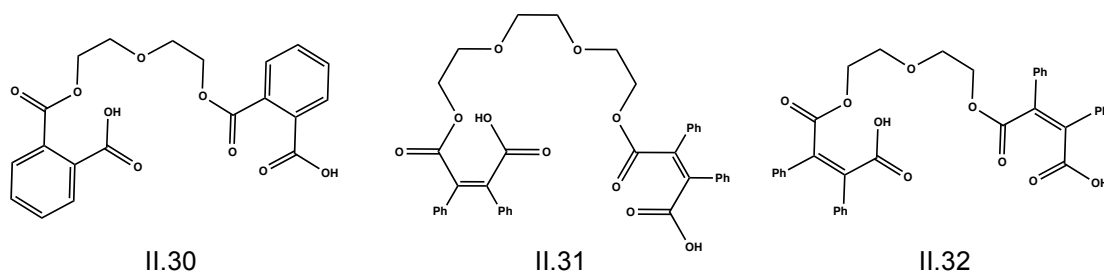
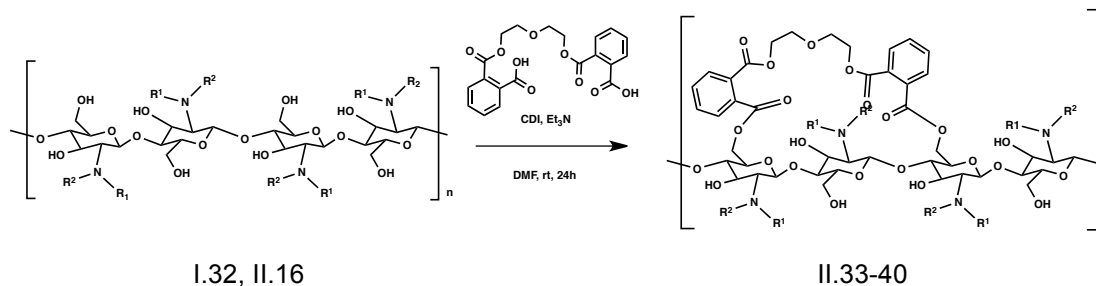


Figure 2.17 Dicarboxylic acids synthesized during this work

co-workers reported the synthesis of dicarboxylic acids starting with different anhydrides and different ethylenoglycol derivatives.<sup>72</sup> This work has inspired us to perform an estimation using Chem3D software in order to predict what should be the appropriate length of the ethylenoglycol chain in the molecular clamp. These studies suggested that a molecule with phthalic anhydride and diethylene glycol should be enough for link two odd units in the *N*-Phth chitosan. Nevertheless three different dicarboxylic acids were synthesized, as shown in Figure 2.17.

The purpose of its synthesis was to understand the role of the ethylenoglycol chain and also the role of the aromatic moiety.

The first step of this strategy or was the *N*-protection with phthalic anhydride and 1,2-diphenyl maleic anhydride, giving the products I.32 and II.16, respectively. In fact the major variation between silylation route and molecular clamp route, is the O-6 esterification between two sugar units.



**Figure 2.18 Example of a molecular clamp reaction scheme**

To establish the protocol of diesterification, a reported procedure was adapted.<sup>72, 73</sup> However, different conditions were tested, starting with different coupling reagents, DIC or DCC. Despite the use of a large excess of TEA, those coupling reagents were no efficient enough to perform the reaction. Then CDI was used instead and proved to be a suitable reagent for this transformation.

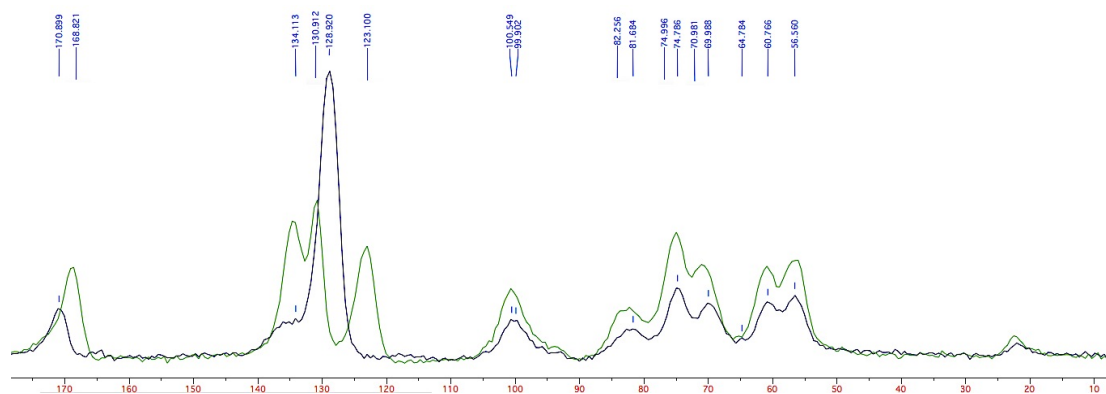


**Figure 2.19 NMR CP/MAS green I.32; black II.33**

NMR CP/MAS and IR spectroscopy confirmed the molecular clamp moiety insertion, once it is shown in NMR CP/MAS spectra the variation in the aromatic region, 134 – 120 ppm after the molecular clamp moiety was insert, 129 ppm, a new signal related to molecular clamp moiety, once he work-up seemed to remove all the remaining molecular clamp that we used and did not react, Figure 2.19. Once the already describe problems were overcome with the procedure it was important to establish the stoichiometry of the molecular clamp to be used in order to promote the link between, two alternate glucosamine units.

In a statistical approach to link every two alternate units the molecular clamp should be used for every four sugar units, leading to 25% (% mol) of molecular clamp of *N*-phthaloyl chitosan. So it was established to use two different amounts of molecular clamp understand the effect of the molecular clamp on the polymer structure. Thus 33% and 66% (% mol) of the

molecular clamp were tested. Since the product was only DMF soluble the reaction could not be followed by TLC, so the solvent was evaporated and then washed with ether to remove eventual molecular clamp residues. A yellow powder was obtained and characterized by NMR CP/MAS and IR.

At this point it was important to understand the influence of molecular clamp moiety on the chitosan structure and check if the clamp used was able to confine the even position or not. To understand that the insertion of the lactyl moiety was tested disregarding the remaining free O-6 positions.

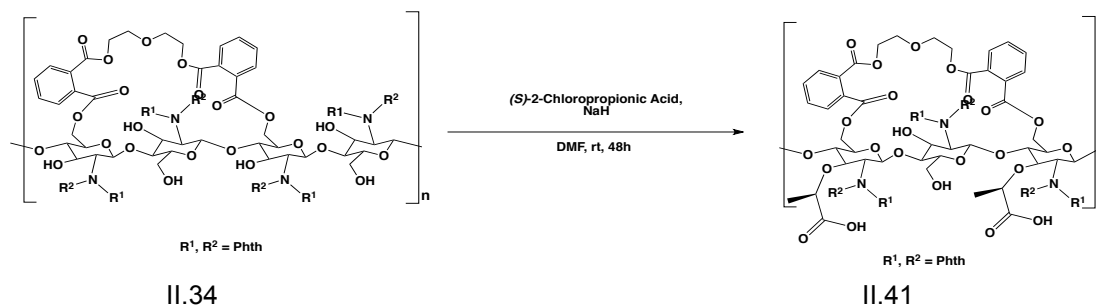


**Figure 2.20 Lactyl unit insertion in a chitosan derivative possessing some free O-6 positions**

The procedure used to lactyl moiety insertion was the same procedure used previously in the silylation route. Starting with *N*-phthaloyl chitosan (I.32) and treating with 66% of molecular clamp (II.30), compound II.34 was obtained. After isolation, DMF evaporation followed by ether washing, to remove the remaining molecular clamp residues, and characterization, by NMR CP/MAS and IR, this compound II.34 was treated with 2 equiv. of (*S*)-2-chloropropionic acid, leading to the formation of II.41, Figure 2.20. Due to the problem of characterization we could not guarantee the  $S_N2$  reaction occur in the O-3 position, or at the O-6 position that were not substituted.

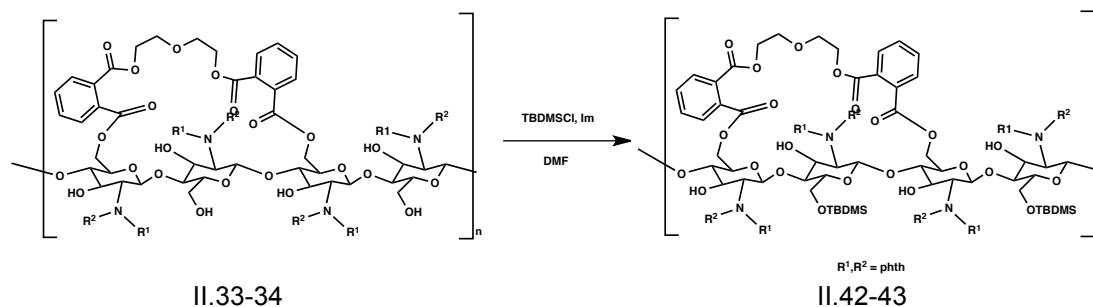


**Figure 2.21 Silylation of the remaining O6 free positions**

In order to guarantee that only the O-3 positions were available for the lactyl moiety insertion, and understand the effect of the molecular clamp on the *N*-phthaloyl chitosan structure and its influence on O-3 positions, the remaining free O-6 positions were protected, Figure 2.21. The choice of the protecting group relied on the fact that only O-6 positions would be protected. Thus, TMS was not used because it was reported the reaction on chitosan O-3 positions. To make sure that every remaining O-6 positions were substituted

with TBDMS, TBDMSCl was used in excess since it is known not to react on O-3 on *N*-phthaloyl chitosan, guaranteeing that every O-6 positions were protected.

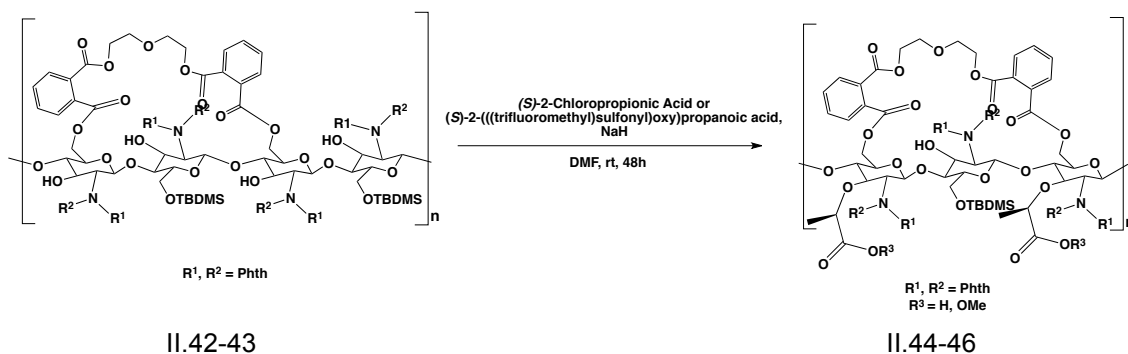


**Figure 2.22 Muramic acid moiety insertion of O6 molecular clamp and O6-TBDMS *N*-phthaloyl chitosan**

To conclude about the efficiency of the molecular clamp route, and the need or not of silylation of the remain O-6 positions after the molecular clamp insertion, the lactyl moiety was introduced, Figure 2.24.

In this step the lactyl moiety insertion was performed in two different ways. The first method was the method already reproduced in the silylation route, 2 and 4 equiv. of (*S*)-2-chloropropionic acid ( $\text{S}_{\text{N}}2$  reaction). The second method consisted on the activation of (*S*)-(-)-2-hydroxypropionic acid ethyl ester, with triflic anhydride. This procedure had the goal of decrease the activation energy of the  $\text{S}_{\text{N}}2$  reaction, once the trifluoromethylsulfonyl group is a better leaving group than the chloride ion. The reaction proceeded with 4 equiv. of the (*S*)-2-(((trifluoromethyl)sulfonyl)oxy)propanoic acid, to give the II.46 sample,. This approach, using

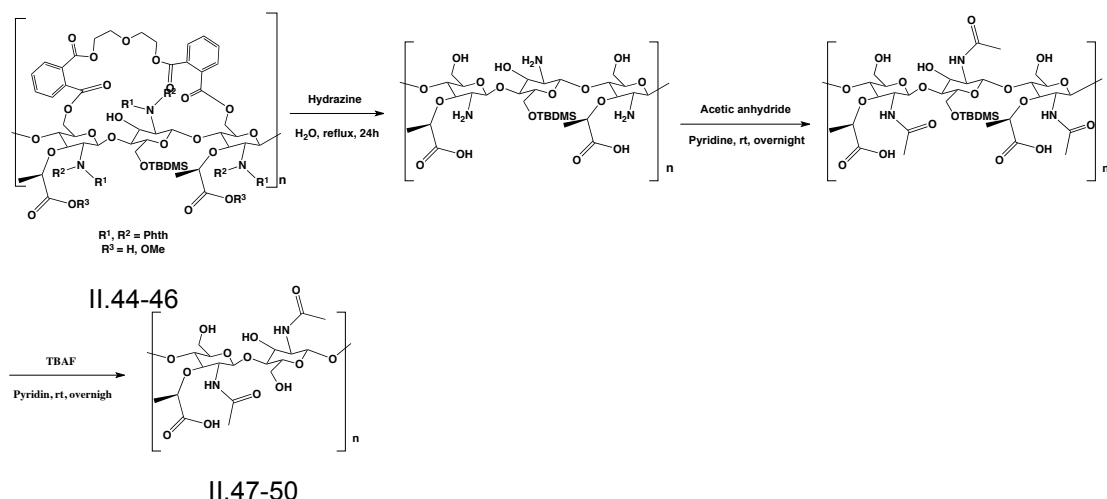


**Figure 2.23 Sequence of deprotection and *N*-acetylation reactions**

the ester instead of the free carboxylic acid on the lactyl reagent implies more synthetic steps in the route towards the NAM-NAG. This approach involves the need to prepare the reagent in order to generate a more electrophilic reagent, and also the hydrolysis of the ester in a more advanced stage by treatment with LiOH.

To complete the synthesis plan, a series of reactions were performed to remove the entire protecting groups and acetylate the amine. It was envisaged that the molecular clamp and the phthaloyl group could be removed at the same step by treatment with hydrazine, while the silyl groups could be easily removed by treatment with TBAF, Figure 2.23.

During the course of this polymeric chitosan modification, molecular clamp route, IR spectroscopy shown to be the best technique to follow reactions. As it is shown in Figure 2.24, after molecular clamp moiety insertion, II.34, the IR spectra exhibited changes, specifically on the  $1661\text{ cm}^{-1}$  band, which was then more intense than the  $1716\text{ cm}^{-1}$  band of

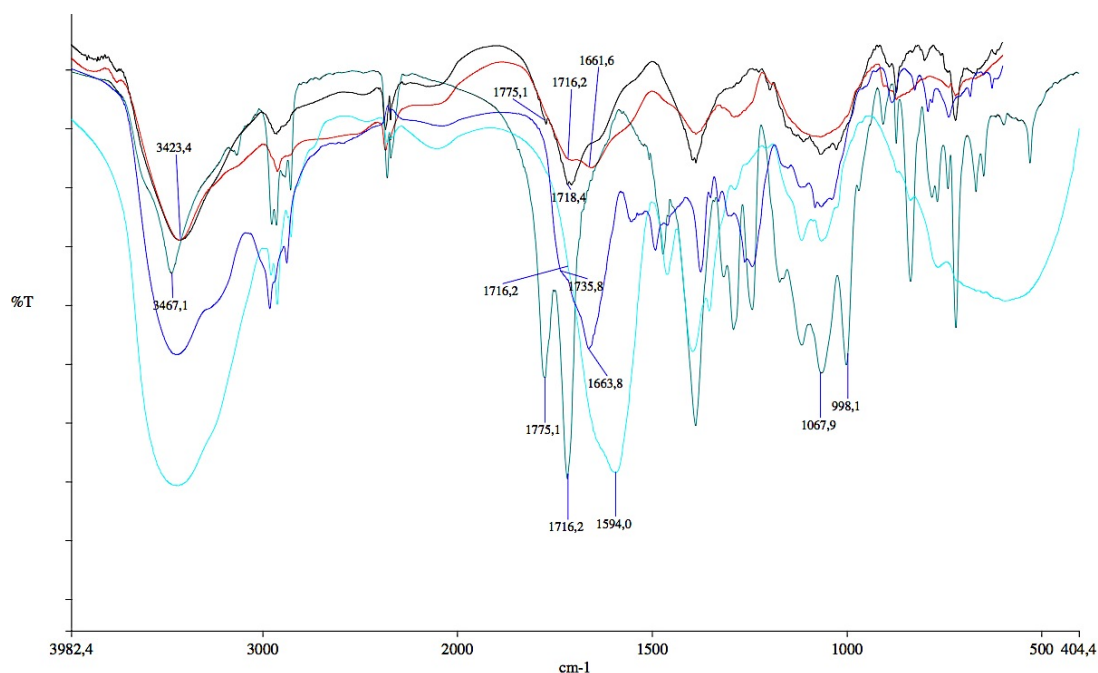


**Figure 2.24 IR spectra of polymeric chitosan modifications, black (I.32); red (II.34); green (II.42); light blue (II.44); blue (II.48)**

the I.32, leading us to conclude that the molecular clamp was successfully introduced. After this step, a silylation of the remaining O-6 positions was performed achieving compound II.44. IR analysis of II.44 shows the shrinkage of the -OH band,  $3467\text{ cm}^{-1}$  and the appearance of the O-Si bands  $1067$  and  $998\text{ cm}^{-1}$ . The next step was the introduction of the lactyl moiety, II.44. IR spectra shows the increase of the -OH band, and the enlargement of the  $1800\text{-}1500\text{ cm}^{-1}$  bands, leading to the appearance of the  $1594\text{ cm}^{-1}$  band, probably due to the presence of carboxylic acid group. The final steps of this route consisted on protecting groups removal and acetylation of the free amine obtaining the II.48. In the IR spectra it can be observed a band at  $1735\text{ cm}^{-1}$ , corresponding to the carbonyl of the carboxylic acid, and  $1663\text{ cm}^{-1}$  corresponding to the carbonyl of the amide group.

Next step of the project consisted on the enzymatic studies in order to understand if the products obtained contained the NAM-NAG sequence and thus which strategy if any had been successful. .

## 2.3 Enzymatic studies of the final products

After the chemical modification of chitosan several products were obtained from the different strategies used. However, the characterization of these compounds revealed the presence of the lactyl moiety but it was not possible to determine the relative positions. Thus to analyse the sequence of the NAM and NAG units generated the enzymatic digestion appeared as a versatile and simple solution. Several enzymes are known to recognize the NAM-NAG sequence of the bacterial cell wall. Lysozymes hydrolyse the  $\beta$ -(1,4) glycosidic bond between the NAM and NAG in the natural substrate PGN.<sup>74</sup>

Thus, in a first stage the enzymatic digestion was performed by the use of two different lytic enzymes, lysozyme and mutanolysin, which hydrolyse between NAM and NAG units. The experiments were carried under several conditions (for 24 and 92 hours) to understand the role of the time of reaction on the hydrolysis profile. Afterwards the products of hydrolysis were analysed by HPLC-UV, to a simple control and compared before and after hydrolysis. Additionally, HPLC-MS was used to identify the result of the hydrolysis. The affinity of the prepared samples for PGRP-SA was also evaluated in order to understand if the samples were recognized by these proteins.

### 2.3.1 Enzymatic digestion

The final products were digested with lysozyme and mutanolysin to understand if there was any NAG-NAM sequence and also to compare with a natural source of PGN from *E. coli*. In a first attempt the products of the silylation route, products, II.22-25, were tested together with the *E. coli* PGN, chitin and chitosan used as control.

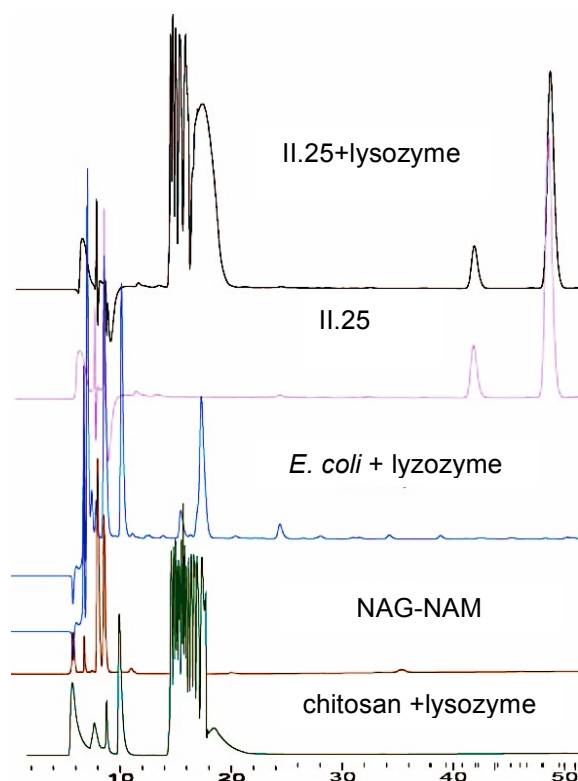
To monitor the experiments a negative control was conducted for every reactions, that consisted on the sample and buffer, without enzyme. The effect of the duration of the hydrolysis reaction, 24 and 92 hours was also tested.

Table 2-2 summarizes the results obtained through HPLC-UV, where it can be observed that, lysozyme, as reported in the literature,<sup>39</sup> recognizes and consequently is able to hydrolyse, chitin and chitosan, with almost the same hydrolysis profile as the synthesized products. This led to the conclusion that the *N*-acetyl moiety has no particular role in the recognition by the lysozyme. However the hydrolysis profile of products II.25, chitin and chitosan are quite different from the lysozyme hydrolysis of *E. coli* PGN. It was also observed that only one of the synthetic samples was hydrolysed by the lysozyme, which may indicate few facts. In the synthesis of the sample II.22 and II.23, the silyl group used, TPS was the bulkiest group that was used. The literature reports that the more bulky the lower the DS will be, TBDMS > TBDPS > TPS, and in fact the TBDPS group has a DS of 0.82, and TPS would have a DS around 0.70.<sup>62</sup>

**Table 2-2 Summary of first enzymatic, lysozyme, digestion**

Sample	time (h)	
	24	92
Chitin	hydrolysed	hydrolysed
Chitosan	hydrolysed	hydrolysed
II.22	N.D.	
II.23		
II.24		
II.25	hydrolysed	hydrolysed
<i>E. coli</i> PGN	hydrolysed	hydrolysed

The lower DS on the O-6 protection opens room for reaction with the (S)-2-chloropropionic acid to occur at this position instead of the O-3, leading to a unit that could not be recognized by lysozyme, once the active site has no affinity to O-6 modifications, as already reported. The sample II.24 gave the same result and was not hydrolysed by the



**Figure 2.25 Comparison of lysozyme hydrolysis profiles, 206 nm absorption**

lysozyme. However its synthesis partner, II.25, was hydrolysed by lysozyme, giving a hydrolysis profile similar to chitin but with more peaks at 206 nm, as it is shown in Figure 2.25. This may indicate that in some extent the sample II.25 managed to incorporate the NAG-NAM sequence in some positions that did not react with (S)-2-chloropropionic acid in the O-6 position, eventually due to the fact of using 4 equiv. of (S)-2-chloropropionic acid

unlike the II.24 2 equiv. were used In fact, not much difference was observed in the profile of the samples which hydrolysis was carried in 24 and 92 hours

With these results in hand, the tests proceeded with all samples from the molecular clamp route. This time mutanolysin was also used with these samples, with the exception of product II.47 that was only tested with lysozyme. Mutanolysin has a larger active site and can hydrolyse PGN with an acetyl group at the O6-position, *Staphylococcus aureus*.<sup>75</sup>

**Table 2-3 Summary of the second enzymatic study (92 hours)**

Sample	Enzyme	
	Lysozyme	Mutanolyzin
Chitin	N.D.	hydrolysed
II.25		N.D.
II.47	hydrolysed	Not tested
II.48	N.D.	hydrolysed
II.49		N.D.
II.50		N.D.

As Table 2-3 shows, in this second enzymatic study the results obtained were different from the results obtained in the first study. This fact suggested that maybe the lysozyme lost its activity, because it is not explainable how can chitin be at a first moment hydrolysed by lysozyme and at a second time only be by mutanolysin. These experiments will

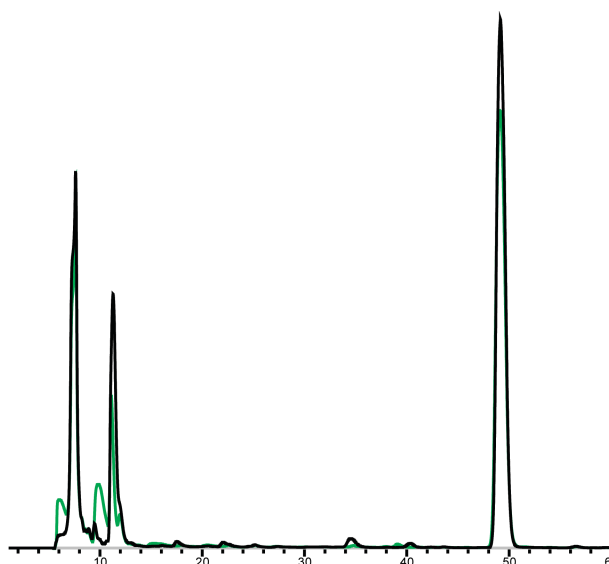


**Figure 2.26 Hydrolysis profile of II.48 treated with mutanolysin; (green); (black) negative control, 206 nm absorption**

have to be repeated to determine the exact lysozyme action on the substracts.

Thus, due to the fact that only the 206 nm absorption was not enough to conclude what was the enzyme's reaction on the sample, the enzymatic hydrolysis products were analysed by a MS detector, in order to understand the meaning of "hydrolysed".

The sample II.48 digested with mutanolysin was analysed. Since the HPLC program was not the same, a study had to be done applying also the negative control to find out where was the difference in both chromatograms, Figure 2.27.

Since the sample concentration was the same in both injections, it was possible to directly compare both of the chromatograms by the intensity. The observation of the negative

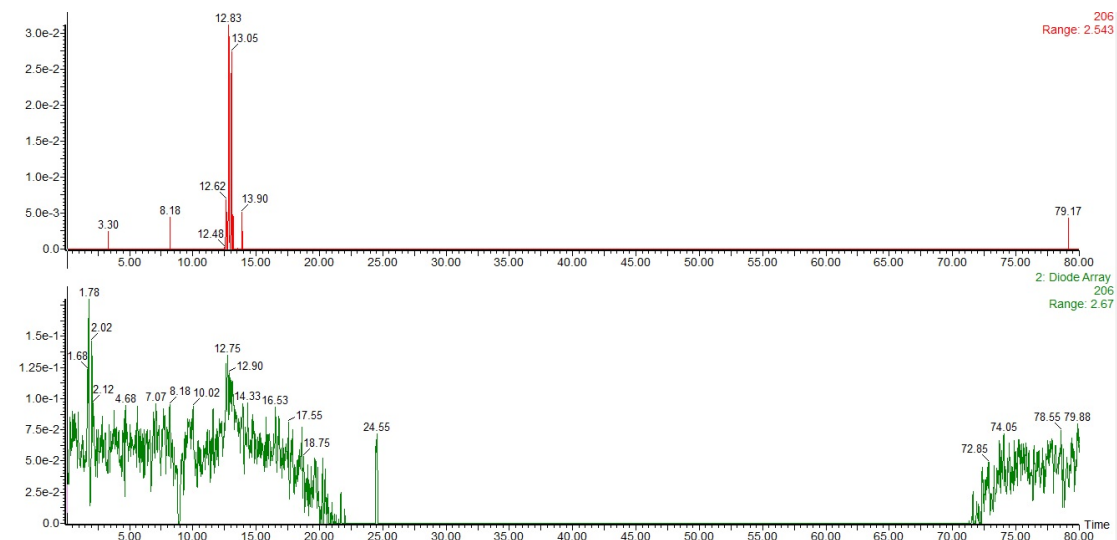


**Figure 2.27 HPLC-UV/MS chromatogram of sample II.48; (red) II.48 + mutanolysin; (green) negative control; 206 nm Absortion**

control was important to ensure that the intensity during the HPLC run was not relevant so every peak that is present on the II.48+mutanolysin chromatogram is derived of the

mutanolysin hydrolysis. To simplify the calculation of all combination of sugar unit, we developed an Octave program that reduced the chromatogram analysis time considerably. The code is shown in the section 6-Appendix. At retention time 8.18 min it can be found, on MS spectra, a  $m/z$  499 peak, that represents a NAG-NAM unit plus one mass unit, since ESI+ was the ionization method. A peak of  $m/z$  703 is also present, which correspond to a oligomer of NAG-NAM-NAG plus two mass units, one derived of the ESI+ and the other only can be explain by the

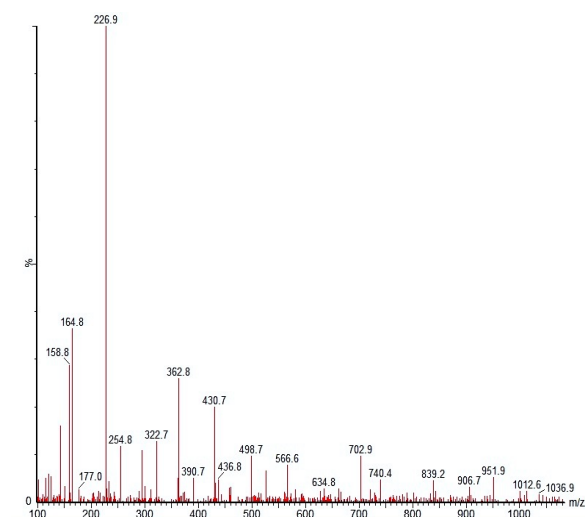


**Figure 2.28 II.48 ESI+ MS, (8.18 min)**

tolerance of the detection mode, one mass unit. The other peaks with retention times 12.48 – 13.90 could not be assigned to any particular oligomer, but they might be peaks that are originated by the ionization of NAG-NAM sequences.

Unfortunately due to the lack of product, we could not realize the HPLC-MS analysis of the sample II.47, and so we could not determinate its hydrolysis product.

### 2.3.2 mCherry-PGRP pull-down assays

Due to the ambiguous enzymatic hydrolysis results, and the loss of activity by the lysozyme, it was decided to preform several PGRP pull-down assays in order to check if this group of proteins could recognize the prepared samples. For this study a mCherry-PGRP-SA was used, PGRP-SA from *D. melanogaster* tagged with a *N*-terminal fluorescent tag that provides a pink colour to the protein. As already reported in Section 1.2, PGRPs are responsible for the Gram-positive bacteria recognition, initiating the Toll pathway cascade. This protein family had conserved a 165-amino acid domain with an evolutionary connection to bacteriophage T7 lysozyme. PGRP-SA has the ability to recognise and bind to natural PGN.<sup>3, 76</sup> PGRP-SA (PDB code 1SXR) has 80% query cover and 44% identify with the human PGRP-1 $\alpha$  (PDB code 1SK3\_A) calculated with BLAST®. Until now there is no crystal structure of *Drosophila* PGRP-SA with any PGN moiety, NAG or NAM, so this experiment may be important to help to unravel the PGRP-SA recognition domain. In other PGRPs there seems to be an almost unchanged amino acid sequence responsible to, what seems to be the PGN's sugar backbone interaction, and a sequence that may change, responsible for the peptide accommodation. However many studies claim that the peptide moiety is almost mandatory to the PGRP binding.<sup>8, 76, 77</sup>

In this study several samples were tested, chitin, II.22-25, II.48, II.49 and II.50, divided in two types of experiment, a first experiment that consisted on a digestion in the presence of PGN, extracted from *Staphylococcus aureus* and a second one without PGN. In order to make sure that all the conclusions and assumptions were right several control samples were used: control sample, A – consisted on heating PGN in the reaction buffer; the control B – PGN reacted with LytA, in order to obtain the PGN's sugar backbone as large as possible (to mimic synthetic samples); control C – PGN reacted with mutanolysin, in order to obtain dimeric/crosslinked NAG-NAM units; and control D – consisted on a mixture of B and C, PGN that reacted with LytA and mutanolysin, in order to obtain small soluble murein fragments, NAG-NAM.

All of these control samples were boiled and centrifuged, and then the pellet was disposed. In the competition assays a reaction mixture was prepared as shown in 4.3.2. The BSA was used as internal loading control.

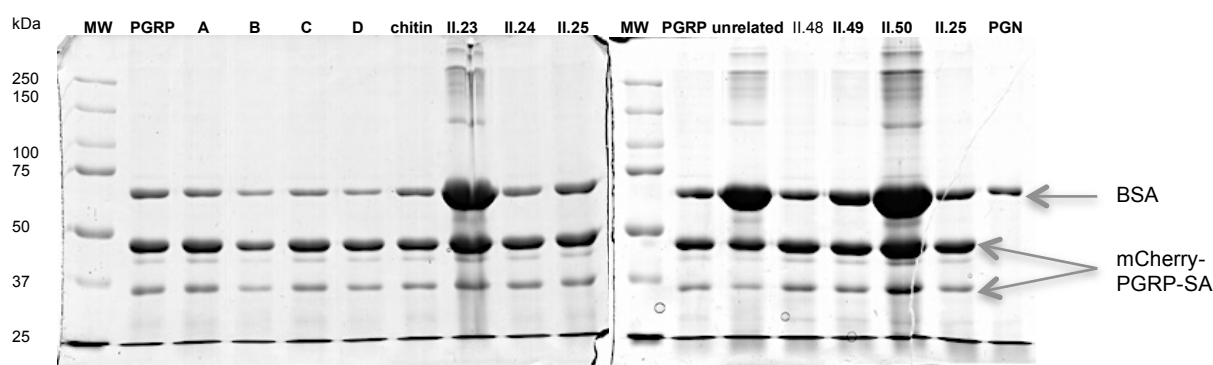
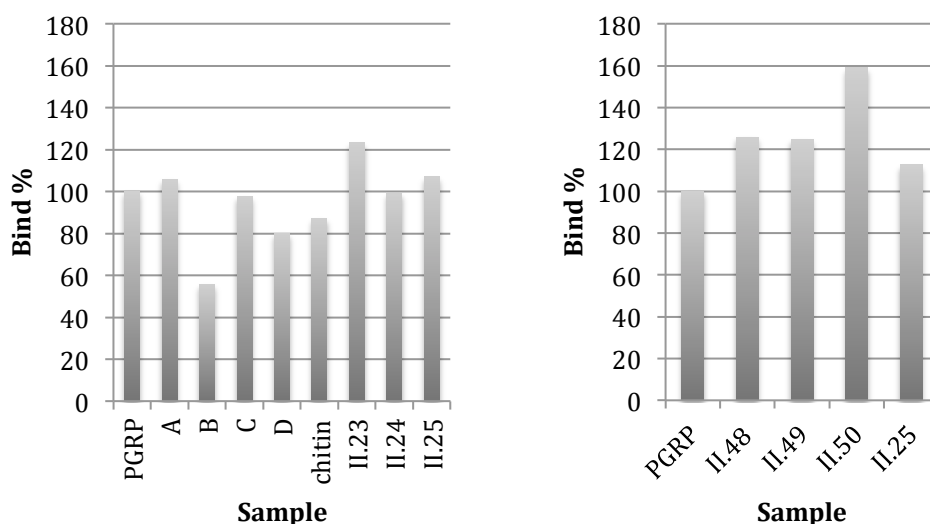


Figure 2.29 8% SDS-PAGE gel electrophoresis of the mCherry-PGRP-SA pull-down assay in the presence of native PGN

Figure 3.30 shows the electrophoresis gel of the mCherry-PGRP-SA pull-down assay in the presence of natural PGN. The synthetic samples were water-soluble and it was observed that once PGRP-SA binds to synthetic samples it forms a water-soluble complex. Once mCherry-PGRP-SA is also water-soluble, and a decrease of the intensity of mCherry-PGRP-SA in the pellet was observed it suggested that a competition between the modified chitosan and the natural PGN could be taking place. That was supported by the direct observation of the electrophoresis gel, and also by the intensity of the bands, using ImageJ software.



**Figure 2.30 mCherry-PRGP-SA percentage of binding of the different samples in the mCherry-PGRP-SA pull-down assay with native PGN**

In Figure 2.30, is shown the percentage of the mCherry-PRGP-SA bounded to the chitosan derivative samples. Taking as 100% the assay where mCherry-PGRP-SA is incubated only with PGN, it is possible to observe that several samples have higher mCherry-PGRP-SA intensity in the pellet than the 100% binding control. These samples that have a higher percentage of binding than the native PGN have also a higher intensity of BSA in the pellet, which could indicate that BSA form some kind of complex with the synthetic samples that turns out to be insoluble. It was also observed that the control sample B, might form a soluble complex with mCherry-PGRP-SA, which explains the decrease the quantity of mCherry-PRGP-SA in the pellet. To understand these results it was decided to repeat the mCherry-PGRP-SA pull-down assay without the native PGN.

Figure 2.32 shows the electrophoresis gels of the mCherry-PGRP-SA pull-down assays without the native PGN. This time it was not possible to define a 100% binding control sample, so the absolute values of mCherry-PGRP-SA intensity are shown, and quantified in Figure 2.32. From the obtaining results, there seems to be a disparity between both II.25 values, so no efforts were concentrated in its analysis. On the other hand, samples II.48, II.49 and II.50 seemed to be the samples that interact the best with mCherry-PGRP-SA. The chitin value seemed to be ambiguous once at the competition assay it did not increase the

percentage of mCherry-PGRP-SA binding, and also as chitin is water-insoluble it was not possible to compare with the other results with water-soluble samples.

At an initial stage of the experiments plan, it was envisaged that in a pull-down assay

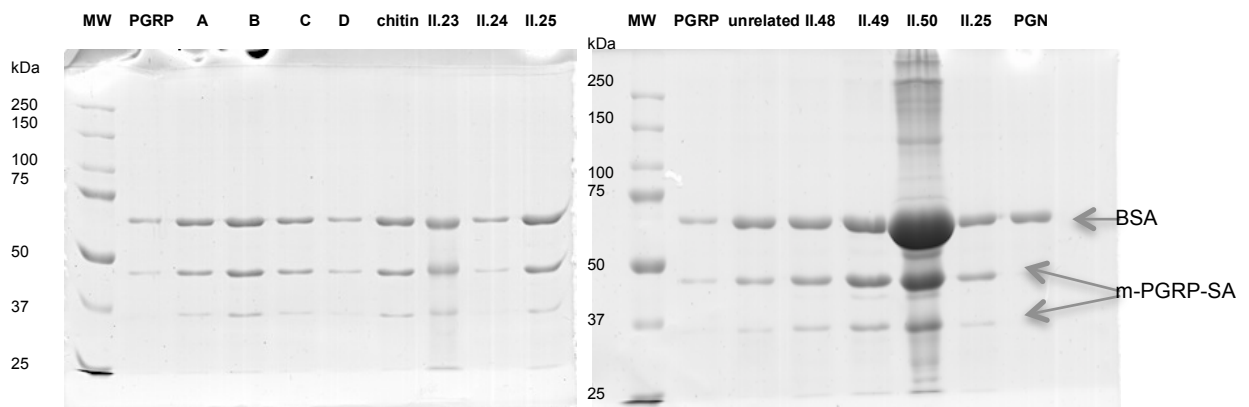


**Figure 2.32 8% SDS-PAGE gel electrophoresis of the mCherry-PGRP-SA pull-down assay without native PGN**

like this, the mCherry-PGRP-SA would be dragged to the pellet, since native PGN is insoluble. However, the results obtained seemed to contradict that thought. As the BSA intensity on the pellet increased, and has been reported the linkage of BSA to PGN and other sugars,<sup>78</sup> it is not possible to assert that the synthetic samples form an insoluble complex with PGRP, leading to increase its intensity on the pellet. It is possible that the synthetic samples

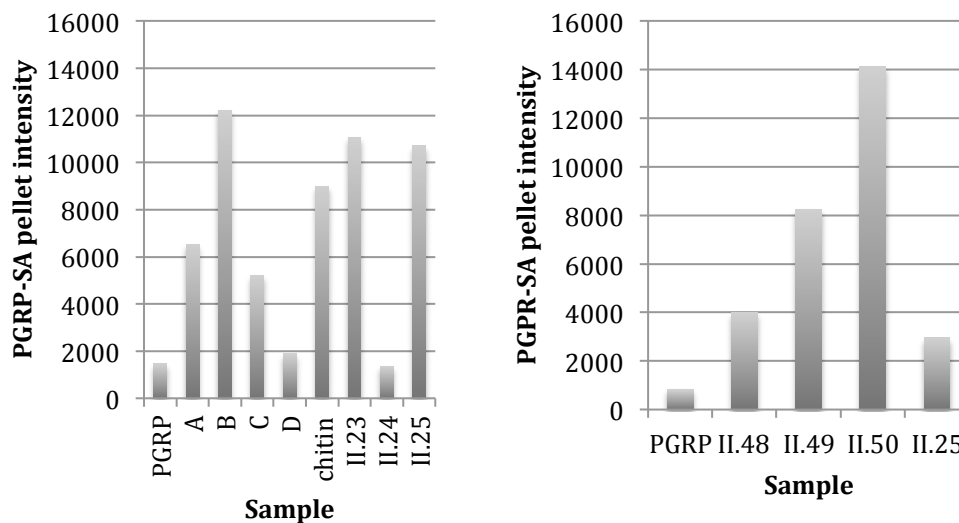


**Figure 2.31 mCherry-PGRP-SA intensity in the PGRP-SA pull-down assay without native PGN**

could form an insoluble complex with BSA and then drag the mCherry-PGRP-SA to the pellet. However, as the BSA intensity value is approximately the same in every control samples, in the completion and none-competition assays, the results strongly suggest that, the prepared samples effectively drag the mCherry-PGRP-SA to the pellet, indicating an affinity to this protein.

At this point the results indicated that the mechanism of mCherry-PRGP-SA recognition was mainly related with the sugar backbone and not so much with the peptide moiety. Once the control sample B seemed to be one that most dragged mCherry-PGRP-SA to the pellet and sample B has a long chain only composed by NAG-NAM units, might be that the peptide moiety leads to lower kD value. However the interaction between the prepared samples and mCherry-PRGP-SA seemed to be quite strong, since it did not broke up during the preparation steps before it was applied on the gel.

The analysis of the mCherry-PGRP-SA pull-down assays seemed to contradict some of the previous enzymatic digestion results. In order to clarify the real composition of the prepared samples it was decided to do a last study using other technic that could help in understanding whether the products prepared on this journey would led to the NAM-NAG polymer.

### 2.3.3 Monosaccharide composition analysis

To finish the product analysis studies, and be able to bring up some conclusions about the research, a monosaccharide composition analysis was performed, This study consists on hydrolysing the prepared samples, with 3 M HCl for 3 and 24 hours according to procedure 4.3.3. Two different times of hydrolysis were used, since this protocol was optimized to monosaccharide composition analysis of native PGN. In this procedure an anionic exchange chromatography was used, with a pH electrode as detection method. This allowed to conclude how much of every monosaccharide was present in the prepared sample. Due to the chemical hydrolysis, the monosaccharides NAG originate glucosamine moieties while the NAM hydrolysis gives muramic acid. By the chromatograms analysis it was possible to conclude that 3 hours of hydrolysis were enough to convert the synthetic samples into monosaccharides.

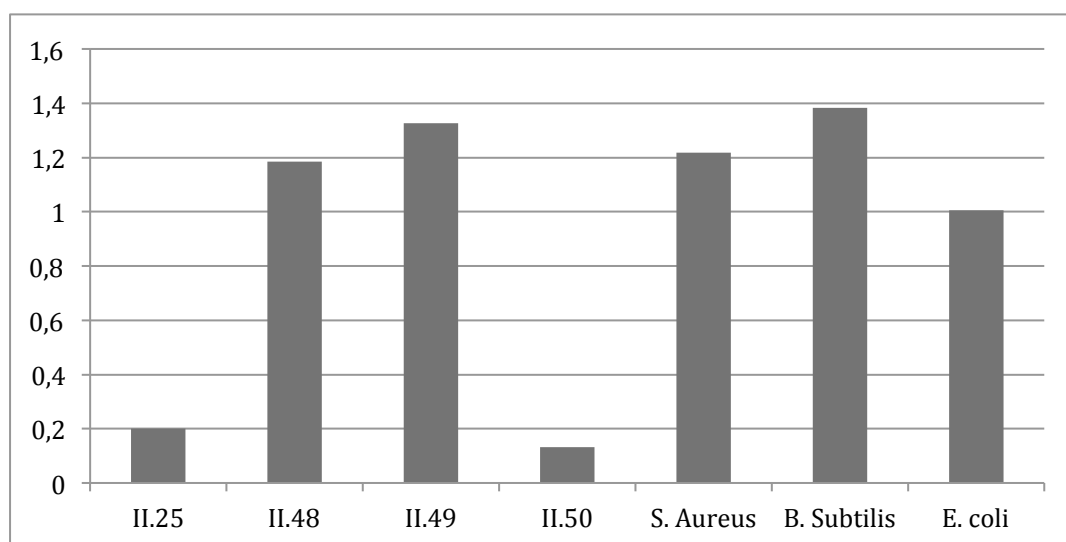


Figure 2.33 Muramic acid: Glucosamine ratio

For this experiment the concentration of the monosaccharides was calculated using a calibration curve, which was made using several concentrations of ribitol, glucosamine,

muramic acid and NAM. The results were obtained by the direct integration of the peak's area in the chromatogram and are summarized in Figure 2.33.

The analysis of the muramic acid-glucosamine ratio obtained for the synthetic samples indicated that the low ratio in the sample II.25 might be related with the DS of the TBDPS group as already was a concern. On the other hand the low ratio of the sample II.50 may be related with the reaction conditions and reagent used to insert the lactyl moiety that was not suitable to chitosan reaction. The strategy to insert the lactyl moiety in the samples II.48 and II.49 was the best that has been embraced. Since sample II.48 was only recognized by mutanolysin, and as a monosaccharide ratio similar to *S. aureus*, it is suspected that maybe, in the acetylation procedure the acetic anhydride could also reacted with the O-6 position. This acetyl group would be removed during the chemical hydrolysis step providing muramic acid unit. However as the sample II.25 was only recognized by lysozyme in the first try, and has a significant ratio, reinforced the lost of lysozyme activity observed.



### 3 Conclusions and final remarks

Since bacterial peptidoglycan is directly associated with bacterial infections and antibiotic resistance, this work contributed to a new and sustainable access to the carbohydrate backbone of the peptidoglycan.

The scientific community has devoted several efforts to the synthesis of bacterial peptidoglycan however these approaches involve long synthetic sequences and laborious isolation. Additionally peptidoglycan isolation in pure and reliable amounts from the bacterial cell-wall is difficult and the presence of contaminations can lead to controversial results.

Thus, in this work a new approach has been explored using a biopolymer, chitosan as the starting material to produce artificial NAM-NAG polymer. In a preliminary study chitosan was hydrolyzed, and several reaction conditions and procedures were tested to obtain chitooligosaccharides of controlled molecular weight. The best conditions involved treatment with concentrated acid and chitooligosaccharides of DP2–15 were obtained and characterized by MALDI-TOF and GPC.

Using the food industry disposal, chitosan, two synthetic strategies were adopted: regioselective O-6 protection with silyl groups – silylation route and di-esterification at two alternate O-6 positions – molecular clamp route.

In the silylation route two different protecting groups were tested in order to generate different steric hindrance, TBDPS and TPS. The introduction of the lactyl moiety was also investigated and several experiments were carried to optimize this step. Best results were obtained when 2 equiv. of (S)-2-chloropropionic acid was used. The reactions were monitored by IR and the products characterized by IR and CP-MAS NMR.

In the molecular clamp route, several molecular clamp scaffolds were prepared, however only one could be tested. For the lactyl moiety insertion the strategy followed the same procedure as described for the silylation route. After the lactyl group had been introduced in both approaches, the protecting groups were removed and the free amino group was acetylated. The final compounds were characterized by IR and NMR spectroscopy.

The isolated products were then hydrolyzed with lysozyme and mutanolysin and analysed by HPLC-UV, in order to evaluate the content of NAM-NAG moieties on these samples. These studies seemed inconclusive to the majority of the samples with the exception of II.48 that provided a different HPLC profile before and after mutanolysin hydrolysis. HPLC-MS analysis showed the presence of two characteristic peaks at  $m/z$  499 – and  $m/z$  703, consistent with NAG-NAM and NAG-NAM-NAG, respectively. The NAG-NAM content of these samples was also evaluated through chemical hydrolysis and ion chromatography exchange. A 1:1.18 ratio was obtained for the sample II.48, very close to the composition of the natural PGN extracted from *S. aureus*'s, 1:1.2.

Apart from that a mCherry-PGRP-SA pull-down assay was also preformed in order to understand the affinity of mCherry-PGRP-SA to these synthetic samples. It was proved that mCherry-PGRP-SA had affinity to these synthetic samples.

These analyses suggested that the molecular clamp route is the best strategy to convert chitosan into NAM-NAG polymer, in which a careful choice of the reaction conditions and reagents is the key to achieve the optimized conversion.

Using this study as preliminary results, the next step consists on optimizing the chitooligomers isolation process, and generates NAG-NAM murein oligomers. After peptide coupling, PGN fragments will be generated and constitute valuable artificial samples of PGN for the *in vivo* studies, in order to conclude if the synthetic PGN fragments will be able to produce an immune response in *D. melanogaster*.

Chitosan has demonstrated to be a good model to achieve artificial NAM-NAG oligomers. This work opens a new platform for achieving PGN fragments with different composition and thus useful for innumerous biological studies.

## 4 Experimental procedure

### 4.1 General Methods

All commercially obtained reagents were used without further purification unless specified. All the mentioned solvents used in the reactions were dried by usual methods.<sup>79</sup>

Molecular sieves 4Å were activated by heating at 300 °C for 3 h. Preparative and analytical TLC was performed with silica gel 60 plates of 1 mm, 0.5 mm and 0.25 mm, respectively. The reactions that could be followed by thin layer chromatography (TLC) silica gel 60 G/UV254 Macherey-Nagel with 0.20 mm Spots detection on TLC was carried with UV light using a 254 nm lamp (Vilber-Lourmat). Additionally, TLC plates visualization was carried with a TLC spray solution of ethanol-sulfuric acid 9:1.

Nuclear Magnetic Resonance (NMR) spectra were recorded at Brüker Advance 400 MHz for <sup>1</sup>H and at 100 MHz for <sup>13</sup>C, in CDCl<sub>3</sub>, DMSO-d<sub>6</sub>, D<sub>2</sub>O or CDCl<sub>3</sub> with chemical shift values (δ) in ppm downfield from TMS (0 ppm) or the solvent residual peak of D<sub>2</sub>O (4.79 ppm), DMSO-d<sub>6</sub> (2.50 ppm) or CDCl<sub>3</sub> (7.24 ppm) as internal standard. The chemical shifts (δ) for a proton spectra were expressed in parts per million (ppm) and the data for proton spectra was presented in the following order: deuterated solvent, signal chemical shift (δ), relative intensity, spin multiplicity (s –singlet, d – doublet, t – triplet, m – multiplet, dd – doublet of duplets), coupling constant (J, in Hz) and molecule peak attribution if possible. The data for carbon spectra was presented in the following order: solvent, chemical shift (δ), molecule attribution if possible. CP MAS - NMR experiments were acquired in a Spectrometer BRUKER AVANCE 400 spectrometer operating at 9.4 T magnetic field (ultrashielded) at Universidade de Aveiro through the PTNMR network service. The mass spectra were obtained on a Micromass AutoSpecQ and a Micromass GTC (MALDI-TOF-MS, Matrix: 2,5-dihydroxybenzoic acid at the chemistry department at FCT-UNL.

Infrared (IR) spectra were recorded on a Brücker Tensor 27 spectrophotometer FTIR spectra were recorded on Perkin-Elmer Spectrum 1000 model apparatus in KBr dispersions for solid samples or NaCl dispersions for oil samples. In each spectra description were only identified the more intense and characteristic bands. The data obtained is presented in the following order: sample support (NaCl or KBr); frequency of the maximum absorption band (ν<sub>max</sub> in cm<sup>-1</sup> attribution to a functional group in a molecule if possible.

Chitosan 80+ low molecular weight was purchased from AltaKitin.

## 4.2 General procedures for chitosan modification

### 4.2.1 Chitosan hydrolysis

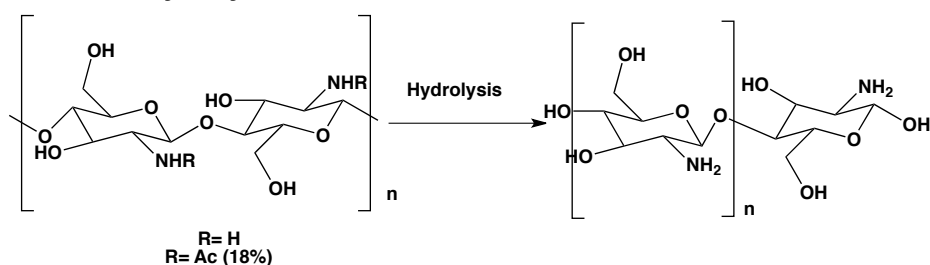


Figure 4.1 Schematic representation of hydrolysis reactions

Table 4-1 Summary of the hydrolysis' work

Entry	Concentration mg/mL	Time (h)	Conditions	Acid	Results <sup>a,b</sup>				
					DA (%)	n	Mn (Da)	Mw (Da)	PDI
1	10	6	Ultrasound bath	5% acetic acid	Nothing occur				
2		4	Ultrasound probe						
3		6	Ultrasound probe						
4	40	6	Ultrasound bath	1M HCl	N. D.				
5		0.5 - 1							
6	20	3	72°C	12M HCl	12	2-18	729	1002	1.37
7		4			2-16				
8		5			11	2-15	674	860	1.28

<sup>a</sup> The acetylation degree was calculated based on equation 1; <sup>b</sup> the n, Mn, Mw and DPI (Mw/Mn) were calculated through MALDI-TOF analysis

#### 4.2.1.1 General procedure for chemical hydrolysis

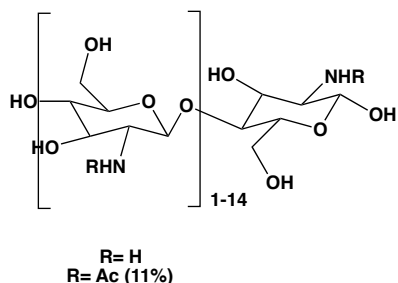
To a 100 mL HCl 12 M solution was added 2 g of chitosan, previously dissolved in a solution of 5% acetic acid to form a gelatin. The suspension was stirred for a period of time as shown in Table 4-1 in a bath at 72°C. The reaction was quenched by addition of ice water and left with stirring for a few minutes. The brown solution obtained was evaporated to dryness, then dissolved in 100 mL of distilled water, and concentrated under vacuum. These operations were repeated twice so as to remove the large amount of HCl.<sup>48</sup>

Product isolation:

1. The product was then dissolved in water, and the pH adjusted to 3 with concentrated NaOH in a flask maintained below 20 °C with an ice bath. The mixture was applied in a dialysis membrane of cellulose ester (CE) with a molecular weight cut off of 500 – 1.000 Da overnight and dialyzed in 1 L

distilled water. The water was renewed and allowed to dialyze for 24 hours. The combined aqueous layers were then concentrated under vacuum and finally were lyophilized.

- The product was treated with 200 mL of cold acetone, and a white powder precipitated. The powder was filtered and dried to give a beige solid



II.8 Starting with commercial chitosan 20% DA using the 4.2.1.1 procedure. An off-white powder was obtained in a yield of 92.5%.

<sup>1</sup>H-NMR (400 MHz; D<sub>2</sub>O): δ 5.37 (t, J = 3.2 Hz, 0.25H), 4.90-4.76 (m, 1H), 3.97 (t, J = 9.5 Hz, 0.344H), 3.89-3.59 (m, 5H), 3.50-3.38 (m, 1H), 3.25 (m, 0.32H), 3.12-3.04 (m, 1H), 3.00-2.91 (m, 0.2H), 1.83-1.80 (m, 0.386H).  
MALDI-TOF: m/z 363.19 [DP1+Na<sup>+</sup>]; 524.30 [DP2+Na<sup>+</sup>]; 685.39 [DP3+Na<sup>+</sup>]; 846.49 [DP4+Na<sup>+</sup>]; 1007.58 [DP5+Na<sup>+</sup>]; 1168.67 [DP6+Na<sup>+</sup>]; 1329.75 [DP7+Na<sup>+</sup>]; 1490.83 [DP8+Na<sup>+</sup>]; 1651.92 [DP9+Na<sup>+</sup>]; 1812.97 [DP10+Na<sup>+</sup>]; 1974.04 [DP11+Na<sup>+</sup>]; 2135.13 [DP12+Na<sup>+</sup>]; 2296.17 [DP13+Na<sup>+</sup>]; 2457.30 [DP14+Na<sup>+</sup>]; 2779.40 [DP15+Na<sup>+</sup>]. IR ν<sub>max</sub>(KBr): 3400 (O-H), 2949 (N-H), 1631 (NHC=O), 1151-1020 (C-O) cm<sup>-1</sup>.

#### 4.2.2 Chitosan N-protection

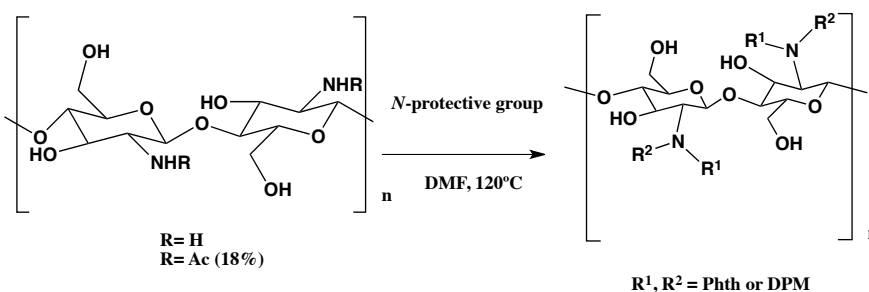
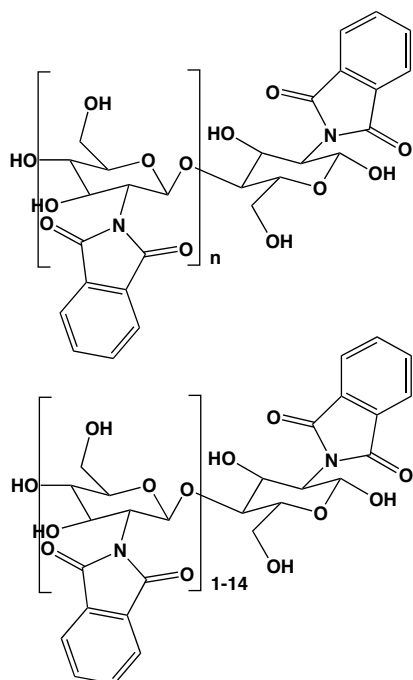


Figure 4.2 Schematic representation of N-protection reactions

To a solution of 5.6 mmol of the anhydride in 6 mL of DMF containing 5% of water was added 0.3 g (1.89 mmol) of chitosan, and the mixture was heated under a nitrogen atmosphere at 120°C with stirring, over night. The reaction mixture was cooled then poured into ice water. The precipitate was collected on a filter, washed with 150 mL of methanol for one hour and dried to give the product.



I.32 starting with commercial chitosan 20% DA using the 4.2.2 procedure. A dark tan solid was obtained 72% yield.

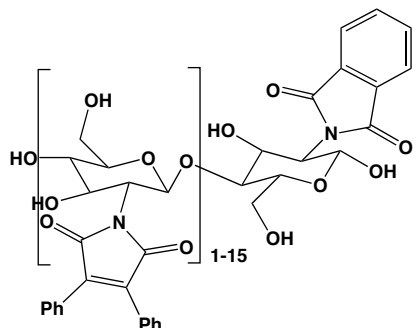
<sup>13</sup>C CP/MAS NMR (101 MHz; None): δ 168.8 (C=O), 134.5, 130.9, 123.1 (Ar), 100.6 (C1), 82.3 (C4), 75.0 (C5), 71.0 (C3), 60.9 (C6), 56.3 (C2).

IR ν<sub>max</sub>(KBr): 3446 (O-H), 2928 (N-H), 1773 and 1717 (C=O), 1641 (C=O), 1196-990 (C-O) cm<sup>-1</sup>.

II.10 starting with II.8 using the procedure 4.2.2. A tan pale powder was obtained in 87% yield.

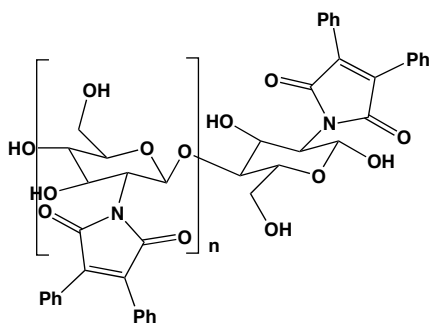
<sup>1</sup>H-NMR (400 MHz; DMSO-d<sub>6</sub>): δ 8.03-7.74 (m, 4H), 5.44-5.00 (m, 2H), 4.75 (s, 1H), 4.23 (m, 3H), 3.72 (s, 2H), 2.91 (s, 1H).

MALDI-TOF: m/z 331 [DP1+Na<sup>+</sup>]; 623,21 [DP2+Na<sup>+</sup>]; 914,29 [DP3+Na<sup>+</sup>]; 1205,37 [DP4+Na<sup>+</sup>]; 1496,44 [DP5+Na<sup>+</sup>]



II.9 starting with II.8 using the procedure 4.2.2. An orange powder was obtained in 44% yield.

$^1\text{H-NMR}$  (400 MHz; aceton- $d_6$ ):  $\delta$  7.55-7.37 (m, 9H), 7.13-7.00 (m, 1H), 6.10-6.07 (m, 0.16H), 5.34-5.26 (m, 1H), 4.87-4.79 (m, 0.5H), 4.52-4.35 (m, 1H), 4.05-3.99 (m, 1H), 3.71-3.68 (m, 2H).  
 $\text{IR } \nu_{\text{max}}$ (KBr): 3437 (O-H), 3063, 1760, 1716, 1659 (C=O), 1581 (Ar), 1151-1010 (C-O)  $\text{cm}^{-1}$ .



II.16 starting with commercial chitosan 20% DA 4.2.2. A tan yellow powder was obtained in 80% yield.

$^{13}\text{C CP/MAS NMR}$  (101 MHz; None):  $\delta$  170.9 (C=O), 136.4, 128.7 (aromatic), 100.0 (C1), 82.6 (C4), 74.6 (C5), 69.9 (C3), 60.4 (C6), 56.4 (C2).  
 $\text{IR } \nu_{\text{max}}$ (KBr): 3446 (O-H), 3066, 1769, 1706, 1652 (C=O), 1575 (Ar), 1154-1018 (C-O)  $\text{cm}^{-1}$ .

## 4.2.3 Chitosan O6-protection

### 4.2.3.1 Molecular Clamp route

#### 4.2.3.1.1 Molecular Clamp synthesis

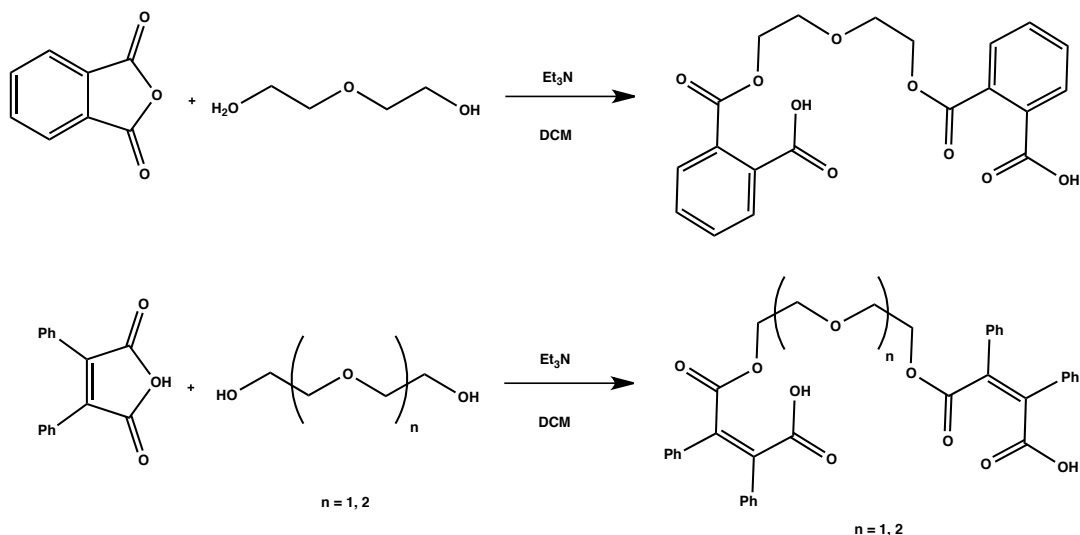
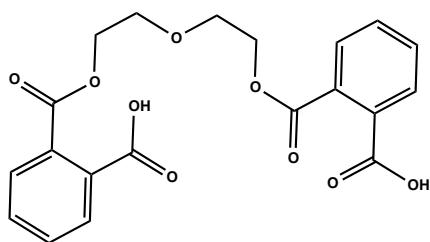


Figure 4.3 Schematic representation of molecular clamp synthesis

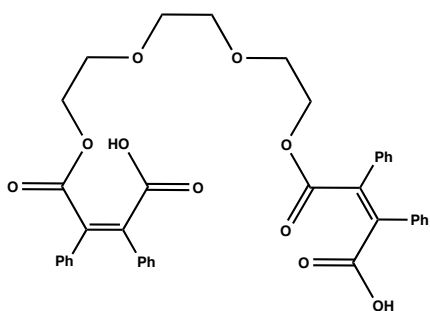
To a solution of anhydride (15.0 mmol) in 100 mL of anhydrous DCM, was added the diol (5.0 mmol) and stirred for 10 minutes, under a nitrogen atmosphere. The reaction mixture

was cooled to 0°C and 15 mmol of anhydrous TEA was added drop-wise. The reaction was stirred overnight at room temperature. The solvent was evaporated, and the residue obtained cooled to 0°C and 200 mL of saturated sodium bicarbonate solution was added. The aqueous layer was washed with ether, 3 x 100 mL. The aqueous layer was collected and cooled to 0°C, acidified with diluted HCl 1 M and extracted with DCM (4 x 100 mL). The combined organic layers were evaporated and dried under reduced pressure to provide the correspondent pure dicarboxylic acid.<sup>72</sup>



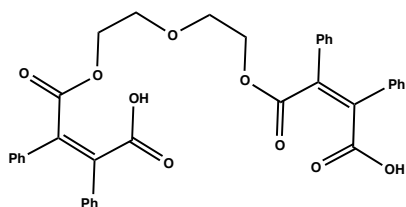
II.30 starting with phthalic anhydride and diethyleneglycol using the procedure 4.2.3.1.1. A colorless oil was obtained in 90% yield.

<sup>1</sup>H-NMR (400 MHz; CDCl<sub>3</sub>): δ 7.80-7.57 (m, 8H), 4.43 (t, *J* = 3.4 Hz, 4H), 3.77 (t, *J* = 3.3 Hz, 4H). <sup>13</sup>C NMR (100 MHz; CDCl<sub>3</sub>): δ 174.7, 167.9, 132.3, 131.9, 131.58, 131.46, 131.0, 129.49, 129.39, 128.9, 69.3, 65.8. IR ν<sub>max</sub>(NaCl): 3054 (O-H), 1726, 1702 (C=O), 1172-1077 (C-O) cm<sup>-1</sup>.



II.31 starting with 1,2-Diphenyl maleic anhydride and triethyleneglycol using the procedure 4.2.3.1.1. A yellow powder was obtained in 89% yield.

<sup>1</sup>H-NMR (400 MHz; CDCl<sub>3</sub>): δ 7.55-7.39 (m, 24H), 3.75 (t, *J* = 4.3 Hz, 4H), 3.69 (s, 4H), 3.63 (t, *J* = 4.3 Hz, 4H). IR ν<sub>max</sub>(KBr): 3390 (O-H), 1842, 1823, 1758, 1629 (C=O), 1180-1000 (C-O) cm<sup>-1</sup>.



II.32 starting with 1,2-Diphenyl maleic anhydride and diethyleneglycol using the procedure 4.2.3.1.1. A yellow powder was obtained in 64% yield.

<sup>1</sup>H-NMR (400 MHz; CDCl<sub>3</sub>): δ 7.58-7.41 (m, 20H), 3.73 (dt, *J* = 57.2, 4.4 Hz, 8H). <sup>13</sup>C-NMR (100 MHz; CDCl<sub>3</sub>): 164.81, 138.17, 131.14, 129.69, 128.93, 127.18, 72.26, 61.87. IR ν<sub>max</sub>(KBr): 3390 (O-H), 1834, 1821, 1755, 1638, 1599 (C=O), 1178-995 (C-O) cm<sup>-1</sup>.

#### 4.2.3.1.2 Molecular Clamp insertion

The dicarboxylic acid (*x* mmol) was dissolved in 3 mL of anhydrous DMF and with CDI was added (2*x* mmol) in, under a nitrogen atmosphere and the mixture was stirred at room temperature for 3 hours. The mixture was added drop-wise to a solution of I.32 (350 mg, 1.2 mmol) and TEA (1.136 mL, 8.16 mmol) in 4 mL of anhydrous DMF, at room temperature under nitrogen atmosphere and the resulting mixture was stirred for 24 hours. The solvent was removed to dryness and the resulting crude washed with 5 mL of methanol in an ice bath, to obtain a yellow solid.

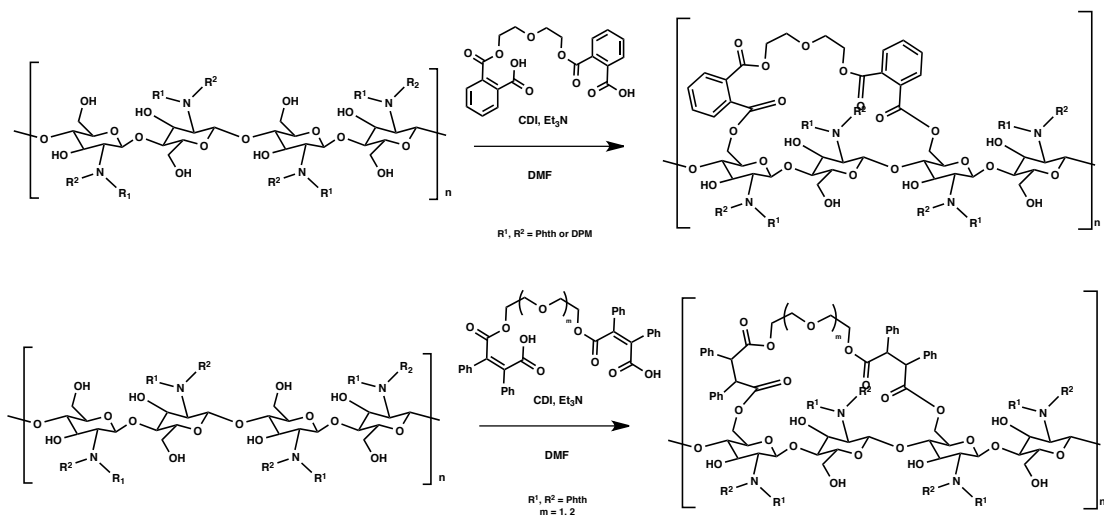
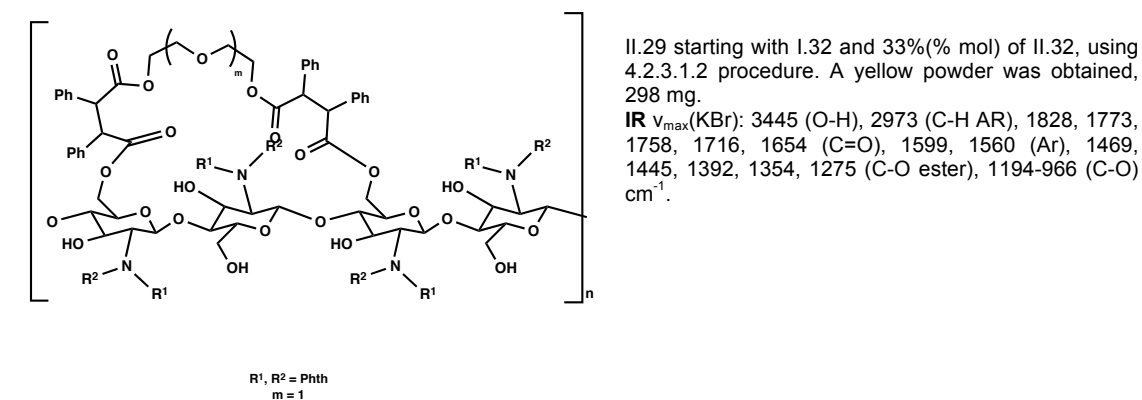
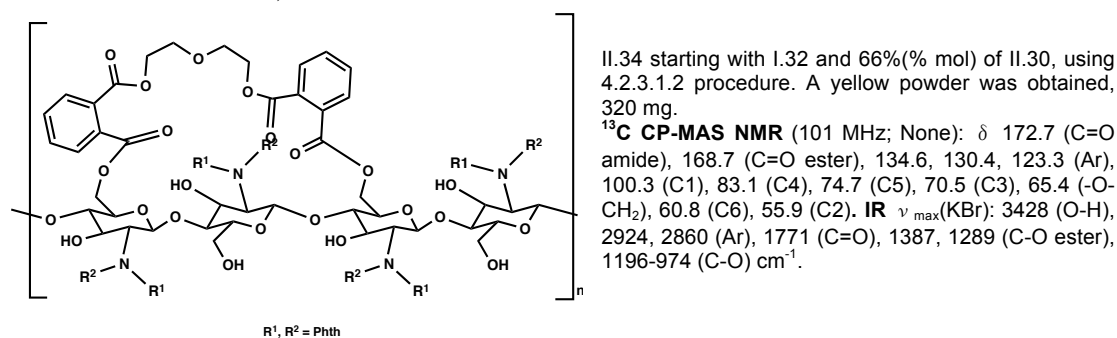
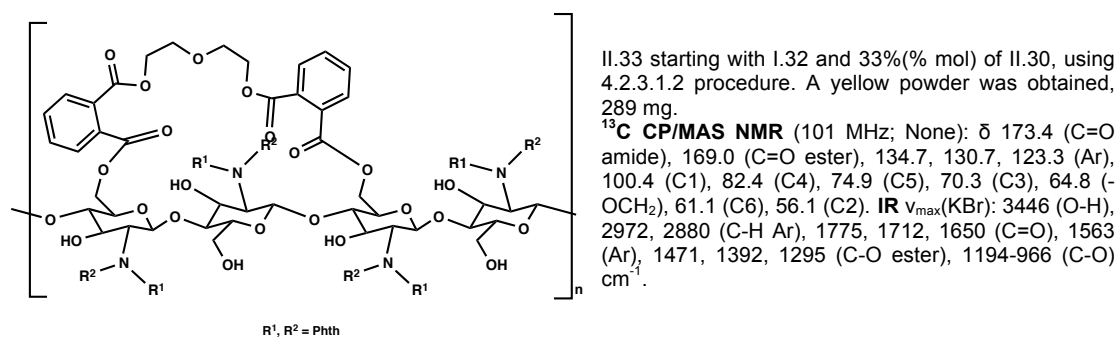
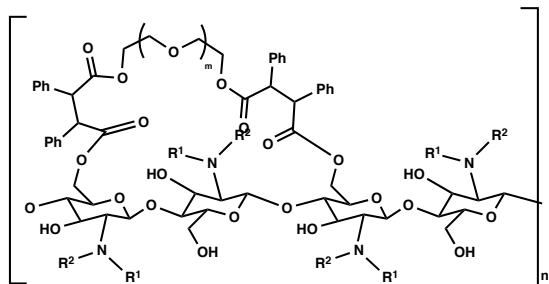
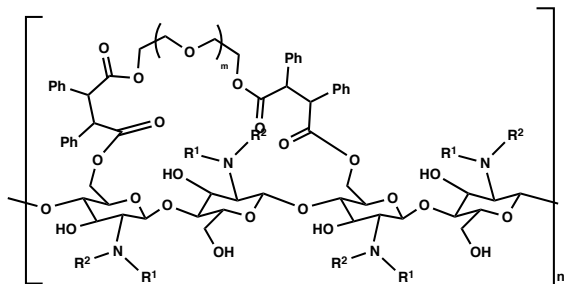


Figure 4.4 Schematic representation of molecular clamp insertion

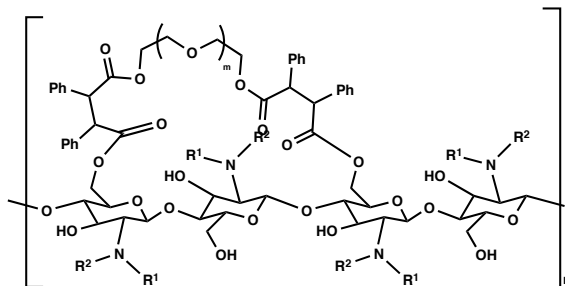




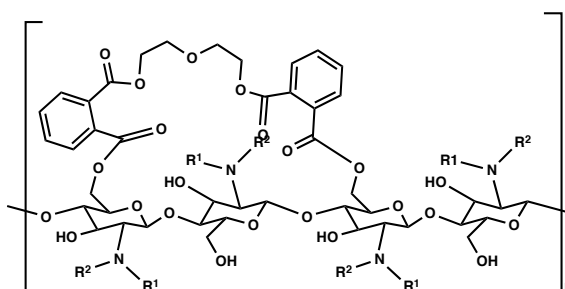
$R^1, R^2 = \text{Phth}$   
 $m = 1$



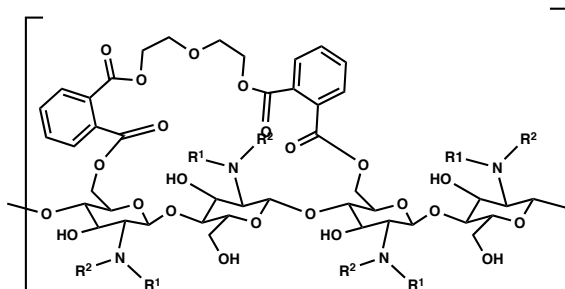
$R^1, R^2 = \text{Phth}$   
 $m = 2$



$R^1, R^2 = \text{Phth}$   
 $m = 2$



$R^1, R^2 = \text{DPM}$



$R^1, R^2 = \text{DPM}$

II.35 starting with I.32 and 66%(% mol) of II.32, using 4.2.3.1.2 procedure. A yellow powder was obtained, 317 mg.

<sup>13</sup>C CP/MAS NMR (101 MHz; None):  $\delta$  172.4 (C=O amide), 168.6 (C=O ester), 134.4, 130.5, 126.3, 123.1 (Ar), 100.3 (C1), 82.8 (C4), 74.5 (C5), 70.8 (-O-CH<sub>2</sub>), 70.1 (C3), 65.6 (-COO-CH<sub>2</sub>), 60.9 (C6), 56.2 (C2). IR  $\nu_{\text{max}}$ (KBr): 3422 (O-H), 2925 (Ar), 1824, 1773, 1758, 1712, 1655 (C=O), 1444, 1390, 1356, 1275 (C-O ester), 1180-998 (C-O) cm<sup>-1</sup>.

II.36 starting with I.32 and 33%(% mol) of II.21, using 4.2.3.1.2 procedure. A yellow powder was obtained, 263 mg.

IR  $\nu_{\text{max}}$ (KBr): 3445 (O-H), 2925 (C-H Ar), 1775, 1714, 1650 (C=O), 1556 (Ar), 1469, 1392, 1318, 1295 (C-O ester), 1196-992 (C-O) cm<sup>-1</sup>.

II.37 starting with I.32 and 66%(% mol) of II.31, using 4.2.3.1.2 procedure. A yellow powder was obtained, 299 mg.

<sup>13</sup>C CP/MAS NMR (101 MHz; None):  $\delta$  173.3 (C=O amide), 168.7 (C=O ester), 134.6, 130.5, 123.2 (Ar), 100.3 (C1), 82.4 (C4), 74.7 (C5), 71.9 (-O-CH<sub>2</sub>), 70.3 (C3), 64.6 (-COOCH<sub>2</sub>), 60.7 (C6), 56.1 (C2). IR  $\nu_{\text{max}}$ (KBr): 3447 (O-H), 2924 (C-H Ar), 1830, 1771, 1709, 1654 (C=O), 1467, 1385, 1329, 1277 (C-O ester), 1196-939 (C-O) cm<sup>-1</sup>.

II.38 starting with II.16 and 33% (% mol) of II.30, using 4.2.3.1.2 procedure. A yellow powder was obtained, 273 mg.

<sup>13</sup>C CP/MAS NMR (101 MHz; None):  $\delta$  170.9 (C=O amide), 134.1, 128.9 (Ar), 100.5 (C1), 81.7 (C4), 74.8 (C5), 70.0 (C3), 64.8 (-COOCH<sub>2</sub>), 60.8 (C6), 56.6 (C2). IR  $\nu_{\text{max}}$ (KBr): 3446 (O-H), 1767, 1705, 1656 (C=O), 1152-1018 (C-O) cm<sup>-1</sup>.

II.39 starting with II.16 and 66% (% mol) of II.30, using 4.2.3.1.2 procedure. A yellow powder was obtained, 342 mg.

<sup>13</sup>C CP/MAS NMR (101 MHz; None):  $\delta$  170.8 (C=O amide), 164.7 (C=O ester), 136.0, 128.9 (Ar), 100.1 (C1), 82.6 (C4), 74.5 (C5), 69.6 (C3), 65.2 (-COOCH<sub>2</sub>), 60.0 (C6), 56.1 (C2). IR  $\nu_{\text{max}}$ (KBr): 3446 (O-H), 1767, 1705, 1652 (C=O), 1599 (Ar), 1151-980 (C-O) cm<sup>-1</sup>.

#### 4.2.3.1.3 O6 remaining groups Silylation

In order to guaranty that every remaining O6 positions became protected we use as

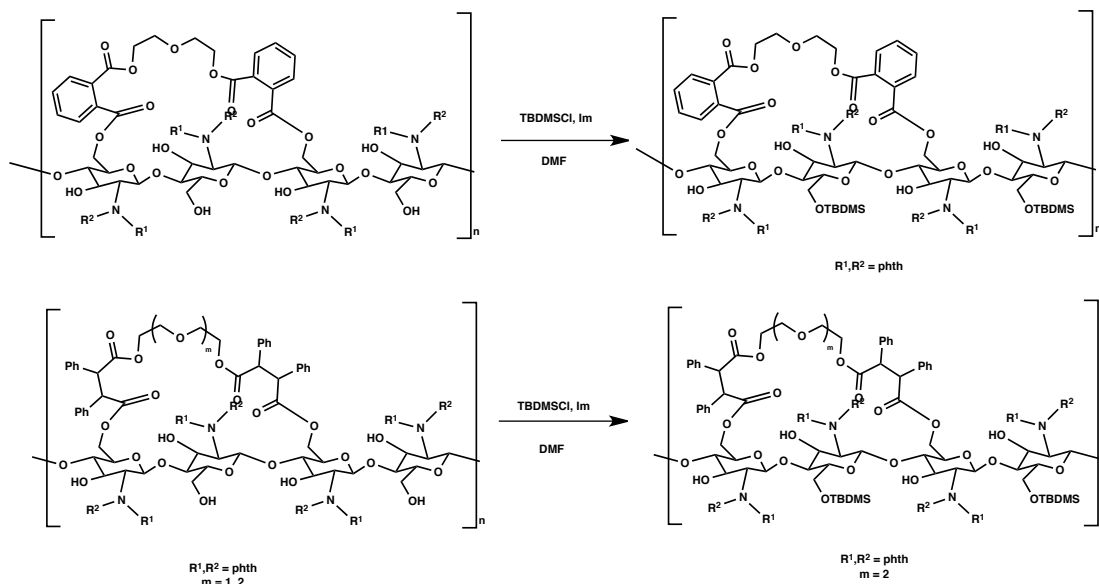
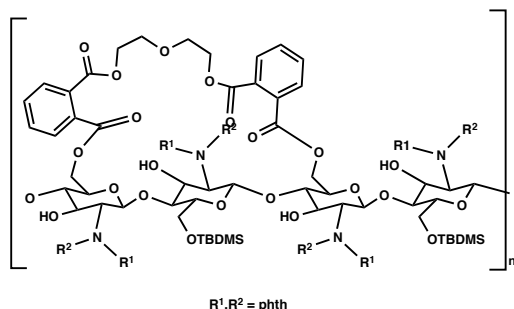


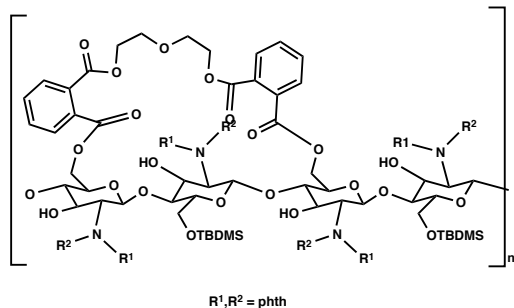
Figure 4.5 Schematic representation of the protection of the remaining O6 free positions

much equivalents of the silyl chloride as the *N*-phthaloylchitosan, so the protocol followed was the same as the 4.2.3.2.



II.42 starting with II.34 using the procedure 4.2.3.2. A yellow powder was obtained, 396 mg.

**IR**  $\nu_{\text{max}}$ (KBr): 3466 (O-H), 1778, 1729, 1646 (C=O), 1471, 1390, 1326 (C-O ester), 1196-970 (C-O), 1119, 1071 (Si-O)  $\text{cm}^{-1}$ .  **$^{13}\text{C}$  NMR CP/MAS** (101 MHz; None):  $\delta$  172.3 (C=O amide), 168.2 (C=O ester), 148.0, 134.4, 131.8, 123.6, 116.8 (Ar), 99.2 (C1), 83.2 (C4), 82.4 (-O-CH<sub>2</sub>), 75.2 (C5), 71.0 (C3), 63.4 (C6), 55.9 (C2), 25.5 (C(CH<sub>3</sub>)<sub>3</sub>), -6.0 (CH<sub>3</sub>)



II.43 starting with II.33 using the procedure 4.2.3.2. A yellow powder was obtained, 351 mg.

**IR**  $\nu_{\text{max}}$ (KBr): 3460 (O-H), 1755, 1718, 1664 (C=O), 1467, 1389, 1322 (C-O ester), 1194-966 (C-O), 1115, 1066 (Si-O)  $\text{cm}^{-1}$ .

#### 4.2.3.1.4 Muramic Acid moiety insertion

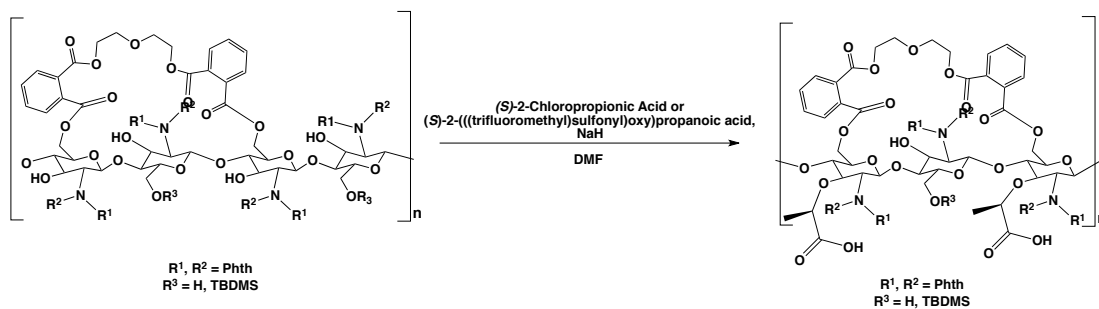
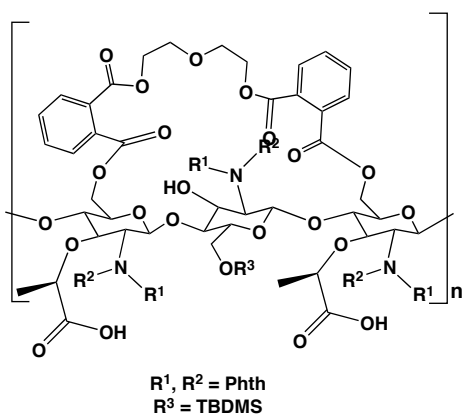


Figure 4.6 Schematic representation of muramic acid moiety insertion

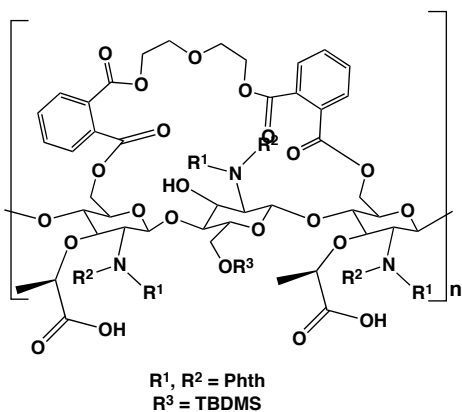
##### 4.2.3.1.4.1 Reaction with (S)-2-Chloropropionic

In this reaction was followed the procedure described in 4.2.4.



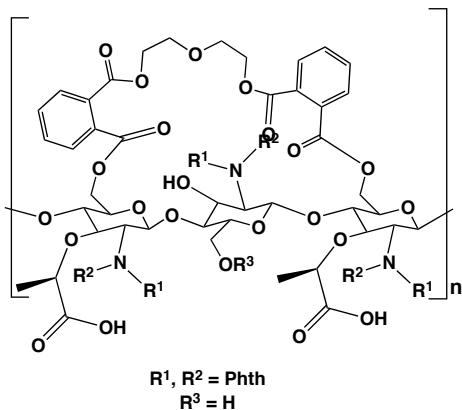
II.44 starting with II.42 and 2 equiv. of (S)-2-Chloropropionic acid using the procedure 4.2.4. A yellow powder was obtained, 218 mg.

IR  $\nu_{\text{max}}$ (KBr): 3422 (O-H), 2957, 2924, 2854 (C-H alkane), 1722-1640 (C=O), 1458, 1259, 1208 (C-O ester), 1090-990 (C-O), 1070 (Si-O)  $\text{cm}^{-1}$ .



II.45 starting with II.42 and 4 equiv. of (S)-2-Chloropropionic acid using the procedure 4.2.4. A yellow powder was obtained, 239 mg.

IR  $\nu_{\text{max}}$ (KBr): 3422 (O-H), 2953, 2924, 2854 (C-H alkane), 1712-1609 (C=O), 1458, 1399 (C-O ester) 1148-988 (C-O), 1081 (Si-O)  $\text{cm}^{-1}$ .



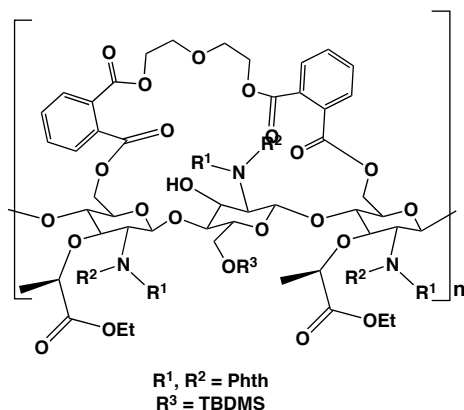
II.41 starting with II.34 and 2 equiv. of (S)-2-Chloropropionic acid using the procedure 4.2.4. A yellow powder was obtained, 223 mg.

IR  $\nu_{\text{max}}$ (KBr): 3435, 3286, 3176 (carboxylic acid), 2961 (alkane), 1706, 1639 (C=O), 1567, 1415 (Ar), 1338, 1247 (C-O ester) 1109-998 (C-O)  $\text{cm}^{-1}$ .

#### 4.2.3.1.4.2 Reaction with hydroxypropionic acid ethyl ester

To a solution of (S)-(-)-2-hydroxypropionic acid ethyl ester (186,27  $\mu$ l, 1,62 mmol) dissolved in dried DCM was added 2,6-lutidine (188,77  $\mu$ l, 1,62 mmol), under inert atmosphere, and the mixture was cooled to  $-78^{\circ}\text{C}$ . Then triflic anhydride (270  $\mu$ l, 1,62 mmol) was added. The mixture was stirred and the mixture was allowed to warm-up to room temperature. The mixture was diluted with 10 mL of a 1:1 mixture hexane:DCM and filtered through celite. The filtrate was concentrated in the vacuum to afford a yellow oil.

This product was used in the general procedure described in 4.2.4. instead of (S)-2-Chloropropionic acid.



II.46 starting with II.43 and 2 equiv. of (S)-(-)-2-hydroxypropionic acid ethyl ester using the procedure 4.2.4. A yellow powder was obtained, 304 mg.

IR  $\nu_{\text{max}}$ (KBr): 3448 (OH), 2961 (alkane), 1777, 1718, 1663 (C=O), 1391 (C-O ester) 1169-1033 (C-O)  $\text{cm}^{-1}$

#### 4.2.3.1.5 Protective groups removal and N-acetylation

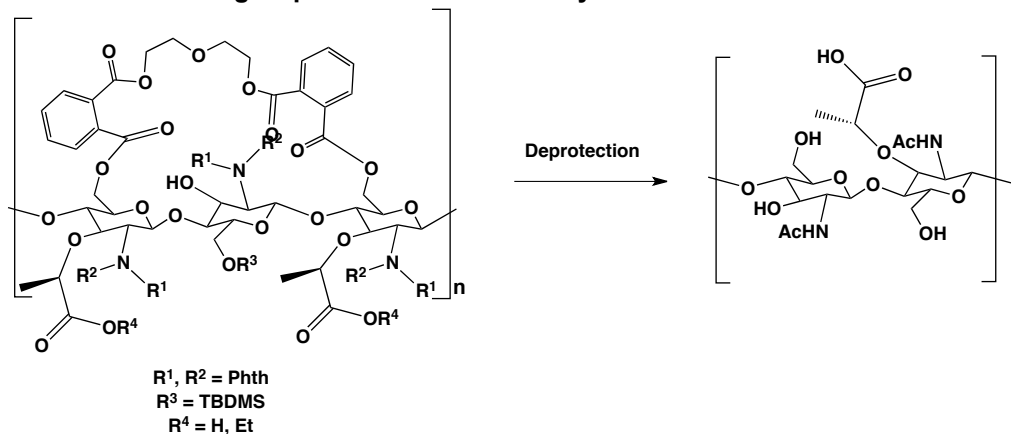


Figure 4.7 Schematic representation of protecting group removal and and N-acetylation reaction

#### 4.2.3.1.5.1 Phthaloyl group and molecular clamp removal

1. In order to guaranty that all of the phthaloyl and molecular clamp groups were removed we used huge excess, 40 equiv. of hydrazine monohydrate in boiling water, in a concentration of 6 M, for 24 hours. Then the solvent was evaporated and washed with 5 mL of distilled water, 5 mL of ethanol and 5 mL

of ethyl ether. The product was not characterized and was all used in the *N*-acetylation procedure to avoid loss of material.

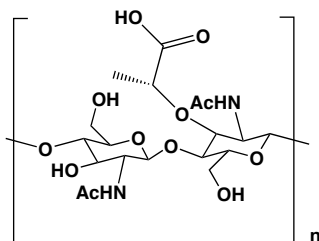
- For II.46, the compound was dissolved in 4,5 mL of distilled water and 4,5 mL of dioxane, and to this solution was added lithium hydroxide monohydrate (66 mg, 1.57 mmol) at room temperature for 2 h30 min. The reaction was quenched by adding a HCl 1 M solution and the pH adjusted to 3. , The solvent was removed and the crude obtained was washed with 1 mL of water, followed by evaporation of solvent. The residue obtained was washed with ethyl ether (2 x 2 mL). The product obtained was not further purified and was used directly in the next step.

#### 4.2.3.1.5.2 *N*-acetylation

The *N*-acetylation was performed according to the procedure described in 4.2.5, without work-up, proceeding to the silyl group removal one pot.

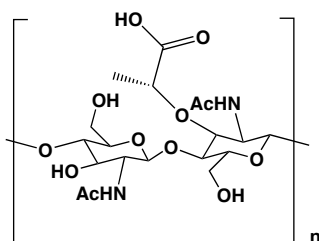
#### 4.2.3.1.5.3 *Silyl group removal*

In order to remove all the silyl groups add 2 equiv. of a solution of TBAF 1 M in THF. The mixture was stirred overnight at room temperature. The solvent was removed, and the dry crude was washed with ethyl ether (x mL) and distilled water (1 mL) and 0.1 mL of NaOH 1 M were added. The water was evaporated and the residue taken to dryness. To the resulting residue was added distilled water (1 mL) and the pH adjusted to 3 with a solution of HCl 1 M. The water was evaporated to give a product.



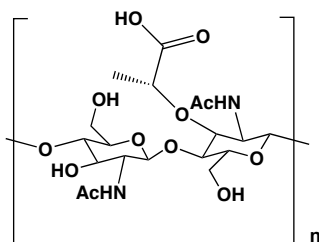
II.47 starting with II.41 followed by the sequence of deprotection procedures 4.2.3.1.5. A yellow powder was obtained, 59 mg.

IR  $\nu_{\max}$ (KBr): 3434 (O-H), 3014, 1732, 1702, 1655 (C=O), 1152, 990 (C-O)  $\text{cm}^{-1}$ .



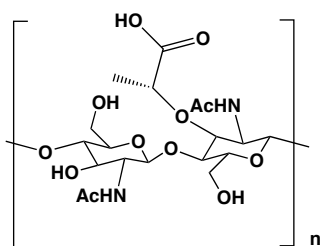
II.48 starting with II.44 followed by the sequence of deprotection procedures 4.2.3.1.5. A yellow powder was obtained, 167 mg.

IR  $\nu_{\max}$ (KBr): 3447 (O-H), 1736, 1663 (C=O), 1162-1009 (C-O)  $\text{cm}^{-1}$ .



II.49 starting with II.45 followed by the sequence of deprotection procedures 4.2.3.1.5. A yellow powder was obtained, 179 mg.

IR  $\nu_{\max}$ (KBr): 3435 (O-H), 1698, 1656 (C=O), 1158-1012 (C-O)  $\text{cm}^{-1}$ .



II.50 starting with II.46 followed by the sequence of deprotection procedures 4.2.3.1.5. A yellow powder was obtained, 194 mg.  
 IR  $\nu_{\max}$ (KBr): 3429 (O-H), 1717, 1651, 1635 (C=O), 1151-1029 (C-O)  $\text{cm}^{-1}$ .

#### 4.2.3.2 Silylation route

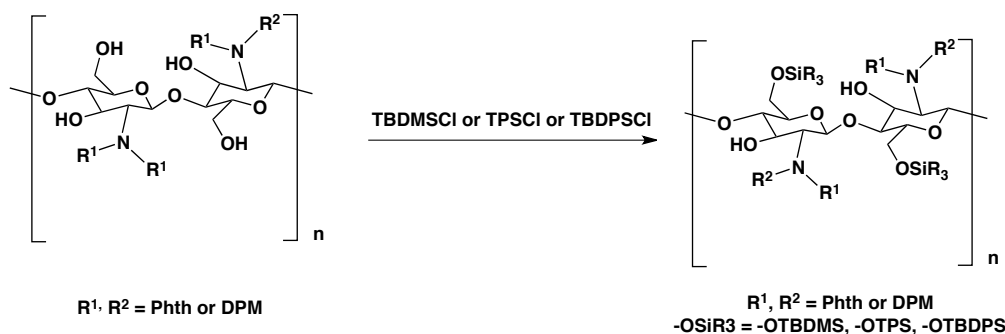
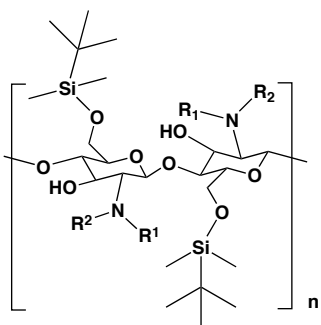


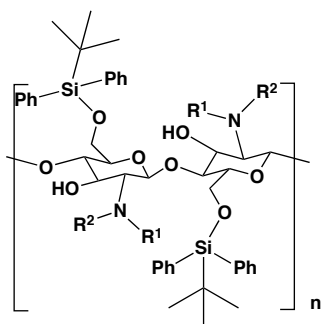
Figure 4.8 Schematic representation of silylation of *N*-protected chitosan

To a suspension of *N*-phthaloylchitosan (0.3 g, 1.05 mmol) and an excess of imidazole (0.581 g, 8.53 mmol) in anhydrous DMF (40 mL) was treated with the respective silyl chloride group in different excess, TBDMSCl (1.14 g, 7.61 mmol), TBDPSCI (1.95 mL, 7.53 mmol), TPSCl (1.45 g, 4.95 mmol). The reaction was stirred at room temperature for 72 hours. The product was precipitated with 50 mL of water/ethanol (1:1 v/v) solution. Then the solid was filtered and washed with 20 mL of water/ethanol and ethyl ether 3 x 5 mL.<sup>62</sup>



$\text{R}^1, \text{R}^2 = \text{Phth}$

I.47 starting with I.32 and TBDMSCl, using 4.2.3.2. A white powder was obtained, 398 mg.  
 IR  $\nu_{\max}$ (KBr): 3435 (O-H), 1779, 1708 (C=O), 1197-963 (C-O) 873 (Si-O)  $\text{cm}^{-1}$ .

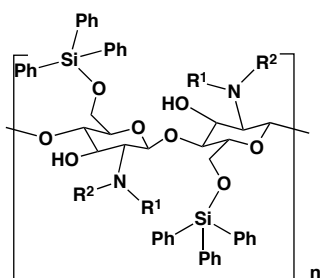


R<sup>1</sup>, R<sup>2</sup> = Phth

I.47 starting with I.32 and TDBPSCI, using 4.2.3.2. A white powder was obtained, 416 mg.

**CP-MAS** <sup>13</sup>C NMR (101 MHz; None): δ 167.8 (C=O), 134.6, 131.2, 127.9, 122.8 (Ar), 98.2 (C1), 82.0 (C4), 75.3 (C5), 69.7 (C3), 62.5 (C6), 56.1 (C2), 26.5 (CH<sub>3</sub>).

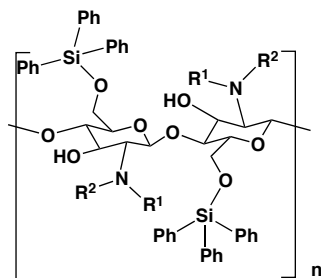
**IR** ν<sub>max</sub>(KBr): 3467 (O-H), 1778, 1718 (C=O), 1193-968 (C-O) 1113, 874 (Si-O) cm<sup>-1</sup>.



R<sup>1</sup>, R<sup>2</sup> = Phth

II.17 starting with I.32 and TPSCI, using 4.2.3.2. A white powder was obtained, 462 mg.

**CP-MAS** <sup>13</sup>C NMR (101 MHz; None): δ 168.6 (C=O), 134.9, 130.5, 128.1, 123.4 (Ar), 99.7 (C1), 82.0, 80.7 (C4), 74.5 (C5), 69.7 (C3), 60.5 (C6), 55.6 (C2). **IR** ν<sub>max</sub>(KBr): 3448 (O-H), 1776, 1717 (C=O), 1196-997 (C-O), 1118, 1095 (Si-O) cm<sup>-1</sup>.

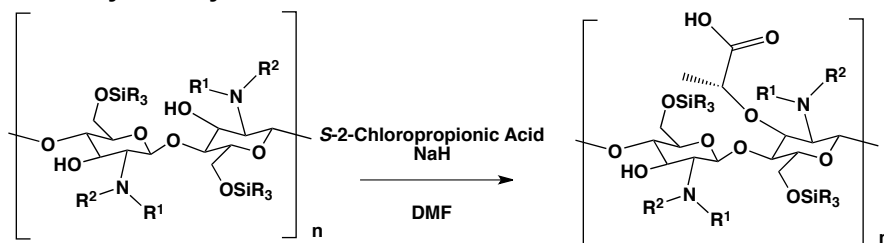


R<sup>1</sup>, R<sup>2</sup> = DPM

II.26 DPM starting with II.16 and TPSCI, using 4.2.3.2. A white powder was obtained, 433 mg of a white powder.

**IR** ν<sub>max</sub>(KBr): 34448 (O-H), 1768, 1707 (C=O), 1102-998 (C-O), 1117 (Si-O) cm<sup>-1</sup>.

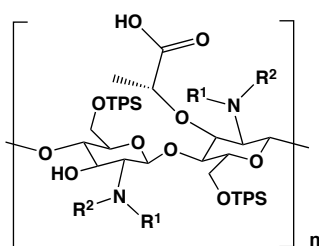
#### 4.2.3.2.1 Lactyl moiety insertion



R<sup>1</sup>, R<sup>2</sup> = Phth or DPM  
-OSiR<sub>3</sub> = -OTPS, -OTBDPS

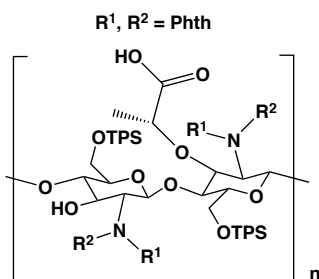
Figure 4.9 Schematic representation of lactyl moiety insertion

In this synthesis step was followed the same procedure as describe in 4.2.4.



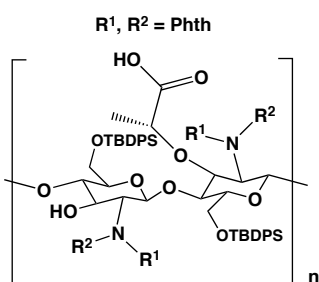
II.20 starting with II.17 and 2 equiv. of S-2-Chloropropionic Acid. A yellow powder was obtained, 178 mg.

IR  $\nu_{\max}$ (KBr): 3392(O-H), 1756, 1732 (C=O), 1593 (C-C Ar), 1109-992 (C-O), 1081 (Si-O)  $\text{cm}^{-1}$ .



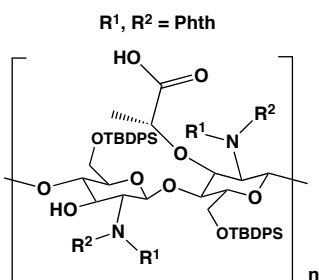
II.21 starting with II.17 and 4 equiv. of S-2-Chloropropionic Acid. A yellow powder was obtained, 189 mg.

IR  $\nu_{\max}$ (KBr): 3382 (O-H), 1830, 1821 (C=O), 1748, 1726 (C=O), 1598 (C-C Ar), 1090-996 (C-O), 1069 (Si-O)  $\text{cm}^{-1}$ .



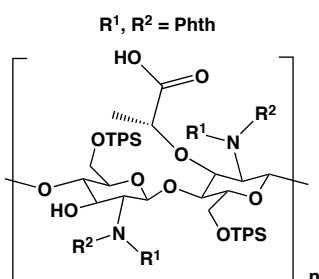
II.18 starting with I.47 and 4 equiv. of S-2-Chloropropionic Acid. A yellow powder was obtained, 167 mg.

IR  $\nu_{\max}$ (KBr): 3432 (O-H), 1724, 1654 (C=O), 1554 (C-C Ar), 1093-991 (C-O), 1113, 1053 (Si-O)  $\text{cm}^{-1}$ .



II.19 starting with I.47 and 2 equiv. of S-2-Chloropropionic Acid. A yellow powder was obtained, 179 mg.

IR  $\nu_{\max}$ (KBr): 3390 (O-H), 1716, 1655 (C=O), 1554 (C-C Ar), 1110-998 (C-O), 1113, 1051 (Si-O)  $\text{cm}^{-1}$



II.27 starting with II.26 and 2 equiv. of S-2-Chloropropionic Acid. A yellow powder was obtained, 149 mg.

IR  $\nu_{\max}$ (KBr): 3448 (O-H), 1768, 1708, 1664 (C=O), 1155-1032 (C-O), 1117, 1072 (Si-O)  $\text{cm}^{-1}$ .

$R^1, R^2 = \text{DPM}$

#### 4.2.3.2.2 Deprotection and *N*-acetylation

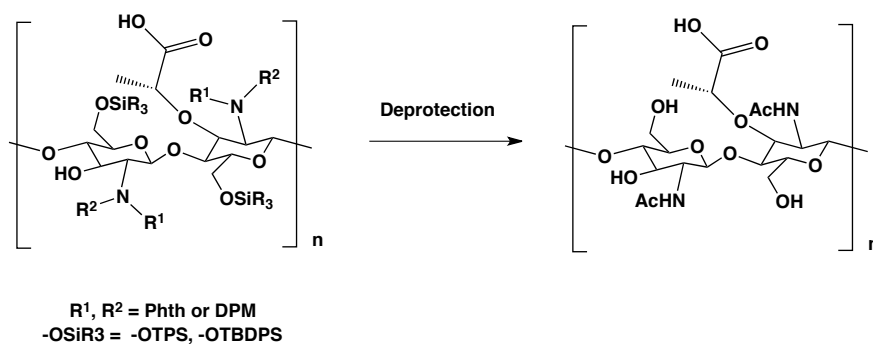


Figure 4.10 Schematic representation of all deprotection reactions and *N*-acetylation

##### 4.2.3.2.2.1 Phthaloyl removal

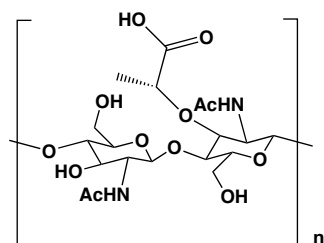
In order to remove the phthaloyl group the procedure described in 4.2.3.1.5.1, was used.

##### 4.2.3.2.2.2 *N*-acetylation

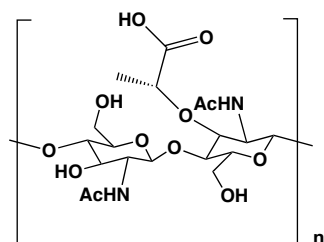
In order to acetylate all the amine groups the procedure described in 4.2.3.1.5.2, was used.

##### 4.2.3.2.2.3 Silyl group removal

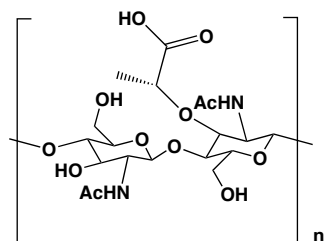
In order to remove all the silyl the procedure described in 4.2.3.1.5.3, was used.



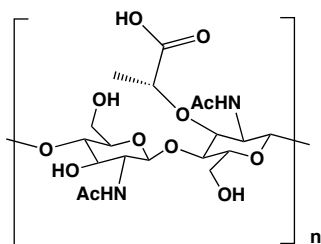
II.22 starting with II.20 followed by the sequence of deprotection procedures 4.2.3.2.2. A yellow powder was obtained, 60 mg.  
IR  $\nu_{\text{max}}$ (KBr): 3435 (O-H), 1718, 1650 (C=O), 1158-998 (C-O)  $\text{cm}^{-1}$ .



II.23 starting with II.21 followed by the sequence of deprotection procedures 4.2.3.2.2. A yellow powder was obtained, 39 mg. Product was not characterized and was used directly in the enzymatic assays.



II.24 starting with II.18 followed by the sequence of deprotection procedures 4.2.3.2.2. A yellow powder was obtained, 49 mg. Product was not characterized and was used directly in the enzymatic assays



II.25 starting with II.19 followed by the sequence of deprotection procedures 4.2.3.2.2. A yellow powder was obtained, 58 mg. Product was not characterized and was used directly in the enzymatic assays.

#### 4.2.4 Muramic Acid moiety insertion

To a 200 mg of  $O_3$ -free chitosan in 5 mL of anhydrous DMF was added NaH (152 mg, 3.8 mmol) at 0°C and was stirred for 1 hour. Then the S-2-Chloropropionic acid was added. The reaction was stirred from 0°C to room temperature for 48 hours. Then the solvent was evaporated to dryness, and the product was diluted with 3 mL of distilled water and acidified with 1 M HCl to pH 3. The residues were washed with ethyl ether, 3 x 5 mL, and the aqueous layers were collected and the solvent was evaporated. The product obtained was dried under vacuum.

#### 4.2.5 N-acetylation

To a solution of *N*-free chitosan, add 20 equiv. of acetic anhydride in 2 mL of dried pyridine at 0°C and let the temperature rise to room temperature over night. Then evaporate the solvent was evaporated to dryness, washed with ethyl ether and 1 mL of distilled water and 0.1 mL of NaOH 1 M were added. The water was removed, and the residue obtained. After that the precipitate was dissolved in 1 mL of distilled water and the pH adjusted to 3 with a solution of HCl 1 M. the water was removed to give the final product.

### 4.3 General procedures to evaluate the final product

#### 4.3.1 Enzymatic digestion

1. To an *ependorf* tube the sample was added (10 mg/mL), in the respective buffer. The enzyme was added, lyzozime (10 mg/mL in ammonium acetate 40 mM, pH 5,25) 1:0.225 (mg of sample: mg of enzyme) or mutanolysin 1:0.15 (mg of sample:  $\mu$ L of enzyme) (10 mg/mL in phosphate 25 mM, pH 5.5);
2. The mixture was incubated for 24 or 92 hours at 37°C 1.200 rpm in a *ependorf* heat plaque;
3. The mixture was boiled in water for 5 minutes;
4. The samples were centrifuged at 13.000 rpm at room temperature for 5 minutes;
5. The same volume of 0,5 M Borate Buffer pH 9.0 was added;
6. Fresh 50 mg/mL  $\text{NaBH}_4$  was added in a ratio of 8.33:1 (mL of mixture: mL of 50 mg/mL  $\text{NaBH}_4$ ) and incubated at room temperature for 2 hours;
7. The sample pH was adjusted to 2.0 with 85% o-phosphoric acid;
8. The samples were centrifuged at 13.000 rpm at room temperature for 5 minutes;
9. The supernatant were collected and store at -20°C.

#### 4.3.1.1 HPLC-UV protocol

Table 4-2 HPLC UV protocol eluent composition

Eluent	200 mM NaHPO4 pH 2.0	Mili-Q water	Methanol (HPLC grade)
A	1 L	900 mL	100 mL
B	1 L	400 mL	600 mL

The HPLC analyses were performed on a Shimadzu® prominence HPLC using a reverse phase C-18 Hypersil column Q = 0,5 mL/min; Oven at 52° C, the volume of injection was not fix and the eluting conditions applied are presented at Table 4-3. The detection was made by absorption at 206 and 280 nm.

Table 4-3 Concentration gradient used during the HPLC-UV program

Time (min)	Solvent A%	Solvent B%
0	100	0
155	0	100
160	0	100
175	100	0
200	100	0

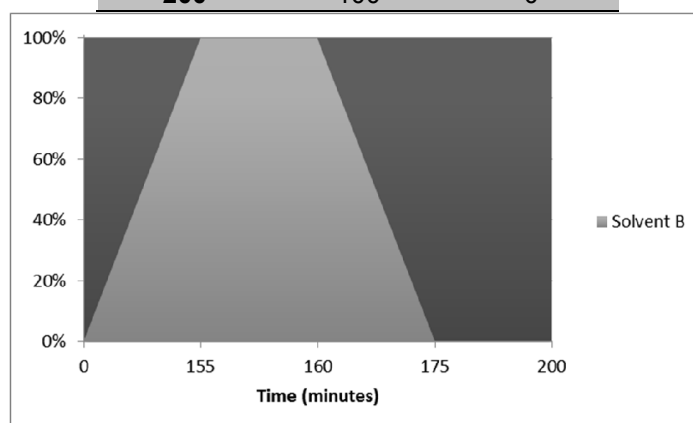


Figure 4.11 HPLC-UV eluent profile

All of the final products were analyzed through this program to check the outcome of the enzymatic hydrolysis.

#### 4.3.1.2 HPLC-MS protocol

The HPLC analyses were performed on a Waters Alliance 2695 (Waters®, Ireland) equipped with a quaternary pump, solvent degasser, auto sampler and column oven, coupled to a Photodiode Array Detector Waters 996 PDA (Waters®, Ireland). The separation was performed on a reversed-phase column (LiCrospher® 100 RP-18, 250x4 mm; 5 µm; Merck®) at 35° C using an injection volume of 20 µL. The mobile phase consisted of Milli-Q water containing 0.5% formic acid (A): MeOH (B) at a flow rate of 0.30 mL/min and the eluting conditions applied are presented at Table 4-4.

**Table 4-4 Concentration gradient used during the HPLC-MS program**

Time (min)	Solvent %A	Solvent %B
0.00	100.0	0.0
30.00	0.0	100.0
50.00	0.0	100.0
60.00	100.0	0.0
80.00	100.0	0.0

Photodiode Array Detector Waters 2996 (Waters®, Ireland) was used to scan wavelength absorption from 205 to 400 nm. MS/MS experiments were performed on Micromass® Quattro Micro triple quadrupole (Waters®, Ireland) with an electrospray in positive ion mode (ESI+), with ion source at 120° C, capillary voltage of 3.0 kV and source voltage of 30V. The compounds were ionized and spectra of the column eluent were recorded in the range m/z 100-2000. High purity nitrogen (N<sub>2</sub>) was used both as drying gas and as a nebulising gas. MassLynx software (version 4.1) was used for data acquisition and processing.

#### **4.3.2 mCherry-PGRP pull-down assay**

The mCherry-PGRP-SA was quantified in the Nanodrop, using PBS Buffer as blank;

Blanks:

A: 20 µL of PGN (10 mg/mL) centrifuged at 13.000 rpm for 5 minutes, pellet was disposed.

B: 20 µL of PGN (10 mg/mL) digested with amidase LytA overnight with the protocol 4.3.1, pellet was disposed.

C: 20 µL of PGN (10 mg/mL) digested with muramidase, Mutanolysin, overnight with protocol 4.3.1, pellet was disposed.

D: 20 µL of PGN (10 mg/mL) digested with muramidase, Mutanolysin, overnight with protocol 4.3.1 and digest with amidase LytA overnight with the protocol 4.3.1, pellet was disposed.

Reaction mixture:

1. 25 µL of BSA 30x (from NEB) – use a master solution;
2. 20 µL of PGN (10 mg/mL) – only in some assays;
3. mCherry-PGRP-SA to 0,3 mg/mL final concentration;
4. Buffer to 300 µL final volume. For each different Protein:Buffer pair tested prepared an empty control;
5. Use 20 µL of MilliQ water instead of PGN;
6. Incubated 30 minutes at 25°C at 1000 rpm;
7. Centrifuged 10 minutes at 3000 rpm;
8. Collected 30 µL of the supernatant and mix it with 30 µL of Loading Buffer at 2x – Unbound Fraction;

9. Resuspend the pellet in 300  $\mu$ L of Buffer and centrifuge for 5 minutes at 6000 rpm;
10. Resuspend the pellet in 300  $\mu$ L of Buffer and centrifuge for 2 minutes at 132000 rpm;
11. Resuspend the pellet in 30  $\mu$ L of Loading Buffer at 1x – Bound Fraction;
12. Apply in an electrophoresis gel both bound and unbound fraction.

#### 4.3.2.1 Electrophoresis

Gel preparation was performed according to Table 4-5. The samples were prepared by adding loading buffer, Table 4-6, containing  $\beta$ -mercaptoethanol in a 1:1 ratio to the sample and boiling them for 5 min, being then immediately applied onto the gel. The gels were ran for 1 h 30 min at a fix voltage 80V in 1x Tris-Glycine buffer, Table 4-7. The samples were prepared in the exact same way as mentioned above.

**Table 4-5 SDS gel composition**

	Running gel 8.0% - 10 mL	Stacking gel 4.0% 6 mL
<b>Acrilamide</b>	2.7 mL	0.8 mL
<b>Tris-HCl, 1.5 M, pH 8.8</b>	2.5 mL	----
<b>Tris-HCl, 0.5 M pH 6.8</b>	----	1.5 mL
<b>SDS 10% (w/v)</b>	0.1 mL	60 $\mu$ L
<b>ddH<sub>2</sub>O</b>	4.65 mL	3.6 mL
<b>TMED</b>	5 $\mu$ L	6 $\mu$ L
<b>PSA 10% (w/v)</b>	50 $\mu$ L	30 $\mu$ L

**Table 4-6 Loading Buffer**

Reagent	Volume (mL)
<b>SDS 10% (w/v)</b>	1.0
<b>Glycerol</b>	0.5
<b>Tris 1M pH 6.8</b>	0.8
<b>Bromophenol blue 0.2% (w/v)</b>	0.1
<b><math>\beta</math>-Mercaptoethanol</b>	0.5
<b>ddH<sub>2</sub>O</b>	2.1

**Table 4-7 Electrophoresis Buffer**

Reagent	Concentration
<b>Tris base</b>	0.025 M, pH 8.8
<b>Glycine</b>	0.102 M
<b>SDS</b>	0.1 % (w/v)

#### 4.3.3 Monosaccharide composition analysis

1. A master solution of HCl was prepared, containing 37.25  $\mu$ L HCl 37% (12 M) and 92.75  $\mu$ L H<sub>2</sub>O per sample;
2. To a 1.5 mL eppendorf was added 20  $\mu$ L of the sample at 10 mg/mL (0.2 mg PGN total) and 130  $\mu$ L of the HCl master solution. Final volume of 150  $\mu$ L at 3 M HCl;
3. The mixture was transferred to a reaction vial and incubated at 95°C for 2 hours;
4. The reaction mixture was transferred into a punctured 1.5 mL Eppendorf;
5. The reaction vial was washed with 100  $\mu$ L of MilliQ H<sub>2</sub>O and added to the Eppendorf;
6. The mixture was lyophilized until completely dryness;

7. Resuspended in 500  $\mu\text{L}$  of MilliQ  $\text{H}_2\text{O}$ ;
8. Lyophilized overnight;
9. The pellet was suspended in 150  $\mu\text{L}$  of MilliQ  $\text{H}_2\text{O}$  before injection and apply 10  $\mu\text{L}$ .

The anionic exchange chromatography analyses were performed on an ICS-5000 Ion Chromatography Systems – Dionex (Thermo Scientific®), and the eluting conditions applied are presented at Table 4-8.

**Table 4-8 Concentration gradient used during the anionic exchange chromatography program**

Time (min)	Flow (mL/min)	Eluent %		
		B	C	D
0	1	1,8	0	0
20	1	1,8	0	0
25	1	1,8	0	20
30	1	1,8	0	20
35	1	1,8	0	80
40	1	1,8	0	80
45	1	1,8	0	0
50	1	1,8	0	0
55	1	1,8	0	0
60	1	1,8	0	0

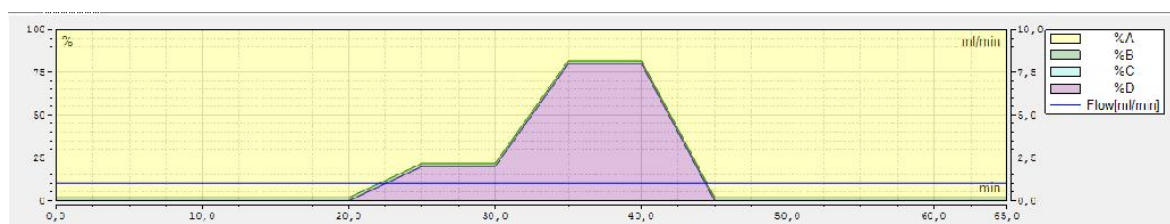


**Figure 4.12 Eluent profile for the anionic exchange chromatography**

**Table 4-9 Eluent Composition**

Eluent	Composition
A	MilliQ $\text{H}_2\text{O}$
B	1M NaOH (Ion Chromatography Grade)
C	Mili-Q $\text{H}_2\text{O}$
D	1M $\text{NaCH}_3\text{COO}$ (HPLC Grade)

## 5 Bibliography

1. Fredrickson, J. K.; Zachara, J. M.; Balkwill, D. L.; Kennedy, D.; Li, S. M. W.; Kostandarithes, H. M.; Daly, M. J.; Romine, M. F.; Brockman, F. J., Geomicrobiology of high-level nuclear waste-contaminated vadose sediments at the Hanford Site, Washington State. *Applied and Environmental Microbiology* **2004**, *70* (7), 4230-4241.
2. Suresh, R.; Mosser, D. M., Pattern recognition receptors in innate immunity, host defense, and immunopathology. *Advances in Physiology Education* **2013**, *37* (4), 284-291.
3. Rubin, G. M.; Yandell, M. D.; Wortman, J. R.; Miklos, G. L. G.; Nelson, C. R.; Hariharan, I. K.; Fortini, M. E.; Li, P. W.; Apweiler, R.; Fleischmann, W.; Cherry, J. M.; Henikoff, S.; Skupski, M. P.; Misra, S.; Ashburner, M.; Birney, E.; Boguski, M. S.; Brody, T.; Brokstein, P.; Celniker, S. E.; Chervitz, S. A.; Coates, D.; Cravchik, A.; Gabrielian, A.; Galle, R. F.; Gelbart, W. M.; George, R. A.; Goldstein, L. S. B.; Gong, F. C.; Guan, P.; Harris, N. L.; Hay, B. A.; Hoskins, R. A.; Li, J. Y.; Li, Z. Y.; Hynes, R. O.; Jones, S. J. M.; Kuehl, P. M.; Lemaitre, B.; Littleton, J. T.; Morrison, D. K.; Mungall, C.; O'Farrell, P. H.; Pickeral, O. K.; Shue, C.; Vosshall, L. B.; Zhang, J.; Zhao, Q.; Zheng, X. Q. H.; Zhong, F.; Zhong, W. Y.; Gibbs, R.; Venter, J. C.; Adams, M. D.; Lewis, S., Comparative genomics of the eukaryotes. *Science* **2000**, *287* (5461), 2204-2215.
4. Chaput, C.; Boneca, I. G., Peptidoglycan detection by mammals and flies. *Microbes and Infection* **2007**, *9* (5), 637-647.
5. Lemaitre, B.; Hoffmann, J., The host defense of *Drosophila melanogaster*. In *Annual Review of Immunology*, Annual Reviews: Palo Alto, 2007; Vol. 25, pp 697-743.
6. Nicolas, E.; Reichhart, J. M.; Hoffmann, J. A.; Lemaitre, B., In vivo regulation of the I kappa B homologue cactus during the immune response of *Drosophila*. *Journal of Biological Chemistry* **1998**, *273* (17), 10463-10469; Weber, A. N. R.; Tauszig-Delamasure, S.; Hoffmann, J. A.; Lelievre, E.; Gascan, H.; Ray, K. P.; Morse, M. A.; Imler, J. L.; Gay, N. J., Binding of the *Drosophila* cytokine Spatzle to Toll is direct and establishes signaling. *Nature Immunology* **2003**, *4* (8), 794-800; Hu, X. D.; Yagi, Y.; Tanji, T.; Zhou, S. L.; Ip, Y. T., Multimerization and interaction of Toll and Spatzle in *Drosophila*. *Proceedings of the National Academy of Sciences of the United States of America* **2004**, *101* (25), 9369-9374.
7. Hu, S. M.; Yang, X. L., dFADD, a novel death domain-containing adapter protein for the *Drosophila* caspase DREDD. *Journal of Biological Chemistry* **2000**, *275* (40), 30761-30764.
8. Kaneko, T.; Yano, T.; Aggarwal, K.; Lim, J. H.; Ueda, K.; Oshima, Y.; Peach, C.; Erturk-Hasdemir, D.; Goldman, W. E.; Oh, B. H.; Kurata, S.; Silverman, N., PGRP-LC and PGRP-LE have essential yet distinct functions in the *Drosophila* immune response to monomeric DAP-type peptidoglycan. *Nature Immunology* **2006**, *7* (7), 715-723.
9. Stoven, S.; Ando, I.; Kadalayil, L.; Engstrom, Y.; Hultmark, D., Activation of the *Drosophila* NF-kappa B factor Relish by rapid endoproteolytic cleavage. *Embo Reports* **2000**, *1* (4), 347-352; Stoven, S.; Silverman, N.; Junell, A.; Hedengren-Olcott, M.; Erturk, D.; Engstrom, Y.; Maniatis, T.; Hultmark, D., Caspase-mediated processing of the *Drosophila* NF-kappa B factor Relish.

*Proceedings of the National Academy of Sciences of the United States of America* **2003**, *100* (10), 5991-5996.

10. Vollmer, W.; Blanot, D.; de Pedro, M. A., Peptidoglycan structure and architecture. *Fems Microbiology Reviews* **2008**, *32* (2), 149-167.
11. Vollmer, W., Structural variation in the glycan strands of bacterial peptidoglycan. *Fems Microbiology Reviews* **2008**, *32* (2), 287-306.
12. Filipe, S. R.; Tomasz, A.; Ligoxygakis, P., Requirements of peptidoglycan structure that allow detection by the Drosophila Toll pathway. *Embo Reports* **2005**, *6* (4), 327-333.
13. Wang, L. H.; Weber, A. N.; Atilano, M. L.; Filipe, S. R.; Gay, N. J.; Ligoxygakis, P., Sensing of Gram-positive bacteria in Drosophila: GGBP1 is needed to process and present peptidoglycan to PGRP-SA. *Embo Journal* **2006**, *25* (20), 5005-5014.
14. Atilano, M. L.; Pereira, P. M.; Yates, J.; Reed, P.; Veiga, H.; Pinho, M. G.; Filipe, S. R., Teichoic acids are temporal and spatial regulators of peptidoglycan cross-linking in Staphylococcus aureus. *Proceedings of the National Academy of Sciences of the United States of America* **2010**, *107* (44), 18991-18996.
15. Zhang, Y.; Fechter, E. J.; Wang, T.-S. A.; Barrett, D.; Walker, S.; Kahne, D. E., Synthesis of heptaprenyl-lipid IV to analyze peptidoglycan glycosyltransferases. *Journal of the American Chemical Society* **2007**, *129* (11), 3080-+.
16. Inamura, S.; Fukase, K.; Kusumoto, S., Synthetic study of peptidoglycan partial structures. Synthesis of tetrasaccharide and octasaccharide fragments. *Tetrahedron Letters* **2001**, *42* (43), 7613-7616.
17. Meroueh, S. O.; Bencze, K. Z.; Heseck, D.; Lee, M.; Fisher, J. F.; Stemmler, T. L.; Mobashery, S., Three-dimensional structure of the bacterial cell wall peptidoglycan. *Proceedings of the National Academy of Sciences of the United States of America* **2006**, *103* (12), 4404-4409.
18. Crich, D.; Dudkin, V., Why are the hydroxy groups of partially protected N-acetylglucosamine derivatives such poor glycosyl accepters, and what can be done about it? A comparative study of the reactivity of N-acetyl-, N-phthalimido-, and 2-azido-2-deoxy-glucosamine derivatives in glycosylation. 2-picolinyl ethers as reactivity-enhancing replacements for benzyl ethers. *Journal of the American Chemical Society* **2001**, *123* (28), 6819-6825.
19. Enugala, R.; Carvalho, L. C. R.; Pires, M. J. D.; Marques, M. M. B., Stereoselective Glycosylation of Glucosamine: The Role of the N-Protecting Group. *Chemistry-an Asian Journal* **2012**, *7* (11), 2482-2501.
20. Enugala, R.; Pires, M. J. D.; Marques, M. M. B., Synthesis of the NAG-NAM disaccharide via a versatile intermediate. *Carbohydrate Research* **2014**, *384*, 112-118.
21. (A)Carvalho, L. R.; Corvo, M. C.; Enugala, R.; Marques, M. M. B.; Cabrita, E. J., Application of HR-MAS NMR in the solid-phase synthesis of a glycopeptide using Sieber amide resin. *Magnetic Resonance in Chemistry* **2010**, *48* (4), 323-330; (B) Unpublished results; (C) Master Thesis "Síntese de peptidoglicano bacteriano reconhecido pelo sistema imunitário" Luísa Carvalho, IST-UTL, 2008.
22. Enugala, R.; Carvalho, L. C. R.; Marques, M. M. B., Towards Glucosamine Building Blocks: Regioselective One-Pot Protection and Deallylation Procedures. *Synlett* **2010**, (18), 2711-2716.
23. Wang, Y. H.; Ye, X. S.; Zhang, L. H., Oligosaccharide assembly by one-pot multi-step strategy. *Organic & Biomolecular Chemistry* **2007**, *5* (14), 2189-2200.

24. Rinaudo, M., Chitin and chitosan: Properties and applications. *Progress in Polymer Science* **2006**, *31* (7), 603-632.
25. Rinaudo, M., Main properties and current applications of some polysaccharides as biomaterials. *Polymer International* **2008**, *57* (3), 397-430.
26. Muzzarelli, R. A. A., Chitins and chitosans for the repair of wounded skin, nerve, cartilage and bone. *Carbohydrate Polymers* **2009**, *76* (2), 167-182.
27. Lamarque, G.; Cretenet, M.; Viton, C.; Domard, A., New route of deacetylation of alpha- and beta-chitins by means of freeze-pump out-thaw cycles. *Biomacromolecules* **2005**, *6* (3), 1380-1388.
28. Shin, Y.; Yoo, D. I.; Jang, J., Molecular weight effect on antimicrobial activity of chitosan treated cotton fabrics. *Journal of Applied Polymer Science* **2001**, *80* (13), 2495-2501.
29. Czechowska-Biskup, R.; Rokita, B.; Ulanski, P.; Rosiak, J. M., Radiation-induced and sonochemical degradation of chitosan as a way to increase its fat-binding capacity. *Nuclear Instruments & Methods in Physics Research Section B-Beam Interactions with Materials and Atoms* **2005**, *236*, 383-390.
30. Torzsas, T. L.; Kendall, C. W. C.; Sugano, M.; Iwamoto, Y.; Rao, A. V., The influence of high and low molecular weight chitosan on colonic cell proliferation and aberrant crypt foci development in CF1 mice. *Food and Chemical Toxicology* **1996**, *34* (1), 73-77.
31. Ikeda, I.; Sugano, M.; Yoshida, K.; Sasaki, E.; Iwamoto, Y.; Hatano, K., EFFECTS OF CHITOSAN HYDROLYSATES ON LIPID ABSORPTION AND ON SERUM AND LIVER LIPID-CONCENTRATION IN RATS. *Journal of Agricultural and Food Chemistry* **1993**, *41* (3), 431-435.
32. Feng, T.; Du, Y.; Li, J.; Wei, Y.; Yao, P., Antioxidant activity of half N-acetylated water-soluble chitosan in vitro. *European Food Research and Technology* **2007**, *225* (1), 133-138.
33. Surini, S.; Akiyama, H.; Morishita, M.; Nagai, T.; Takayama, K., Release phenomena of insulin from an implantable device composed of a polyion complex of chitosan and sodium hyaluronate. *Journal of Controlled Release* **2003**, *90* (3), 291-301.
34. Mucha, M., Rheological characteristics of semi-dilute chitosan solutions. *Macromolecular Chemistry and Physics* **1997**, *198* (2), 471-484.
35. Gupta, B.; Arora, A.; Saxena, S.; Alam, M. S., Preparation of chitosan-polyethylene glycol coated cotton membranes for wound dressings: preparation and characterization. *Polymers for Advanced Technologies* **2009**, *20* (1), 58-65.
36. Muzzarelli, R. A. A., Biomedical Exploitation of Chitin and Chitosan via Mechano-Chemical Disassembly, Electrospinning, Dissolution in Imidazolium Ionic Liquids, and Supercritical Drying. *Marine Drugs* **2011**, *9* (9), 1510-1533.
37. Kurita, K.; Kojima, T.; Nishiyama, Y.; Shimojoh, M., Synthesis and some properties of nonnatural amino polysaccharides: Branched chitin and chitosan. *Macromolecules* **2000**, *33* (13), 4711-4716.
38. Franca, E. F.; Lins, R. D.; Freitas, L. C. G.; Straatsma, T. P., Characterization of Chitin and Chitosan Molecular Structure in Aqueous Solution. *Journal of Chemical Theory and Computation* **2008**, *4* (12), 2141-2149.
39. Sannan, T.; Kurita, K.; Iwakura, Y., Studies on Chitin, 1. *Die Makromolekulare Chemir* **1975**, *176*, 1191-1195; Sannan, T.; Kurita, K.; Iwakura, Y., Studies on Chitin, 2. *Makromol. Chem.* **1976**, *177*, 3589-3600.

40. Kadokawa, J.; Takegawa, A.; Mine, S.; Prasad, K., Preparation of chitin nanowhiskers using an ionic liquid and their composite materials with poly(vinyl alcohol). *Carbohydrate Polymers* **2011**, *84* (4), 1408-1412; Wang, W. T.; Zhu, J.; Wang, X. L.; Huang, Y.; Wang, Y. Z., Dissolution Behavior of Chitin in Ionic Liquids. *Journal of Macromolecular Science Part B-Physics* **2010**, *49* (3), 528-541; Wu, Y.; Sasaki, T.; Irie, S.; Sakurai, K., A novel biomass-ionic liquid platform for the utilization of native chitin. *Polymer* **2008**, *49* (9), 2321-2327; Mourya, V. K.; Inamdar, N. N., Chitosan-modifications and applications: Opportunities galore. *Reactive & Functional Polymers* **2008**, *68* (6), 1013-1051; Kurita, K., Controlled functionalization of the polysaccharide chitin. *Progress in Polymer Science* **2001**, *26* (9), 1921-1971.
41. Hirai, A.; Odani, H.; Nakajima, A., DETERMINATION OF DEGREE OF DEACETYLATION OF CHITOSAN BY H-1-NMR SPECTROSCOPY. *Polymer Bulletin* **1991**, *26* (1), 87-94; Suginta, W.; Chuenark, D.; Mizuhara, M.; Fukamizo, T., Novel b-N-acetylglucosaminidases from *Vibrio harveyi* 650: Cloning, expression, enzymatic properties, and subsite identification. *BMC Biochemistry* **2010**, *11* (40); Bahrke, S.; Einarsson, J. M.; Gislason, J.; Haebel, S.; Letzel, M. C.; Peter-Katalinic, J.; Peter, M. G., Sequence Analysis of Chitooligosaccharides by Matrix-Assisted Laser Desorption Ionization Postsorce Decay Mass Spectrometry. *Biomacromolecules* **2002**, *3* (4), 696-704.
42. Popa-Nita, S.; Lucas, J. M.; Ladaviere, C.; David, L.; Domard, A., Mechanisms Involved During the Ultrasonically Induced Depolymerization of Chitosan: Characterization and Control. *Biomacromolecules* **2009**, *10* (5), 1203-1211.
43. Cabrera, J. C.; Cutsem, P. V., Preparation of chitooligosaccharides with degree of polymerization higher than 6 by acid or enzymatic degradation of chitosan. *Biochemical Engineering Journal* **2005**, *25*, 165-172.
44. Alves, N. M.; Mano, J. F., Chitosan derivatives obtained by chemical modifications for biomedical and environmental applications. *International Journal of Biological Macromolecules* **2008**, *43* (5), 401-414; Gupta, B.; Agarwal, R.; Alam, M. S., Textile-based smart wound dressings. *Indian Journal of Fibre & Textile Research* **2010**, *35* (2), 174-187; Patel, M. P.; Patel, R. R.; Patel, J. K., Chitosan Mediated Targeted Drug Delivery System: A Review. *Journal of Pharmacy and Pharmaceutical Sciences* **2010**, *13* (4), 536-557; Petkar, K. C.; Chavhan, S. S.; Agatonovik-Kustrin, S.; Sawant, K. K., Nanostructured Materials in Drug and Gene Delivery: A Review of the State of the Art. *Critical Reviews in Therapeutic Drug Carrier Systems* **2011**, *28* (2), 101-164; Morris, G. A.; Kok, M. S.; Harding, S. E.; Adams, G. G., Polysaccharide drug delivery systems based on pectin and chitosan. *Biotechnology and Genetic Engineering Reviews, Vol 27* **2010**, *27*, 257-283; Muzzarelli, R. A. A.; Boudrant, J.; Meyer, D.; Manno, N.; DeMarchis, M.; Paoletti, M. G., Current views on fungal chitin/chitosan, human chitinases, food preservation, glucans, pectins and inulin: A tribute to Henri Braconnot, precursor of the carbohydrate polymers science, on the chitin bicentennial. *Carbohydrate Polymers* **2012**, *87* (2), 995-1012; Yang, T.-L., Chitin-based Materials in Tissue Engineering: Applications in Soft Tissue and Epithelial Organ. *International Journal of Molecular Sciences* **2011**, *12* (3), 1936-1963; Park, B. K.; Kim, M.-M., Applications of Chitin and Its Derivatives in Biological Medicine. *International Journal of Molecular Sciences* **2010**, *11* (12), 5153-5165; Deng, C.;

- Li, F. F.; Griffith, M.; Ruel, M.; Suuronen, E. J., Application of Chitosan-Based Biomaterials for Blood Vessel Regeneration. *Polymers and Organic Chemistry* **2010**, *297*, 138-146; Chaudhury, A.; Das, S., Recent Advancement of Chitosan-Based Nanoparticles for Oral Controlled Delivery of Insulin and Other Therapeutic Agents. *Aaps Pharmscitech* **2011**, *12* (1), 10-20; Jayakumar, R.; Chennazhi, K. P.; Srinivasan, S.; Nair, S. V.; Furuike, T.; Tamura, H., Chitin Scaffolds in Tissue Engineering. *International Journal of Molecular Sciences* **2011**, *12* (3), 1876-1887; Muzzarelli, R. A. A., Chitosan composites with inorganics, morphogenetic proteins and stem cells, for bone regeneration. *Carbohydrate Polymers* **2011**, *83* (4), 1433-1445.
45. Allan, G. G.; Peyron, M., MOLECULAR-WEIGHT MANIPULATION OF CHITOSAN .1. KINETICS OF DEPOLYMERIZATION BY NITROUS-ACID. *Carbohydrate Research* **1995**, *277* (2), 257-272.
46. Zamani, A.; Taherzadeh, M. J., PRODUCTION OF LOW MOLECULAR WEIGHT CHITOSAN BY HOT DILUTE SULFURIC ACID. *Bioresources* **2010**, *5* (3), 1554-1564.
47. Einbu, A.; Vårum, K. M., Depolymerization and De-N-acetylation of Chitin Oligomers in Hydrochloric Acid. *Biomacromolecules* **2007**, *8*, 309-314.
48. Trombotto, S.; Ladaviere, C.; Delolme, F.; Domard, A., Chemical preparation and structural characterization of a homogeneous series of chitin/chitosan oligomers. *Biomacromolecules* **2008**, *9* (7), 1731-1738.
49. Yalpani, M.; Pantaleone, D., An examination of the unusual susceptibilities of aminoglycans to enzymatic hydrolysis. *Carbohydrate Research* **1994**, *259*, 159-175; Aiba, S., STUDIES ON CHITOSAN .4. LYSOZYMIC HYDROLYSIS OF PARTIALLY N-ACETYLATED CHITOSANS. *International Journal of Biological Macromolecules* **1992**, *14* (4), 225-228.
50. Chen, R. H.; Chang, J. R.; Shyur, J. S., Effects of ultrasonic conditions and storage in acidic solutions on changes in molecular weight and polydispersity of treated chitosan. *Carbohydrate Research* **1997**, *299*, 287-295; Kjartansson, G. T.; Zivanovic, S.; Kristbergsson, K.; Weiss, J., Sonication-Assisted Extraction of Chitin from Shells of Fresh Water Prawns (*Macrobrachium rosenbergii*). *Journal of Agricultural and Food Chemistry* **2005**, *54*, 3317-3323.
51. Wasikiewicz, J. M.; Yeates, S. G., "Green" molecular weight degradation of chitosan using microwave irradiation. *Polymer Degradation and Stability* **2013**, *98* (4), 863-867; Ajavakoma, A.; Supsvetsonb, S.; Sombooth, A.; Sukwattanasinitta, M., Products from microwave and ultrasonic wave assisted acid hydrolysis of chitin. *Carbohydrate Polymers* **2012**, *90*, 73-77.
52. Ifuku, S.; Miwa, T.; Morimoto, M.; Saimoto, H., Preparation of highly chemoselective N-phthaloyl chitosan in aqueous media. *Green Chemistry* **2011**, *13* (6), 1499-1502.
53. Kurita, K.; Ikeda, H.; Yoshida, Y.; Shimojoh, M.; Harata, M., Chemoselective protection of the amino groups of chitosan by controlled phthaloylation: Facile preparation of a precursor useful for chemical modifications. *Biomacromolecules* **2002**, *3* (1), 1-4.
54. Ifuku, S.; Matsumoto, C.; Wada, M.; Morimoto, M.; Saimoto, H., Preparation of highly regioselective amphiprotic chitosan derivative via "click chemistry". *International Journal of Biological Macromolecules* **2013**, *52*, 72-76.

55. Pestov, A. V.; Kodess, M. I.; Matochkina, E. G.; Yatluk, Y. G., Selective mono-N-2-carboxyethylation of chitosan in the presence of magnesium halides. *Carbohydrate Polymers* **2011**, *86* (2), 783-788.
56. Badawy, M. E. I.; Rabea, E. I., Characterization and antimicrobial activity of water-soluble N-(4-carboxybutyryl) chitosans against some plant pathogenic bacteria and fungi. *Carbohydrate Polymers* **2012**, *87* (1), 250-256.
57. Skorik, Y. A.; Pestov, A. V.; Kodess, M. I.; Yatluk, Y. G., Carboxyalkylation of chitosan in the gel state. *Carbohydrate Polymers* **2012**, *90* (2), 1176-1181.
58. Xu, T.; Xin, M. H.; Li, M. C.; Huang, H. L.; Zhou, S. Q., Synthesis, characteristic and antibacterial activity of N,N,N-trimethyl chitosan and its carboxymethyl derivatives. *Carbohydrate Polymers* **2010**, *81* (4), 931-936.
59. Xu, T.; Xin, M. H.; Li, M. C.; Huang, H. L.; Zhou, S. Q.; Liu, J. Z., Synthesis, characterization, and antibacterial activity of N,O-quaternary ammonium chitosan. *Carbohydrate Research* **2011**, *346* (15), 2445-2450.
60. Ren, J. M.; Li, Q.; Dong, F.; Feng, Y.; Guo, Z. Y., Phenolic antioxidants-functionalized quaternized chitosan: Synthesis and antioxidant properties. *International Journal of Biological Macromolecules* **2013**, *53*, 77-81.
61. Yang, J. H.; Luo, K.; Li, D. L.; Yu, S. S.; Cai, J.; Chen, L. Y.; Du, Y. M., Preparation, characterization and in vitro anticoagulant activity of highly sulfated chitosan. *International Journal of Biological Macromolecules* **2013**, *52*, 25-31; Kurita, K.; Sugita, K.; Kodaira, N.; Hirakawa, M.; Yang, J., Preparation and evaluation of trimethylsilylated chitin as a versatile precursor for facile chemical modifications. *Biomacromolecules* **2005**, *6* (3), 1414-1418; Ma, G. P.; Yang, D. Z.; Kennedy, J. F.; Nie, J., Synthesize and characterization of organic-soluble acylated chitosan. *Carbohydrate Polymers* **2009**, *75* (3), 390-394; Watanabe, T.; Kodaira, N.; Ikeda, H.; Kurita, K., Synthesis and some properties of silylated chitins as key intermediates for chemical modifications. *Polymer Bulletin* **2012**, *68* (7), 1845-1855.
62. Binette, A.; Gagnon, J., Regioselective silylation of N-phthaloylchitosan with TBDMS and TBDPS groups. *Biomacromolecules* **2007**, *8* (6), 1812-1815.
63. Munro, N. H.; Hanton, L. R.; Moratti, S. C.; Robinson, B. H., Preparation and graft copolymerisation of thiolated beta-chitin and chitosan derivatives. *Carbohydrate Polymers* **2009**, *78* (1), 137-145.
64. Zou, Y. Q.; Khor, E., Preparation of c-6 substituted chitin derivatives under homogeneous conditions. *Biomacromolecules* **2005**, *6* (1), 80-87.
65. Morita, Y.; Sugahara, Y.; Takahashi, A.; Ibonai, M., PREPARATION OF CHITIN-P-TOLUENESULFONATE AND DEOXY(THIOCYANATO) CHITIN. *European Polymer Journal* **1994**, *30* (11), 1231-1236.
66. Holappa, J.; Nevalainen, T.; Savolainen, J.; Soininen, P.; Elomaa, M.; Safin, R.; Suvanto, S.; Pakkanen, T.; Masson, M.; Loftsson, T.; Jarvinen, T., Synthesis and characterization of chitosan N-betainates having various degrees of substitution. *Macromolecules* **2004**, *37* (8), 2784-2789.
67. Ifuku, S.; Wada, M.; Morimoto, M.; Saimoto, H., Preparation of highly regioselective chitosan derivatives via "click chemistry". *Carbohydrate Polymers* **2011**, *85* (3), 653-657; Liu, H. Q.; Zhao, Y. C.; Cheng, S.; Huang, N.; Leng, Y. X., Syntheses of novel chitosan derivative with excellent solubility, anticoagulation, and antibacterial property by chemical modification. *Journal of Applied Polymer Science* **2012**, *124* (4), 2641-2648.

68. Umemura, T.; Hirakawa, M.; Yoshida, Y.; Kurita, K., Quantitative protection of chitin by one-step tritylation and benzoylation to synthesize precursors for chemical modifications. *Polymer Bulletin* **2012**, *69* (3), 303-312.
69. Satoh, T.; Kano, H.; Nakatani, M.; Sakairi, N.; Shinkai, S.; Nagasaki, T., 6-Amino-6-deoxy-chitosan. Sequential chemical modifications at the C-6 positions of N-phthaloyl-chitosan and evaluation as a gene carrier. *Carbohydrate Research* **2006**, *341* (14), 2406-2413.
70. Huang, J.; Chen, W. W.; Hu, S.; Gong, J. Y.; Lai, H. W.; Liu, P.; Mei, L. H.; Mao, J. W., Biochemical activities of 6-carboxy beta-chitin derived from squid pens. *Carbohydrate Polymers* **2013**, *91* (1), 191-197.
71. Guan, R. J.; Wang, Q.; Sundberg, E. J.; Mariuzza, R. A., Crystal structure of human peptidoglycan recognition protein S (PGRP-S) at 1.70 angstrom resolution. *Journal of Molecular Biology* **2005**, *347* (4), 683-691; Guan, R. J.; Brown, P. H.; Swaminathan, C. P.; Roychowdhury, A.; Boons, G. J.; Mariuzza, R. A., Crystal structure of human peptidoglycan recognition protein I alpha bound to a muramyl pentapeptide from Gram-positive bacteria. *Protein Science* **2006**, *15* (5), 1199-1206.
72. Muthusamy, S.; Gnanaprakasam, B.; Suresh, E., Desymmetrization of cyclic anhydrides using dihydroxy compounds: Selective synthesis of macrocyclic tetralactones. *Organic Letters* **2006**, *8* (9), 1913-1916.
73. Wakao, M.; Fukase, K.; Kusumoto, S., Chemical synthesis of cyclodextrins by using intramolecular glycosylation. *Journal of Organic Chemistry* **2002**, *67* (23), 8182-8190.
74. McKenzie, H. A.; White, F. H., LYSOZYME AND ALPHA-LACTALBUMIN - STRUCTURE, FUNCTION, AND INTERRELATIONSHIPS. *Advances in Protein Chemistry* **1991**, *41*, 173-315.
75. Calandra, G. B.; Cole, R. M., LYSIS AND PROTOPLAST FORMATION OF GROUP-B STREPTOCOCCI BY MUTANOLYSIN. *Infection and Immunity* **1980**, *28* (3), 1033-1037.
76. Guan, R. J.; Mariuzza, R. A., Peptidoglycan recognition proteins of the innate immune system. *Trends in Microbiology* **2007**, *15* (3), 127-134.
77. Chang, C. I.; Pili-Floury, S.; Herve, M.; Parquet, C.; Chelliah, Y.; Lemaitre, B.; Mengin-Lecreulx, D.; Deisenhofer, J., A Drosophila pattern recognition receptor contains a peptidoglycan docking groove and unusual L,D-carboxypeptidase activity. *Plos Biology* **2004**, *2* (9), 1293-1302; Royet, J.; Dziarski, R., Peptidoglycan recognition proteins: pleiotropic sensors and effectors of antimicrobial defences. *Nature Reviews Microbiology* **2007**, *5* (4), 264-277.
78. Dziarski, R., CELL-BOUND ALBUMIN IS THE 70-KDA PEPTIDOGLYCAN, LIPOPOLYSACCHARIDE, AND LIPOTEICHOIC ACID BINDING-PROTEIN ON LYMPHOCYTES AND MACROPHAGES. *Journal of Biological Chemistry* **1994**, *269* (32), 20431-20436; Sogorb, M. A.; Carrera, V.; Benabent, M.; Vilanova, E., Rabbit serum albumin hydrolyzes the carbamate carbaryl. *Chemical Research in Toxicology* **2002**, *15* (4), 520-526.



## 6 Appendix